Securing Crucial Biodiversity, Carbon and Water Stores in the Congo Basin Peatlands

Model Documentation of the Hydrological Decision Support System

Technical Report
Project Number: 11826037

09-Jan-2026

Prepared for UNEP

Executive Summary

The Congo Basin peatlands, particularly those in the Cuvette Centrale region, represent one of the world's most significant terrestrial carbon stores and are vital for biodiversity and hydrological stability. In response to increasing pressures from land use change, infrastructure development, and climate variability, the United Nations Environment Programme (UNEP) initiated a project titled **"Securing Crucial Biodiversity, Carbon and Water Stores in the Congo Basin Peatlands by Enabling Evidence-Based Decision Making and Good Governance".** This initiative led to the development of a Hydrological Decision Support System (HDSS), designed to provide scientific guidance for sustainable peatland management in the Lac Télé/Lac Tumba landscape.

The HDSS provides a scientific basis for evaluating the potential impacts of various development interventions and climate scenarios on peatland hydrology and carbon dynamics. It supports decision-makers by providing guidance on the likely consequences of locally relevant interventions - identified through a consultative stakeholder process - on water balance and soil carbon stocks.

Model and HDSS development

At the heart of the HDSS is a conceptual hydrological model tailored to the unique conditions of the Cuvette Centrale peatlands. Due to limited georeferenced data, the model adopts a simplified but robust structure that captures the essential hydrological processes governing peatland function. It distinguishes between rainfall-driven and river-influenced regimes, enabling the simulation of both interfluvial domes and riparian zones. The model domain is a 40 km by 2.88 km slice through a peat dome, discretized into 80-meter grid cells, and initialized under saturated conditions. The simulation period spans from 2000 to 2019.

The hydrological model, built using the MIKE SHE platform, simulates the full water cycle, including precipitation, evapotranspiration, infiltration, groundwater flow, and overland flow. Actual evapotranspiration is calculated using the Kristensen & Jensen method, with reference evapotranspiration derived from the Priestley-Taylor equation. Leaf Area Index (LAI) data from MODIS and Copernicus Earth observation datasets are used to represent vegetation dynamics, while spatial climate inputs are sourced from ERA5 reanalysis data. The model captures a bimodal seasonal rainfall pattern and reveals a long-term trend of declining precipitation and increasing evapotranspiration.

Soil hydraulic properties are parameterized based on literature and previous modeling efforts. In the unsaturated zone, the model uses Richards' Equation. The saturated zone includes peat and clay layers, with peat depths ranging from 1.15 to 4 meters. Overland flow is modeled using a 2D diffusive wave approximation, with detention storage set at 6.5 cm to reflect microtopographic variability.

Calibration of the model was conducted against field data from Dargie et al. (2017) and Crezee et al. (2022). The shape parameter of the soil water retention curve and the reference evapotranspiration increased by 5% to better model seasonal water table fluctuations. The model successfully reproduces observed patterns, including spatial variation in groundwater depth and seasonal drying trends linked to climate change. Water balance analysis shows that rainfall and evapotranspiration are by far the most important hydrological fluxes in the region, with evapotranspiration slightly exceeding precipitation during the simulation period.

To assess carbon dynamics, the hydrological model is coupled with a carbon accumulation and decay model inspired by DigiBog. Litter material generated by plant growth is divided into leaves, wood and roots. The decomposition of organic matter under oxic and anoxic conditions is simulated with a dual exponential decay function, including both the fast decay of labile compounds and the slow decomposition of recalcitrant material. Peat decay is more intense under oxic conditions, i.e. if air-filled porosity exceeds 10%, and increases exponentially with temperature. The parameters used to describe peat accumulation and decay are derived from field data in the Congo peatlands (Young et al., 2023).

Under baseline conditions, annual net soil carbon loss is estimated at 4.72 kg C/m², while permanently waterlogged scenarios result in a soil carbon loss of 2.82 kg/m²/yr.

Development interventions, climate change scenarios and hydrological regimes

The HDSS evaluates seven development interventions—baseline, road construction, operational road, settlement development, forest fire (deforestation), oil palm plantation, and rice cultivation—under three climate scenarios (current, SSP1-2.6 sustainable growth, SSP3-7.0 severe impact) and two hydrological regimes (rainfall-driven and river-influenced).

The development interventions were identified through stakeholder consultations in Brazzaville. Each intervention alters vegetation cover, topography, and soil hydraulic properties, with significant implications for water table dynamics and the soil carbon stock. The generalized development interventions derived from the stakeholder consultations are the following:

Table 0-1 Generalized development interventions

Code	Name	Description
A	Baseline without Intervention	Vegetation and topography of the peatlands are according to the current conditions - between 2010 and 2020
B	Road Built and Operational	(a) A raised impervious road is built 1 meter above the natural surface. It is finished and operational. (b) Vegetation is removed, and the soil surface is flattened. (c) The road embankment is filled with permeable gravel. (d) The underlying peat is compressed due to the road's weight.
C	Road during Construction	(a) A raised impervious road is being built 1 meter above the natural surface. (b) Vegetation is removed, and the soil surface is flattened. (c) The road embankment is filled with permeable gravel. (d) The underlying peat is compressed due to the road's weight. (e) During construction, drainage is installed 2 meters below the ground, i.e., 1 meter below the surrounding surface.
D	Settlements Developed	(a) A settlement is developed in the peatland forest. (b) The topography is raised by 50 cm to prevent flooding. (c) Vegetation is cleared, and the soil surface is partially paved. (d) The peat is compressed under the load of buildings.
E	Forest Fire – Deforestation	(a) A forest fire completely clears the vegetation. (b) As a result, soil properties change: bulk density increases, and specific yield decreases.
F	Palm Plantation replaces Forest	Deforestation and Conversion to Oil Palm Plantations: (a) Natural vegetation is cleared to establish additional oil palm plantations. (b) Oil palms thrive with a mean water level 40 cm to 60 cm below ground. There is drainage at 50 cm depth. (c) Vegetation properties are altered according to 15-year-old mature oil palm plantation. (d) The microtopography is smoothed due to clearing. (e) Soil properties change by drainage: increased bulk density, reduced specific yield, and reduced hydraulic conductivity at saturation. (f) The topography is lowered by 50 cm due to soil subsidence induced by drainage.
G	Rice Cultivation replaces Forest	Deforestation and Conversion to Rice Cultivation: (a) Natural vegetation is removed and replaced with rice paddies. Rice is the most common seasonally flooded crop in the Cuvette Centrale. (b) There are two harvests per year. Vegetation and surface properties/roughness vary with crop stage.

Climate change scenarios are modeled using the delta change method, applying monthly scaling factors to precipitation, evapotranspiration, and temperature. From the IPCC AR6 emission scenarios the following to form part of the scenario definitions:

Table 0-2 Climate change scenarios

Code	Name	Description
1	Current Climate	Rainfall, temperature and evapotranspiration between 2010 and 2020 are chosen to represent the current climate conditions.
2	CC Sustainable Growth	SSP1-2.6: (a) Global warming is limited to around 1.5°C-2°C above pre-industrial levels. (b) This scenario is in line with the objectives of the Paris Agreement and represents an optimistic future with sustainable economic growth and minimal impact on climate change.
3	CC Severe Impact	SSP3-7.0: (a) Projected warming: 3°C-4°C by 2100, with severe climatic consequences. (b) This scenario represents a high-risk future, characterized by significant climate change, social inequalities and environmental degradation.

To reflect the hydrological diversity of the Cuvette Centrale, the hydrological model incorporates two distinct representations: one for rainfall-driven peatlands and another for those influenced by river flooding. This ensures that both hydrological regimes are adequately captured:

Table 0-3 Hydrological regimes

Code	Name	Description
1	Rain-fed	Rainfall and Evapotranspiration only: The hydrological processes in the peatlands are only driven by rainfall and evapotranspiration. This is mostly the case in interfluvial peat domes, mostly located in the Republic of Congo.
2	River-fed	Rainfall and Evapotranspiration plus River Water Levels: The hydrological processes in the peatlands are driven by rainfall and evapotranspiration, as well as fluctuating water levels in bordering water bodies (e.g., river reaches). This is mostly the case in the riparian peatlands, mostly located in the Democratic Republic of Congo.

The hydrological regions are represented in the models as model boundary conditions: in the rainfall driven configuration, the western and eastern boundaries have a constant head set at surface level. These water levels fluctuate in the river-fed models. Boundary conditions are model drivers like the climate model drivers. The model structure and parameterization are designed to align with the region's hydrological, climatic, and geomorphological characteristics, while also accounting for existing data gaps.

By combining the seven development interventions with three climatic scenarios and two hydrological regimes, the HDSS generates results for 42 different scenarios.

Scenarios evaluation method with indicators

Behind each scenario definition is a comprehensive model with its input parameters and simulation results. The evaluation of scenarios makes use of indicators that are derived from the detailed simulation results. The following indicators are defined to allow simplified evaluation of scenarios and comparisons:

Table 0-4 Indicators used to generate results

Name	Indicator Description
Carbon Flux Inside	Carbon stock change in kg per m2 per year inside the footprint of the intervention
Carbon Flux Outside	Carbon stock change in kg per m2 per year outside the footprint of the intervention
Oxic Depth Inside	Average oxic depth inside the footprint of the intervention: Depth in the soil where oxygen is still present, affecting nutrient cycling, i.e., carbon transformations. This influences the rate of organic matter decomposition and thus carbon sequestration.
Oxic Depth Outside	Average oxic depth outside the footprint of the intervention: Depth in the soil where oxygen is still present, affecting nutrient cycling, i.e., carbon transformations. This influences the rate of organic matter decomposition and thus carbon sequestration.
GWT Depth Inside	Average ground water table depth inside the footprint of the intervention - in meters below the surface
GWT Depth Outside	Average ground water table depth outside the footprint of the intervention - in meters below the surface

Summary of results

The hydrological and carbon emission impacts of the interventions are assessed within and around the intervention footprint. Indicator values are summarised in the table below. Values highlighted in red and green indicate, respectively, high and low soil carbon losses.

Table 0-5 Results of development scenarios in current climate in rain-fed peatlands

Indicator Short Name	Unit	Indicator Values for Scenarios						
		A.1.1	B.1.1	C.1.1	D.1.1	E.1.1	F.1.1	G.1.1
Oxic Depth Inside	m	0.20	0.92	2.12	0.37	0.18	0.73	0.14
Groundwater Depth Inside	m	0.15	1.06	2.00	0.40	0.14	0.73	0.10
Carbon Flux Inside	kg/m^2/year	**-4.72**	0.00	0.00	-8.77	-4.67	-15.64	-3.77
Oxic Depth Outside	m	0.20	0.13	0.68	0.16	0.20	0.77	0.20
Groundwater Depth Outside	m	0.15	0.05	0.68	0.10	0.16	0.79	0.15
Carbon Flux Outside	kg/m^2/year	**-4.72**	-2.90	-14.26	-3.80	-4.78	-15.01	-4.70

Table 0-6 Results of development scenarios in current climate in river-fed peatlands

Indicator Short Name	Unit	Indicator Values for Scenarios						
		A.1.2	B.1.2	C.1.2	D.1.2	E.1.2	F.1.2	G.1.2
Oxic Depth Inside	m	0.12	0.89	2.12	0.34	0.12	0.71	0.09
Groundwater Depth Inside	m	0.03	1.03	2.01	0.35	0.03	0.69	0.00
Carbon Flux Inside	kg/m^2/year	**-2.82**	0.00	0.00	-8.10	-3.17	-14.55	-2.46
Oxic Depth Outside	m	0.12	0.07	0.61	0.09	0.12	0.65	0.12
Groundwater Depth Outside	m	0.03	-0.05	0.59	-0.01	0.03	0.64	0.03
Carbon Flux Outside	kg/m^2/year	**-2.82**	-1.40	-12.88	-2.08	-2.85	--13.53	-2.79

Climate change scenarios

Water levels in the peatland are expected to drop under both SSP1-2.6 and SSP3-7.0. Although rainfall should increase by 1.5% annually under SSP1-2.6, the rise in actual evapotranspiration is sharper. Under SSP3-7.0, a substantial increase in actual evapotranspiration coupled with a slight decrease in rainfall leads to lower water levels. As water levels drop under climate change, peat decay increases.

Conclusions

The scenario analyses conducted highlight several critical vulnerabilities of the peatlands, arising from their hydrological sensitivity, the nature of development interventions, and the impacts of climate change.

- **Hydrological Vulnerabilities**: The peatlands are highly sensitive to changes in water table levels. Lowering of the groundwater table - whether through drainage, infrastructure development, or prolonged dry periods - exposes peat to oxic conditions, thereby accelerating decomposition and increasing carbon losses. The loss of microtopography and increased overland flow further exacerbate water loss, particularly in areas where natural surface features are altered.
- **Vulnerabilities from Development Interventions**: Infrastructure development, such as road construction, settlement expansion, and conversion to agriculture (e.g., oil palm or rice cultivation), typically involves drainage and compression of peat soils. These interventions result in a significant lowering of the water table, increased oxic depth, and enhanced peat decomposition. Removal of natural vegetation and smoothing of the land surface reduce the peatland's capacity to retain water and buffer against hydrological extremes.
- **Climate Change Vulnerabilities**: With climate change, the peatlands of the Cuvette Centrale are expected to become drier. Evapotranspiration rates are projected to increase substantially, driven by rising temperatures in the region. This projection is particularly concerning for the Cuvette Centrale, where peatlands are more vulnerable to drought than their Southeast Asian counterparts due to lower annual precipitation. The region could experience longer and more intense dry seasons, leading to lower water tables, an increased risk of fire, and accelerated carbon loss. These findings should be interpreted with caution given the high uncertainty of CMIP6 rainfall projections.

In summary, the Congo Basin peatlands are highly vulnerable to hydrological disturbance, unsustainable land use, and climate change. Maintaining high water tables, protecting natural vegetation, and restoring degraded areas are essential to safeguard their carbon stocks, biodiversity, and hydrological functions.

Applicability and limitations

The Hydrological Decision Support System (HDSS) enhances understanding and the management of the Congo Basin peatlands. By integrating hydrological processes with carbon dynamics and climate projections, the HDSS can be used to help assess how water table fluctuations—driven by climate variability and human interventions—affect carbon losses from peat soils.

Despite data limitations and the necessity of using conceptual simplifications, the HDSS successfully captures key hydrological patterns and the critical role of groundwater depth and soil saturation in determining peatland carbon fluxes. Furthermore, it offers actionable insights for sustainable land-use planning that can lay the foundation for evidence-based governance, long-term monitoring, and stakeholder engagement—essential components for safeguarding one of the world's most carbon-rich and ecologically vital ecosystems.

Future efforts should focus on improving in-situ data collection, refining soil hydraulic parameters, and expanding the spatial resolution of the model. Nonetheless, the HDSS represents a significant step towards the application of integrating hydrology, carbon dynamics, and climate projections into a unified decision support framework for sustainable management and conservation of peatlands in the Congo Basin.

Contents

1 Introduction

The Congo Basin peatlands represent one of the world's most significant stores of terrestrial carbon, biodiversity, and freshwater resources. Protecting these ecosystems is critical not only for regional environmental integrity but also for global climate regulation. However, the peatlands face increasing pressures from local development, land use change, and climate variability, all of which can profoundly alter their hydrological and ecological balance.

In response to these challenges, the project "Securing Crucial Biodiversity, Carbon and Water Stores in the Congo Basin Peatlands by Enabling Evidence-Based Decision Making and Good Governance", implemented by UNEP, aims to support sustainable peatland management in the Lac Télé/Lac Tumba landscape. Central to this effort is the development of a Hydrological Decision Support System (HDSS), which provides a scientific basis for evaluating the potential impacts of various development interventions and climate scenarios on peatland hydrology and carbon dynamics.

This report documents the modelling approach and scenario analyses underpinning the HDSS. The model is designed for the Cuvette Centrale peatlands, reflecting their hydrological, climatic, and geomorphological characteristics. It supports decision-makers by providing guidance on the likely consequences of locally relevant interventions - identified through a consultative stakeholder process - on water balance and soil carbon stocks.

The following chapters describe the purpose and rationale for the modelling approach, the structure and verification of the model, the definition and evaluation of scenarios, and the key findings and recommendations for sustainable peatland management.

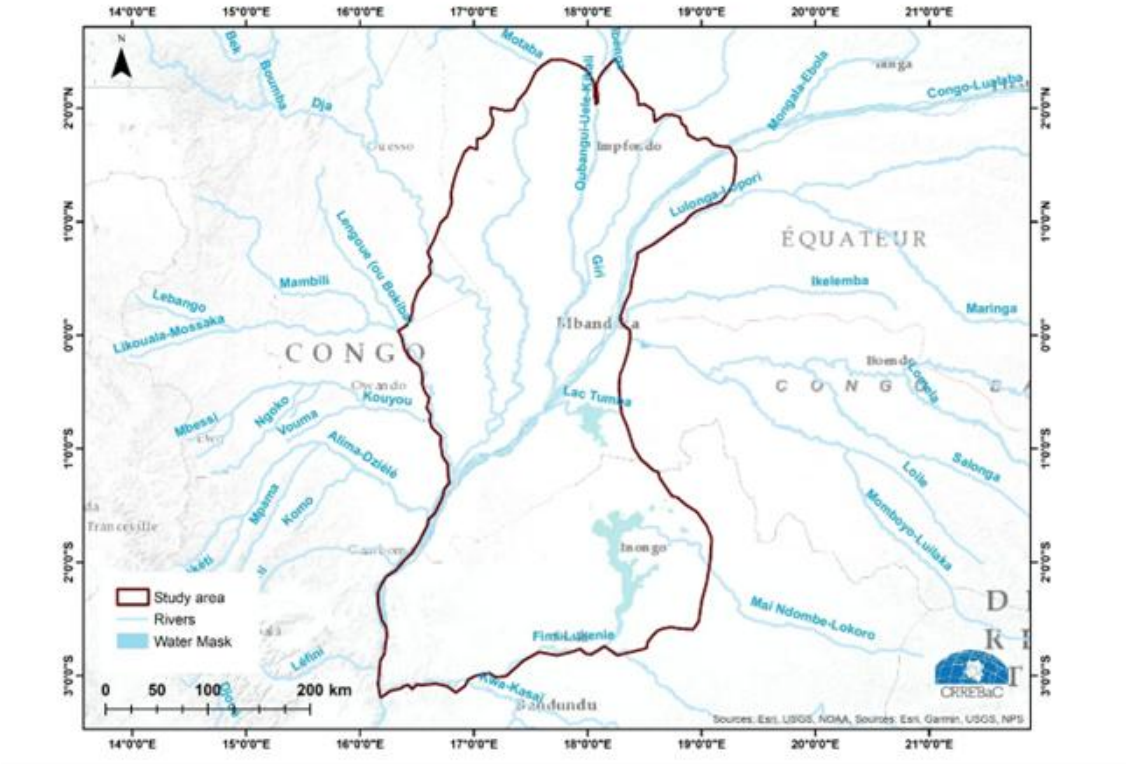

Figure 1.1 Overview of the Lac Tele Lac Tumba project landscape

2 Modelling Approach: Purpose, Rationale, and Methodology

The modelling approach adopted in this study is tailored to the hydrological and ecological context of the Cuvette Centrale peatlands in the Congo Basin.

2.1 Purpose and Rationale

The purpose of the model is to provide scientifically grounded guidance for decision-makers when preparing for planning interventions that may affect the peatland ecosystem, with a particular focus on estimating changes in the soil carbon stock.

Key aspects of the rationale include the following:

1. **Experimental Modelling Approach**: Due to limited availability of adequate georeferenced and comprehensive data for the region, developing a fully spatially explicit model was not feasible. Instead, an “experimental”, conceptual model has been developed, focusing on the key hydrological processes that govern peatland function. This approach is fit-for-purpose, allowing robust scenario analysis while acknowledging uncertainties.
2. **Addressing Hydrological Diversity**: The Cuvette Centrale peatlands exhibit hydrological diversity, with some areas influenced solely by rainfall and others also affected by river flooding. The model addresses this by establishing two types of hydrological representations, ensuring that both rainfall driven and river-influenced peatlands are adequately captured.
3. **Appropriate Model Development**: The model is designed to reflect the key characteristics of the Cuvette Centrale peatlands. Its structure, assumptions, and parameterization reflect the hydrological, climatic, and geomorphological conditions of this region, as well as the available data and knowledge gaps.
4. **Spatial Extent and Sensitivity**: The spatial extent of the model was determined through experimentation with the range of effects of different local interventions, ensuring that the model domain is appropriate for the scenarios under consideration.
5. **Locally Derived Interventions**: The set of interventions analysed in the scenario analysis was derived from a consultative process involving regional stakeholders, notably through a dedicated workshop held in Brazzaville in March 2025. As a result, all interventions reflect local development and management scenarios.

2.2 General Modelling Approach

Peatlands are wetlands characterized by the accumulation of organic matter under saturated, anoxic conditions. They store approximately one-third of global soil carbon despite covering only 3% of the land surface (Gorham, 1991). Peatland hydrology - particularly the position and variability of the water table - is central to their ecological functioning and carbon dynamics. Surface water inputs (rainfall, overland flow) and losses (evapotranspiration, runoff, drainage) regulate the water table, which in turn controls redox conditions in the peat profile. When water levels drop, oxygen infiltrates deeper peat layers, stimulating microbial decomposition and increasing CO_2 emissions. Conversely, saturated conditions promote methane (CH_4) production but limit CO_2 release. Thus, understanding the hydrology is essential for predicting and managing the climate impact.

Tropical peatlands, found in regions such as Southeast Asia, the Congo Basin, and the Amazon, are particularly vulnerable to hydrological disturbance. Unlike temperate peatlands, tropical systems are often deeper, with faster rates of carbon accumulation, and are exposed to more intense anthropogenic pressures such as deforestation, canal drainage, and agricultural conversion (Page et al., 2011; Dargie

et al., 2017). Drainage and drying increase aerobic decomposition and fire susceptibility, resulting in disproportionately high CO_2 emissions per area.

The peatlands of the Cuvette Centrale in the Congo Basin are among the largest tropical peat deposits on Earth, yet their hydrology remains insufficiently understood. Dargie et al. (2017) revealed the vast extent and carbon storage capacity of these systems, establishing their significance for global climate regulation. More recently, Apers et al. (2022) investigated seasonal water table dynamics, uncovering spatial variability in hydrological controls and highlighting the need for further in situ monitoring. These studies form the foundation of a growing but still limited understanding of how these peatlands function and respond to environmental change.

Given the limited availability of data for the region, the model is conceptual rather than georeferenced. Nevertheless, it is validated using the best available literature and field data. To improve understanding of the carbon dynamics in the Cuvette Centrale peatlands, this conceptual hydrological model is coupled with an approach that estimates the storage and decay of soil carbon based on water table fluctuations and heuristics derived from relevant scientific studies.

2.3 Overview of Model Structure

1. **Hydrological Representation**: The model simulates key processes of the water cycle, including precipitation, evapotranspiration, infiltration, groundwater flow, and overland flow. It distinguishes between rainfall driven and river-influenced peatland conditions.
2. **Scenario Analysis**: The model supports the evaluation of locally relevant interventions, as identified through the stakeholder workshop, and their impacts on hydrology and soil carbon stocks.
3. **Outputs**: Key outputs include groundwater levels, soil water content, and estimated change in soil carbon stocks, providing indicators for environmental management and policy.

3 Modelling the Peatland Hydrology of the Cuvette Centrale

The baseline model aims to reproduce the current water balance in the peatlands of the Cuvette Centrale in the Congo Basin. Specifically, it seeks to accurately[1] simulate the seasonal and interannual fluctuations of the groundwater table, capture the dynamics and evolution of soil moisture, and estimate actual evapotranspiration. An accurate hydrological representation of the area is essential for understanding its carbon dynamics.

3.1 Methodology

3.1.1 The MIKE SHE Hydrological Model

MIKE SHE is a hydrological modelling system designed to simulate the entire land phase of the hydrological cycle. Developed by DHI, it encompasses all key water cycle processes, including precipitation, evapotranspiration, overland flow, unsaturated and saturated subsurface flow, and channel flow in rivers and lakes. MIKE SHE is part of the MIKE Zero platform and supports GIS integration.

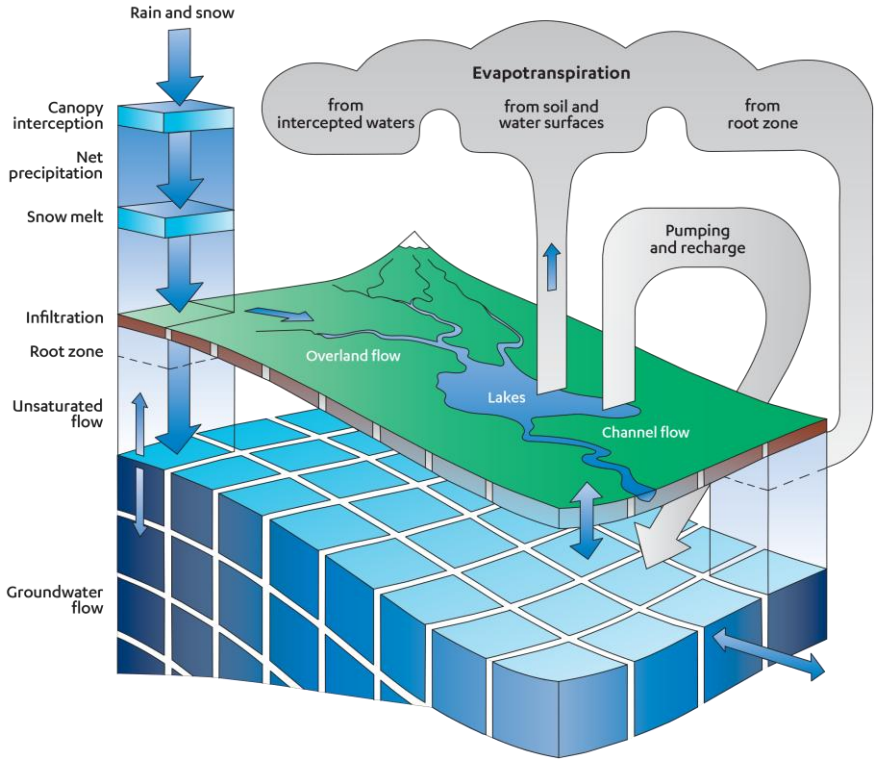

Figure 3.1 MIKE SHE models the whole water cycle

Peatlands are characterized by shallow water tables and close interactions between the aquifer and surface water. An integrated surface-subsurface modelling tool such as MIKE SHE enables accurately representing the complex dynamics. MIKE SHE supports the representation of key processes such as soil moisture variation in the unsaturated zone, overland flow and lateral flow in the saturated zone, which are critical to understanding peatland behaviour. The tool can use spatially distributed inputs and outputs, which allow modeling of heterogeneity in rainfall, evaporation, vegetation, soil, and topography.

[1] Accuracy: The datasets that were available for model development have limitations for applicability. However, any datasets that could be obtained have been compiled and quality controlled. So, the model setup and results are accurate vis-à-vis the scope and quality of the datasets used.

3.1.2 Building a MIKE SHE Model

The MIKE SHE model is developed as follows:

- **Definition of simulation specifications**: selection of both the computational engines for surface flow representation (Finite Difference) and for the unsaturated zone (Richards' Equation); selection of calculation time steps;
- **Definition of the modeled domain and the resolution of the model grid**;
- **Definition of meteorological inputs and evapotranspiration characteristics based on land use**: spatialized at the plot scale, with land use typologies and associated properties (e.g., vegetation development stage);
- **Definition of the hydrogeological model structure and the properties of the layers in the saturated zone**: hydraulic conductivity, specific yield, specific storage
- **Definition of the characteristics for modeling infiltration processes in the unsaturated zone**: particularly soil profiles (soil water content, hydraulic conductivity) and the choice of infiltration modeling parameters;
- **Definition of characteristics for surface flow modeling**: including surface roughness, interception zones, and initial conditions;
- **Definition of exported outputs (types of variables) and their export frequency.**

3.1.3 Key Processes of the Water Cycle

Peatlands are broadly classified into ombrotrophic and minerotrophic types based on their sources of water and nutrients. Ombrotrophic peatlands, such as raised bogs, are rainfall driven, receiving water exclusively from atmospheric precipitation. In contrast, minerotrophic peatlands, which include fens and swamp forests, are groundwater- or surface water-fed, meaning they receive inputs from mineral-rich sources like rivers, lakes, or subsurface flow. Both rainfall driven and river-fed peatlands were found in the Cuvette Centrale (Dargie et al. 2017; Crezee, 2022).

MIKE SHE models the main processes of the water cycle: precipitation, evapotranspiration, infiltration through the unsaturated zone, groundwater flow and overland flow. The simplified water balance is the following:

$$P + Q = ET + GW + OL + \Delta S$$

where

- P represents precipitation,
- Q is river inflow (>0 if inflow, <0 if outflow),
- ET is evapotranspiration
- GW is exchange with groundwater: >0 for seepage and <0 for groundwater recharge
- OL is incoming (<0) or outcoming (>0) overland flow
- ΔS is surface ponding.

The balance between rainfall and evapotranspiration is key to understand the hydrological behaviour of peatlands. Q results from the gradient between the river water level (boundary condition) and the groundwater level.

MIKE SHE allows adjustment of the different fluxes. The volume of precipitation is obtained from rainfall earth observation data. The parameters calibrated here were adjusted to better predict the volumes of evapotranspiration (ET), groundwater exchange (GW), overland flow (OL), and surface storage (ΔS).

3.1.4 Numerical Methods

The tool provides a flexible modelling framework where both physical based methods and simpler conceptual approaches could be used to simulate the various processes (see available methods Figure 3.2). The methods retained for the current study are described below.

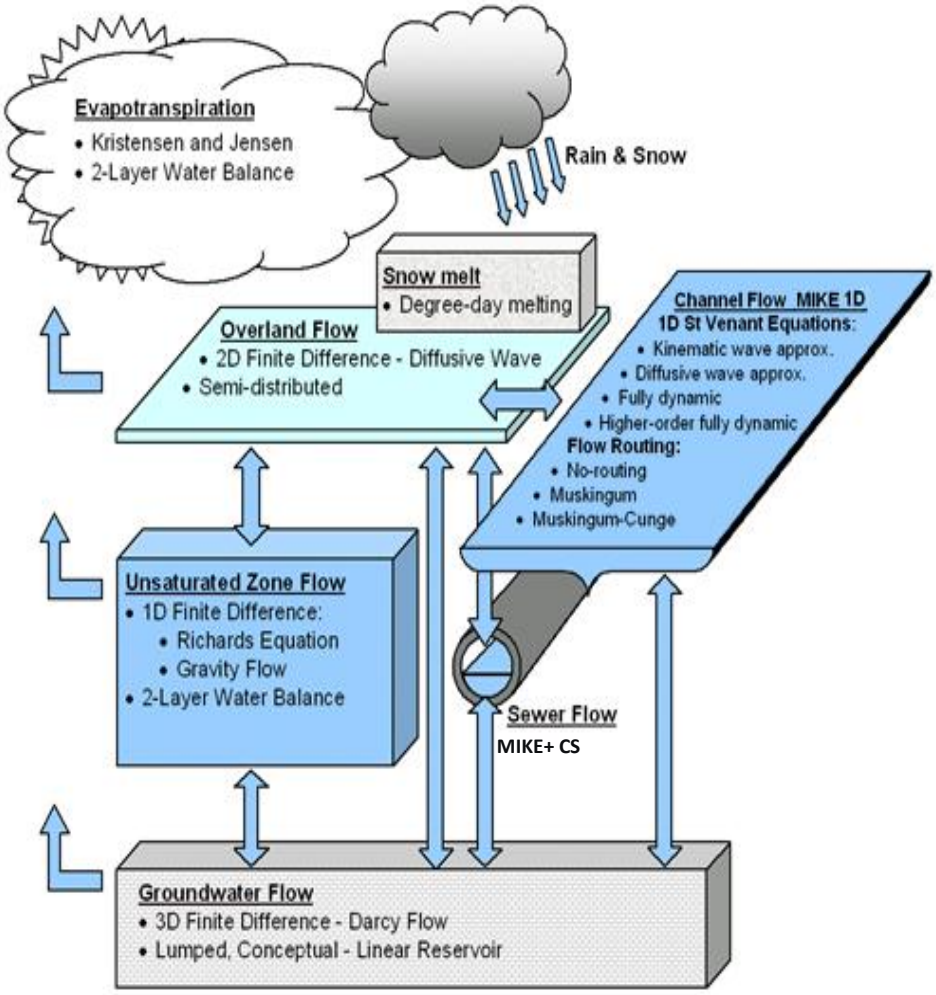

Figure 3.2 Overview of the numerical methods used to simulate the water cycle processes in MIKE SHE

Actual evapotranspiration is computed with the Kristensen and Jensen method, which is an empirical approach used to estimate actual evapotranspiration based on root water uptake, soil moisture status, and crop development, offering a simple and fast alternative to more physically based models.

Overland flow is simulated using the 2D finite difference method with the diffusive wave approximation, which includes bed friction, gravity, and hydrostatic pressure terms, assuming negligible inertial forces—suitable for modeling slow flood wave propagation and surface runoff over large areas.

Richards' equation models vertical unsaturated flow in the soil using a full capillarity-based approach, enabling detailed simulation of water content and fluxes, and is recommended for fine-textured soils or when high accuracy in moisture profiles is required.

In the saturated zone, groundwater flow is resolved using the 3D finite difference method based on Darcy's law, enabling detailed simulation of groundwater levels, flow, and interaction with surface water, particularly important for complex hydrogeological systems.

3.1.5 Generated outputs

Spatialized outputs are generated by the model for the entire simulation period. The most relevant outputs in this context include:

- Groundwater levels and depth of the groundwater table[2]
- Soil water content and saturation levels
- Key components of the water balance: actual evapotranspiration, infiltration to the saturated zone, overland flow, and lateral groundwater flow toward the boundaries of the model domain.

Groundwater levels and soil water contents are then used to estimate carbon dioxide dynamics (see section 4).

3.2 Model Development

3.2.1 Model domain and topography

Peatlands often develop into dome-shaped structures - known as peat domes - due to the accumulation of organic matter over centuries under consistently waterlogged, rainfall driven conditions. These domes are typically higher in the centre, where peat accumulation is greatest, and gently slope outward, creating a natural gradient that drives lateral water flow from the dome to its edges.

There is limited information on soil type, land use, topography, etc. in the peatlands, and especially limited information on spatial variations. For this reason, developing a georeferenced model of the peatlands is challenging. Instead, an “experimental” - non-georeferenced - model is developed, building on as much information as possible from the peatlands.

The model is set up as a rectangle with a length of 40.00 km and a width of 2.88 km (see Figure 3.3). The cell size is 80m x 80m, giving a length of 500 cells and a width of 36 cells. The rectangle represents a slice through a peat dome. For simplicity’s sake, it is assumed that the rectangle is aligned so the y-direction is South-North and the x-direction is West-East. The conceptual dome slice is located between two rivers to the west and east of the model. With this, both rain-fed peatlands in the center of the dome and river-fed peatlands on the edge of the dome can be simulated.

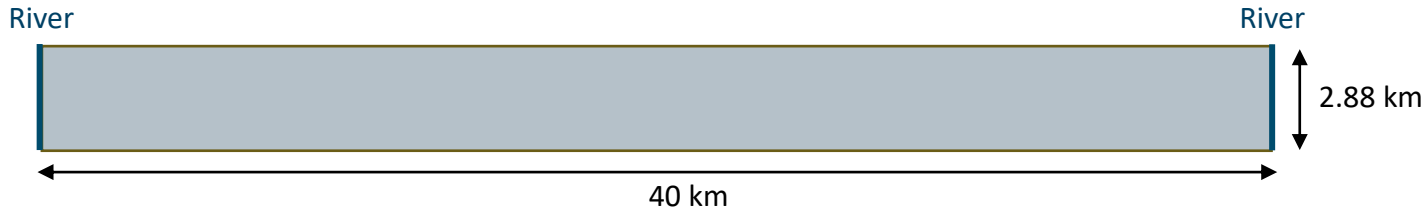

Figure 3.3 Conceptual model area

The model is set up for the period 2000-2019. The dome is assumed to be fully saturated at the start of the simulation, with an initial water level corresponding to the topography.

Topography measurements were made in the peatlands of the Cuvette Centrale by Dargie et al. (2017) and Crezee et al. (2022). Their findings indicate that peat domes in the Cuvette Centrale are extremely flat, with very low topographic gradients despite their large spatial extent. According to Crezee, these domes typically rise only 1 to 3 meters over tens of kilometres, creating a subtle convex profile that is nonetheless hydrologically significant. A very flat dome is thus modelled.

[2] Groundwater research in the Congo Basin remains limited, resulting in a scarcity of empirical data to support the validation of groundwater level simulations.

Based on the surrounding topography and water levels, a dome was created which had an elevation of 307 m at one end and 309 m at the other end. The dome reaches a maximum height of 3 m. The dome height is constant in the y-direction, thus representing a slice through the dome. The dome as seen from the side in shown in Figure 3.4. Slopes are higher at the edges of the dome.

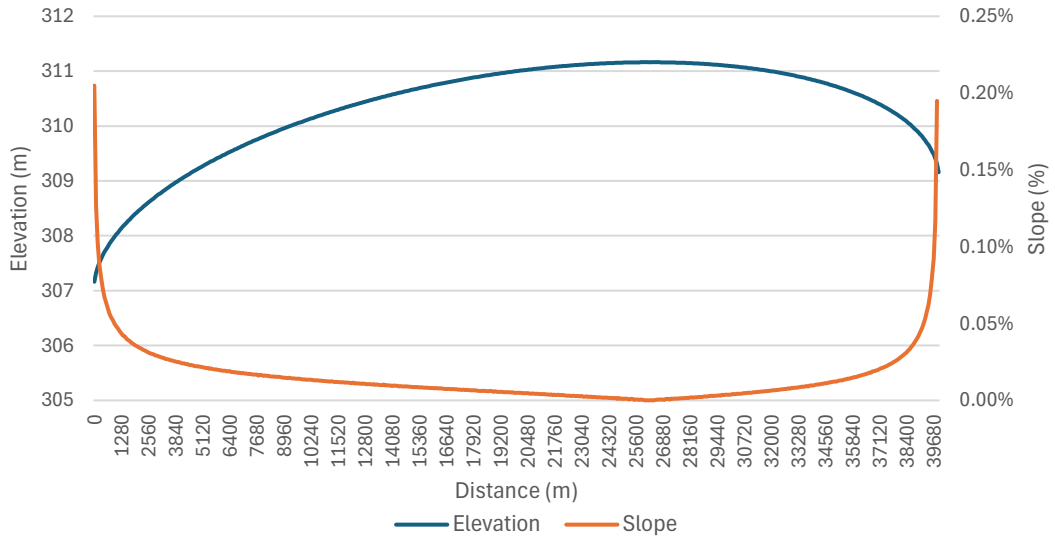

Figure 3.4 Representation of the dome seen from the side. The dome height is constant in the y-direction

3.2.2 Evapotranspiration

In MIKE SHE, actual evapotranspiration is calculated using the Kristensen and Jensen method. This approach relies on several physical parameters, including reference evapotranspiration, leaf area index (LAI) and root depth.

Reference evapotranspiration is computed using the Priestley-Taylor equation, which is a simplification of the widely known Penman-Monteith equation:

$$ET_0 = \alpha \cdot \frac{\Delta}{\Delta + \gamma} \cdot \frac{(R_n - G)}{\lambda}$$

Where:

- ET_0: Reference evapotranspiration
- α : Priestley–Taylor coefficient (typically ~1.26 under well-watered conditions)
- Δ: Slope of the saturation vapor pressure curve
- γ: Psychrometric constant
- R_n: Net radiation at the surface
- G: Soil heat flux (often negligible over daily scales)
- λ: Latent heat of vaporization

The net radiation is computed using the mean daily temperature, the minimum and maximum daily temperatures, the relative humidity and the latitude of the area. Temperature data are obtained from the ERA5 numerical weather model, and catchment average temperatures are calculated for the catchment shown in Figure 3.7 following the same procedure as for rainfall in section 3.2.2.

To better fit the observed water table levels, the reference evapotranspiration timeseries that was computed with the Priestley-Taylor method was then multiplied by 1.05 (see calibration section).

The LAI is derived from Earth observation datasets provided by Copernicus and MODIS and incorporates seasonal variation. A mean monthly value extracted for the extent of the Cuvette Centrale is used as input parameter in the model. The root depth is assumed to be constant at 1 meter.

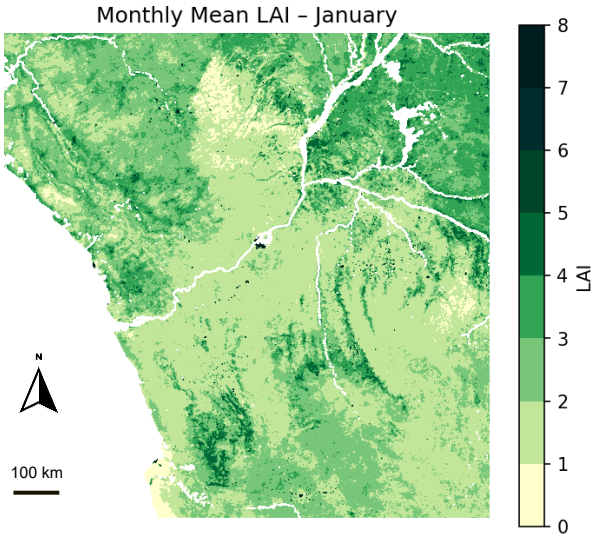

Figure 3.5 Monthly mean Leaf Area Index (LAI) in January between 2020 and 2024
Source: MODIS Earth Observation MYD15A2H Dataset

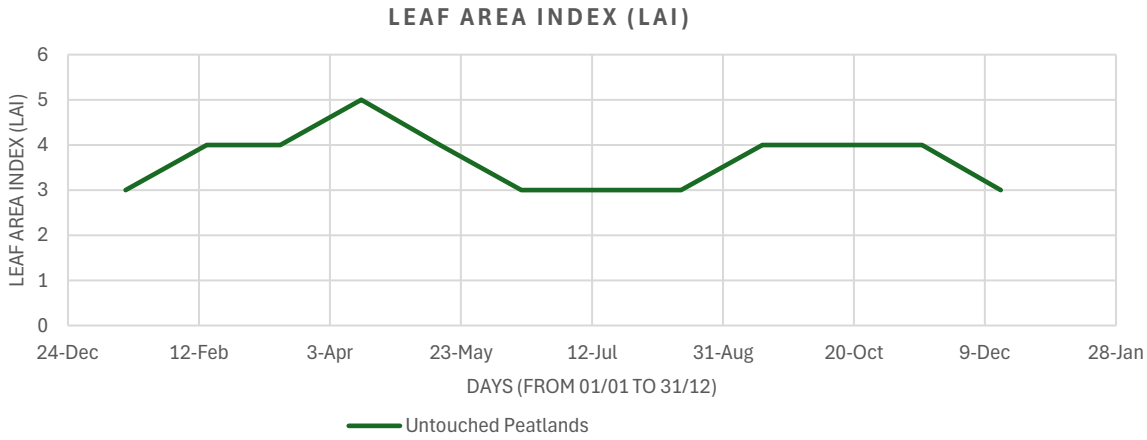

Figure 3.6 Annual variations of the Leaf Area Index (LAI) used in the model
Derived from the MODIS Earth Observation MYD15A2H Dataset

3.2.3 Rainfall

Daily rainfall time series are obtained from the ERA5 numerical weather model from ECWMF (European Center of Mid-range Forecast). ERA5 is a gridded product with a continuous period from 2nd of January 1981 to 10th of January 2025 when the data was processed. The gridded data is converted to a one-dimensional precipitation timeseries by calculating the catchment average rainfall for the sub-catchment in the peatlands shown in Figure 3.5. The sub-catchment is covering the Likouala Aux Herbes River drainage area and is considered representative.

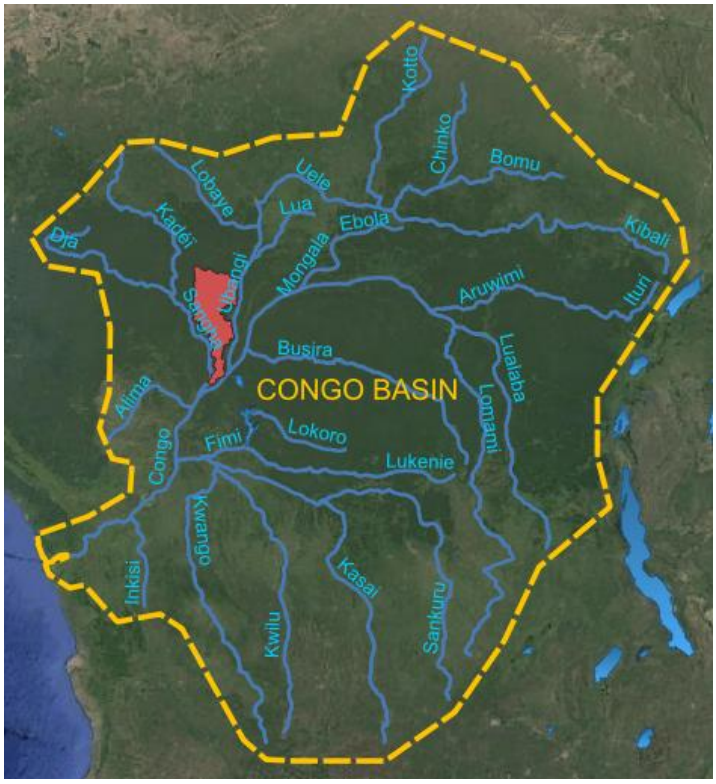

Figure 3.7 Representative sub-catchment (red) located in the Congo peat lands.

ERA5 provide a long continuous time series allowing to analyse how the climate has changed over the last 43 years. Figure 3.10 shows average annual daily rainfall together with reference evapotranspiration. Over the 43 years ERA5 shows a decline in precipitation and an increase in reference evapotranspiration from the top plot.

Monthly fluctuations of the daily precipitation and potential evapotranspiration are detailed Figure 3.8[3]. A bimodal seasonal rainfall pattern is distinguishable with two dry seasons and two wet seasons. Reference evapotranspiration varies less between months. Yearly climate timeseries are analysed for the period 1981-2024 (see Figure 3.9). An increasing trend is noticeable for reference evapotranspiration. There seems to be a decreasing trend for rainfall, which is coherent with recent scientific studies made in the Congo Basin (Sonwa et al., 2020; Cook et al., 2020). However, the trend appears to be less pronounced since 2000 (see Figure 3.10).

[3] Note: Validating these global datasets - given the many uncertainties of climate data representation in the cuvette centrale - is inherently challenging. Tapping into local knowledge to validate these global datasets could help mitigating. However, as reported under several studies, also local knowledge of data is ambiguous.

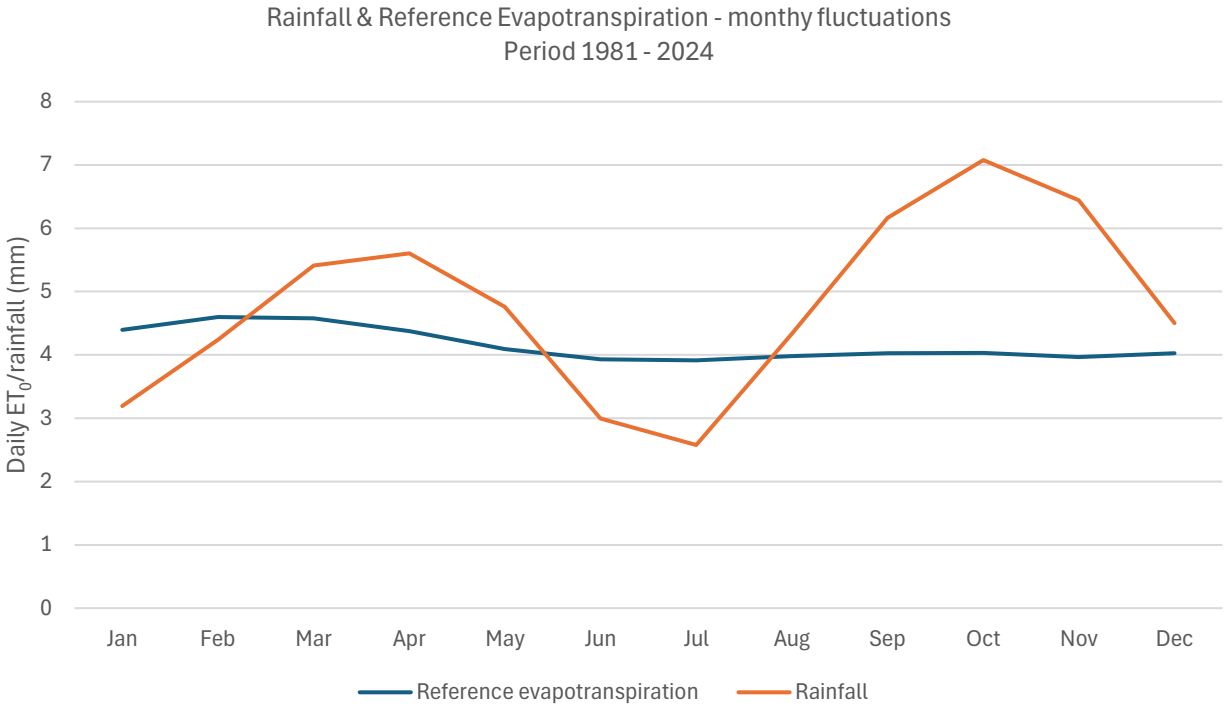

Figure 3.8 Monthly fluctuations of the daily rainfall and reference evapotranspiration for the period 1981-2024

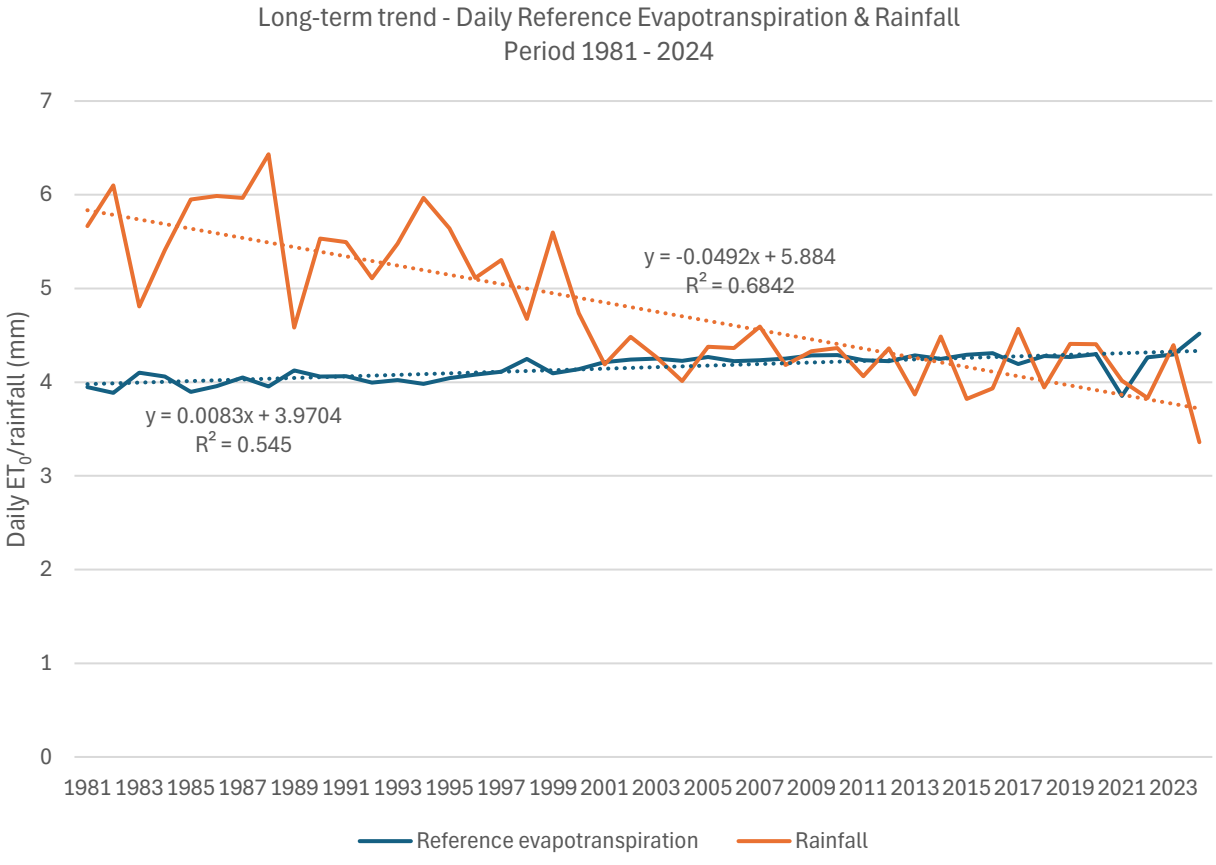

Figure 3.9 Long-term trends of the daily rainfall and reference evapotranspiration for the period 1981-2024

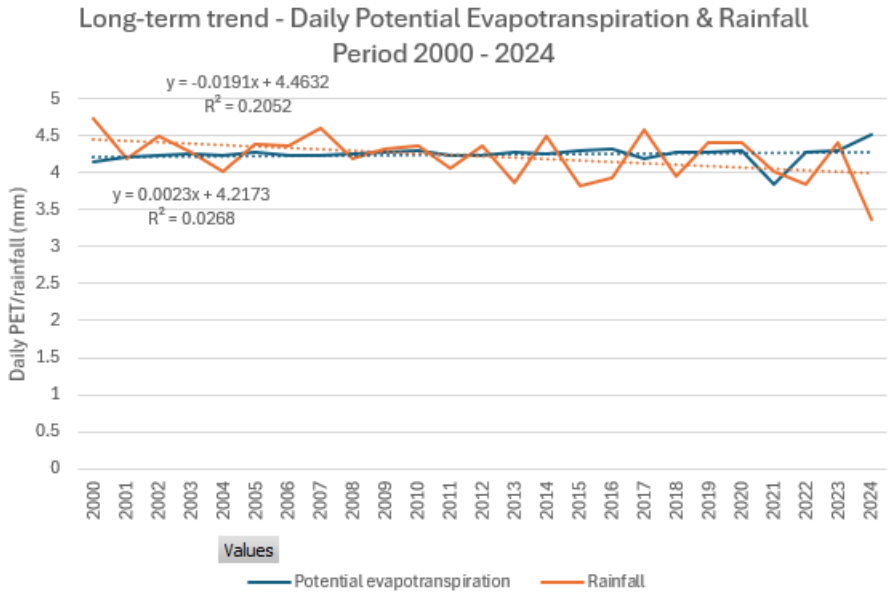

Figure 3.10 Yearly annual rainfall (orange) and reference evapotranspiration (blue) with linear trend lines

3.2.4 Unsaturated Zone

The infiltration to the unsaturated zone is modelled with the Richard's Equation. The equation requires the following parameters:

- Hydraulic conductivity at saturation (Ksat)
- Shape parameters of the conductivity curve (α, n, l)
- Saturated moisture content (θ_s)
- Residual moisture content (θ_r)
- Shape parameters of the retention curve (α, n)

No field measurements of these parameters were made in the Cuvette Centrale[4]. Thus, parameter values of other peatlands are used here. Apers et al. (2022) developed a tropical peatland model and used them to simulate peatland hydrology in the Cuvette Centrale. They chose the soil hydraulic properties based on a thorough literature review in tropical peatlands. The hydraulic conductivity at saturation used in the model was taken from this study. Other parameters, such as the shape parameters of the conductivity and retention curves were taken from a previous peatland model in Denmark and calibrated to better fit the situation of the Cuvette Centrale. Saturated and residual moisture contents (respectively 0.80 and 0.29) were also taken from the previous Danish peatland model but are coherent with Apers' estimates (0.88 and 0.3).

[4] It is recommended to plan for in-situ data collection in the future to improve the quality of the hydrological model.

Table 3-1 Parameters describing the soil properties used in the model setup

Parameter	Value
Hydraulic conductivity at saturation K_s (m/s)	6 x 10^{-5}
Shape parameters of the conductivity curve	α = 0.067 cm^{-1}
	n = 1.446
	l = 0.5
Saturated moisture content θ_s	0.80
Residual water content θ_r	0.29
Shape parameters of the retention curve	α = 0.2 cm^{-1}
	n = 1.813
Specific Yield* (θ_s-θ_{FC})	0.47

*where θ_{FC} is the water content at field capacity

The soil column is discretized vertically in 13 cells, with cell depth ranging from 5 cm in the uppermost grid points to 1 m in the bottom of the profile. This discretization allows to better represent the exchanges between surface and subsurface water.

3.2.5 Saturated Zone

The saturated zone is the essential model component because the peatlands are generally flooded and thus within the saturated zone. The saturated zone consists of a thick peat layer overlaying a clay base.

According to Dargie's measurements along transects in interfluvial peatlands of the Republic of Congo, peat in the area is in average 2.4 m deep with a maximum depth of 5.9 m. Crezee (2022) measured peat thickness along transects in the Democratic Republic of Congo (DRC) and found out that the average peat depth was slightly higher (3.3m), with peat depth reaching 7 m in one transect. An average peat depth of 3.3 m was thus taken in this model. The peat depth ranges between 1.15 m at the edges of the model to 4 m in the centre.

The 3D finite difference method based on Darcy's law requires the following parameters in MIKE SHE:

- Vertical and horizontal hydraulic conductivity (K)
- Specific Yield (S_y) (= porosity)
- Specific Storage (S_s)

The vertical hydraulic conductivity of peat is set at 10^{-5} m/s. This value is in the same order of magnitude as the hydraulic conductivity at saturation in the unsaturated zone derived from the article of Apers et al (6 x 10^{-5} m/s). However, it is slightly lower to account for the peat compression with depth. Peat tends to accumulate in horizontal layers which makes it anisotropic with a higher conductivity in the horizontal x and y-directions than in the vertical z-direction. A higher horizontal conductivity is thus taken here. The parameter values are detailed in the Table 3-2. The hydraulic properties of clay are taken from previous projects.

Table 3-2 Physical properties of the saturated zone

Parameter	Peat	Clay
Vertical Hydraulic conductivity K_v (m/s)	10^{-5}	10^{-7}
Horizontal Hydraulic conductivity K_h (m/s)	10^{-4}	5 x 10^{-6}
Specific Yield S_y	0.47	0.15
Specific Storage S_s	0.001	0.004

3.2.6 Overland Flow

Overland flow is simulated using the 2D finite difference method with the diffusive wave approximation. One parameter governing surface runoff velocity is the Manning-Strickler coefficient, which varies

according to land use. The lower the coefficient value, the rougher the area and the slower the runoff. A roughness coefficient of 10 $m^{1/3}/s$ is used in this study.

Another parameter used to set up the overland flow component of a MIKE SHE model is detention storage. It is used to limit the amount of water that can flow over the ground surface. The depth of ponded water must exceed the detention storage before water will flow as sheet flow to the adjacent cell. For example, if the detention storage is set equal to 2 mm, then the depth of water on the surface must exceed 2 mm before it will be able to flow as overland flow. This is equivalent to the trapping of surface water in small ponds or depressions within a grid cell.

The ground surface in tropical peatland forests has microforms: elevated surface areas called hummocks and depressions called hollows. This microtopography affects lateral discharge as water is stored in hollows before flowing laterally. Lampela et al. (2016) studied the microtopography in natural tropical peatlands in Indonesia and found that the surface elevation measurements can be approximated by a zero-mean normal distribution with a standard deviation σ of 16 cm. For a normal distribution, the mean absolute error (MAE) can be approximated in the following way:

$$MAE \approx \sigma \times \sqrt{\frac{2}{\pi}} \approx 13\ cm$$

Where σ is the sample's standard deviation

The detention storage value is thus taken as 13/2 = 6.5 cm.

3.2.7 Boundary Conditions

The northern and southern boundary conditions of the dome are no-flow boundaries. It is assumed that water flows to or from the rivers on either side of the dome and that there is negligible flow in the y-direction.

In the rainfall driven configuration, the western and eastern boundaries have a constant head set at surface level.

In the river-fed scenario, time-varying water level timeseries are used for the western and eastern boundaries of the peat dome model. These time series are derived from the Database for Hydrological Time Series of Inland Waters (DAHITI), developed by the German Geodetic Research Institute (see Schwatke et al., 2015). The database compiles satellite altimetry measurements from multiple missions since 1985.

Virtual altimetry stations are available in the Cuvette Centrale, including along the Likouala, Sangha, Likouala aux Herbes, and Oubangui rivers in the Republic of Congo (RoC), and the Congo, Ngiri, Lulonga, and Ruki rivers as well as Lake Tumba in the Democratic Republic of Congo (DRC). Based on data availability for the 2012–2019 simulation period, stations were selected in the lower reaches of the Likouala aux Herbes, Oubangui, and Ngiri rivers. The locations of these stations and their data coverage are shown in **Error! Reference source not found.**. While all selected stations provide c ontinuous coverage for 2016–2019, coverage is more limited during 2012–2015, with only one station providing data along each of the three selected rivers.

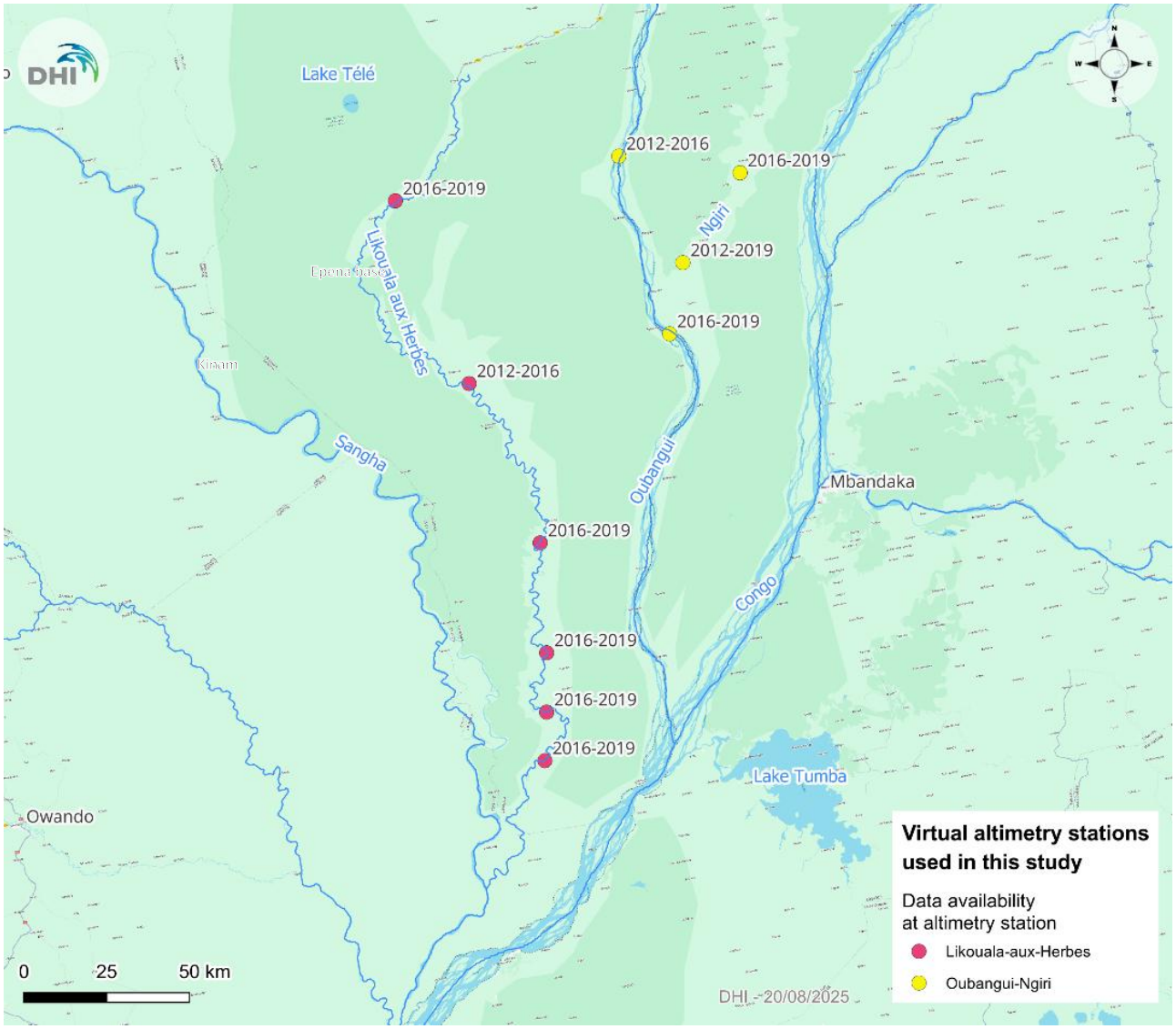

Figure 3.11 Location of the selected altimetry stations and data coverage periods during the 2012-2019 simulation period

Data is averaged over two clusters and used to define the model boundaries: Stations along the Likouala-aux-Herbes River are used for the western boundary, while those along the Oubangui and Ngiri rivers are used for the eastern boundary. The averaged time series are then smoothed using a Gaussian filter. For 2012, when no data are available from the Likouala-aux-Herbes cluster, data from the Oubangui–Ngiri cluster are applied to both clusters.

Water levels in both groups are adjusted so that their mean values over the simulation period match the ground elevation at the respective boundary. In this way, the mean boundary water levels are consistent across the rain-fed and river-fed configurations. The time series of boundary water levels for the simulation period are shown in Figure 3.12. The average annual amplitude between maximum and minimum water levels is slightly higher in the Oubangui–Ngiri cluster (3.8 m) than in the Likouala-aux-Herbes cluster (3.55 m).

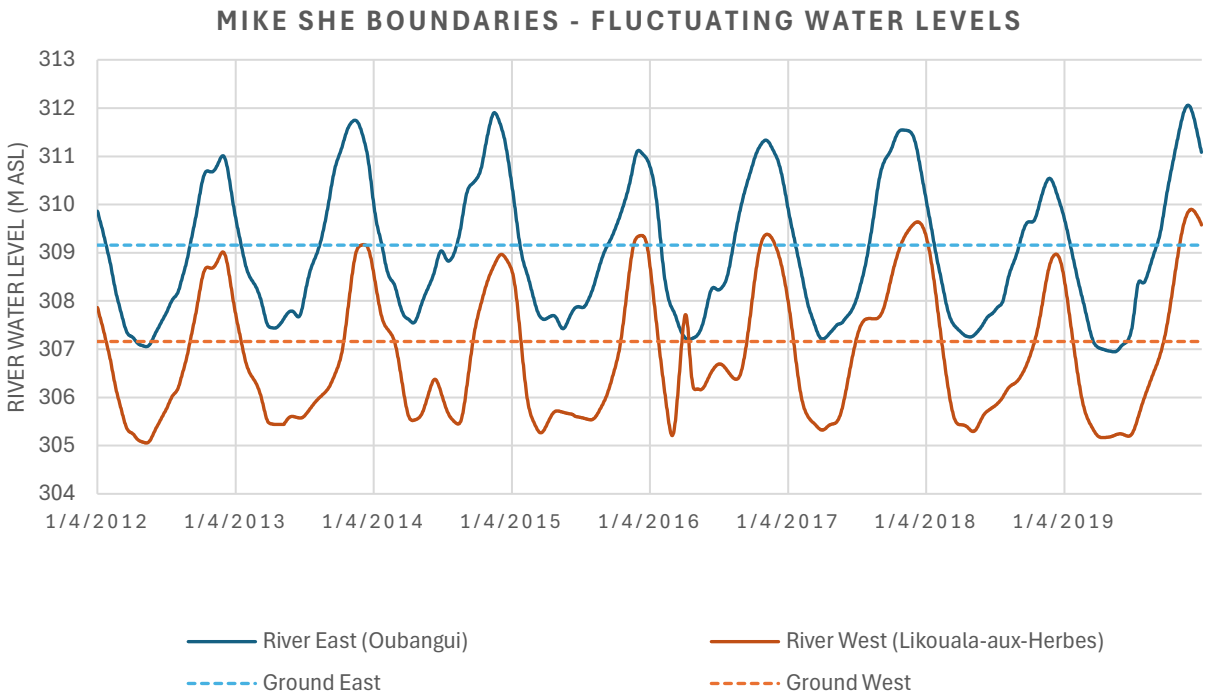

Figure 3.12 Fluctuating water levels used as model boundaries

Weather and hydrometric data measurements have been carried out at the Epena base, located in the upper reaches of the Likouala aux Herbes River. These data were recently published and analysed in a joint report by the Réserve Communautaire du Lac Télé and the Wildlife Conservation Society[5]. Water levels measured at Epena between 2016 and 2017 are compared in **Error! Reference source not found.** with the average water levels of the Likouala aux Herbes cluster.

Both datasets show a similar amplitude of 4-5 m between low and high levels. While the overall water level trends are comparable, the timeseries obtained from earth observation display a lag of 1-2 months compared to the field measurements. This lag is expected, as the satellite-derived values are computed as averages from virtual stations located downstream of Epena (see station locations in Figure 3.11). This concise analysis at Epena suggests that the earth observation approach provides reliable estimates of river water levels.

[5] Romani, T., & Ossere, J. (2025, avril). Rapport d'expertise – Météo (température et pluie) et hauteur d'eau de la rivière Likouala aux Herbes à la Base d'Epena (2000-2023) (Version 1). Ministère de l'Économie Forestière; Réserve Communautaire du Lac Télé; Wildlife Conservation Society.

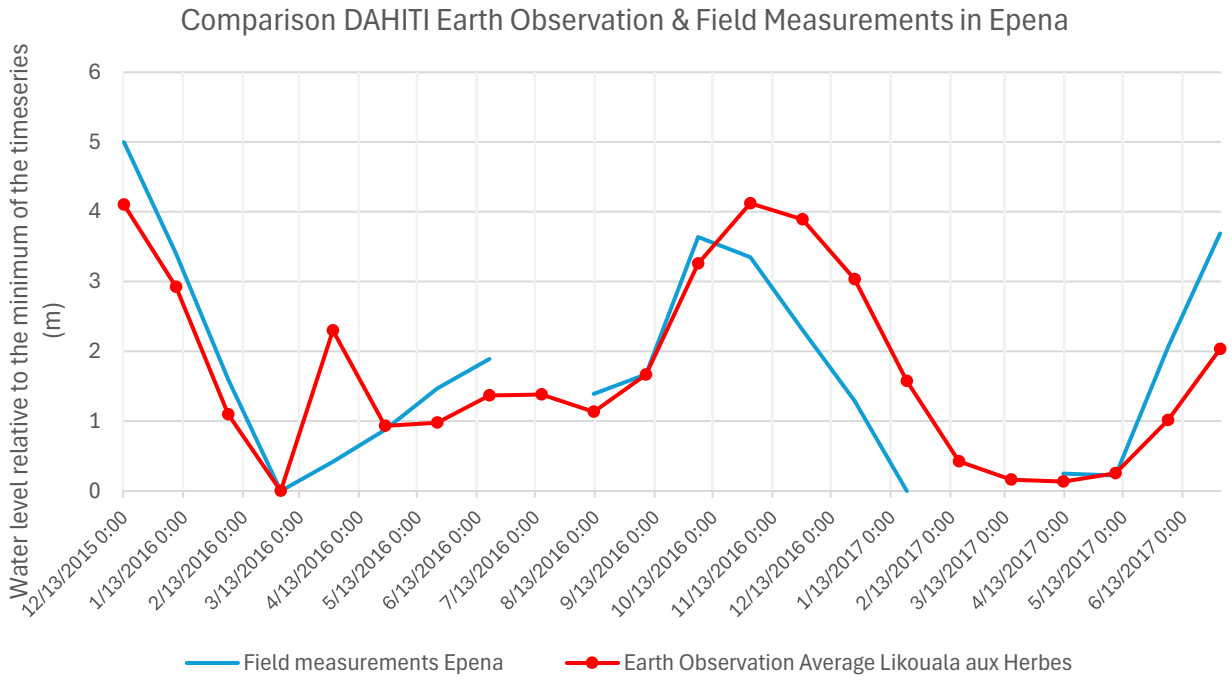

Figure 3.13 Comparison between water levels obtained from earth observation and field measurements in Epena

3.3 Model Calibration and Results

Calibration involves ensuring that models accurately reflect the hydrology of the peatlands. The various model parameters are adjusted by comparing the model results with measurements from literature.

There are a few water table measurements for the area to calibrate the hydrological model. Dargie et al. (2017) measured the depth of the water table along several transects in interfluvial peatlands of the Republic of Congo. Crezee et al. (2022) took water table measurements along transects in interfluvial and river-influenced peatlands of the Democratic Republic of Congo (DRC).

Since the hydrological model is conceptual in nature, attempting to match its simulated outputs to an observed timeseries at a given location would be misguided. The purpose of calibrating the model here is rather to accurately reproduce the average water table level and its seasonal fluctuations.

3.3.1 Calibration Data

Water table depth measurements were made by Dargie et al. along several transects in the Congolese Cuvette Centrale (see Figure 3.14). There are common patterns between the transects. Water table is low between March and June and high between September and December. The water table remains above ground for several months in a row: the forest is flooded. During the 2013-2014 period, the average water table is roughly at surface level.

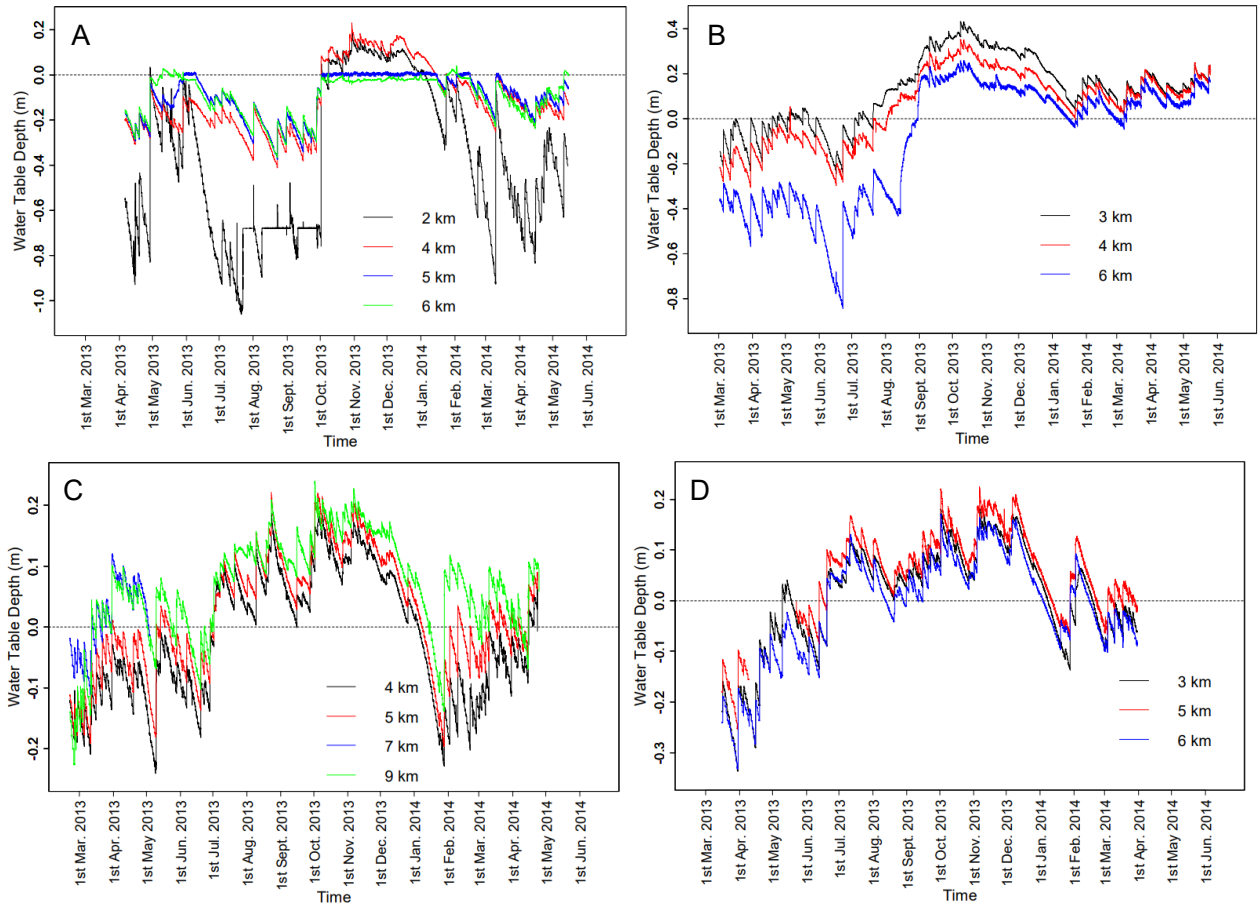

Figure 3.14 Time series of water table levels along the A) Bondoki B) Bondzale C) Ekolongouma and D) Itanga interfluvial transects. Distances from the river located at the beginning of each transect are indicated. The black timeseries in transect A isn't in peatland but in a seasonally flooded forest.
Source: Dargie et al., 2015

Crezee (2022) took water table depth measurements along several transects in DRC peatlands in 2018-2019 (see Figure 3.15). The two transects differ because Lokolama has much less river impact than Ikelemba. The water table is low between June and August 2019 and high in 2018 and late 2019. The average water table depth is between 0 and -20 cm depending on the point on the transect.

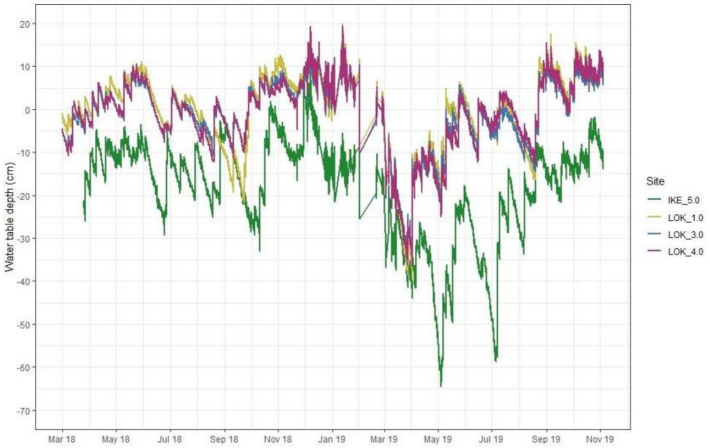

Figure 3.15 Time series of water table levels along the Lokolama and Ikelemba transects. Distances from the river located at the beginning of each transect are indicated.
Source: Crezee, 2022

3.3.2 Water Table Depth – Rain-fed scenario

Water table depths for a transect along the x-axis are displayed Figure 3.16 for the period 2012-2019. Water level timeseries are similar between the rain-fed and river-fed scenarios for the 10 km and 25 km points. Regarding the point located 2 km away from the western boundary, only the results of the rain-fed model are included.

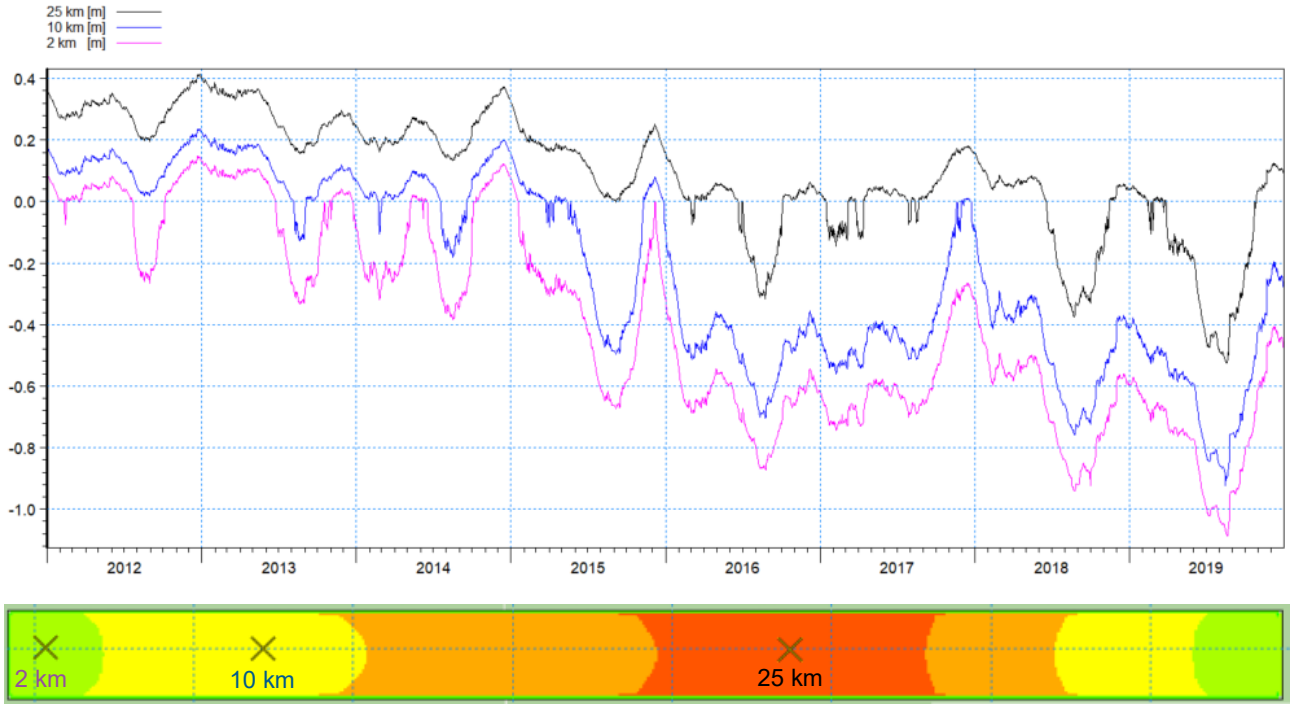

Figure 3.16 Simulated water table depth along a transect in the x-direction. Distances from the river located at the beginning of the transect are indicated.

The water table depth gradually decreases at all points throughout the simulation period. This drying trend can be explained by the concomitant increase in temperature and thus reference evapotranspiration and decrease in rainfall (see section 3.2.2). Seasonal fluctuations are clearly noticeable: the water table is high during the wet season (September to November, March to May) and low during the dry season. Due to the specific yield characteristics of peat, where water table rise depends on the peat's pore space and hydraulic conductivity, a given amount of rainfall will cause greater changes in the water table below the peat surface than above it. This explains why water table shifts are more important below ground than above ground.

In the model, water table depth decreases with distance from the river. This is due to increased lateral groundwater flow to the river in the peripheral steep areas (see slope profile Figure 3.4). Mean water table levels relative to surface and surface elevation are superimposed in

Figure **3.17**. The water table depths drop at the edges of the model as the water table depth is set to 0 at the west and east boundaries.

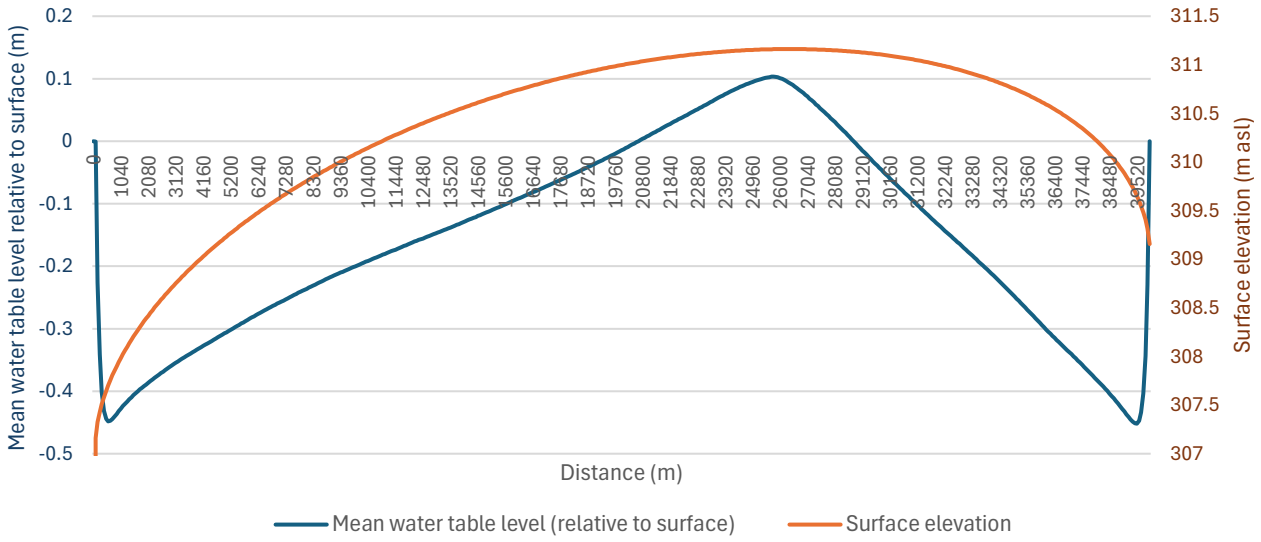

Figure 3.17 Mean groundwater table depth and level along the length of the dome slice.

The fluctuations of the simulated water levels during the period 2013-2014 differ from the water measurements taken by Dargie (Figure 3.14). Indeed, Dargie's measurements show a gradual increase in the groundwater table in 2013 followed in 2014 by a gradual decrease. Simulated timeseries are characterized by a decrease in 2014 followed by two peaks in late 2013 and early 2014. Simulated mean water levels are in the same range as observed values within a distance between 0 and 10 km from the river.

In 2018-2019, the simulated water table depths have similar trends in the simulated and observed timeseries. Both timeseries show an important drop between March and August and peaks in late 2018 and late 2019. The water table levels are in average higher in the measurements than in the simulation. This better alignment with results in 2018-2019 than in 2013-2014 could stem from the location of the precipitation data used in this study. Indeed, data was extracted from a point located in the Democratic Republic of Congo South of the Equator. Precipitation patterns there show a major dry season between June and August and a minor dry season in December-January. This contrasts with the area of the Cuvette Centrale located North of the Equator, where the major dry season happens in December-January and the minor dry season between June and August.

3.3.3 Water Table Depth – River-fed scenario

Water levels at the peat dome centre and near the western boundary are shown in Figure 3.18. The results indicate that the Likouala aux Herbes River seasonally floods the lower areas of the peatland (upper graphs). This additional inflow produces a sustained rise in the water table compared to the baseline rainfall driven scenario. In the rainfall driven baseline, several successive dry years create an imbalance in the water budget and cause the water table to gradually decline over the simulation period. This downward trend does not occur in the river-fed scenario, where the aquifer is replenished by seasonal floods. Near the boundary, the water table remains above ground most of the time, except during the dry season (upper left).

Low river levels appear to affect the water table only in the first two cells near the boundary, where it drops below the rainfall driven baseline during some dry years (upper left). No additional drops in the water table due to low river levels are observed three cells away from the boundary (upper right).

The lower-left graph shows the water table in a cell located 4 km from the boundary at an elevation of 309 m. Although river levels regularly exceed 309 m, the cell did not flood until late 2017. This is because overland flow is not instantaneous; it depends on ground roughness and detention storage. In MIKE SHE, overland flow into a neighbouring cell occurs only when the ponded water depth exceeds

the detention storage value, i.e. 65 mm in the baseline scenario. This explains why the water table diverges from the rainfall driven baseline only in 2017, after an extended period of flooding at the boundary. Once a cell is flooded, the water table consistently remains above the rainfall driven baseline, even when river levels drop.

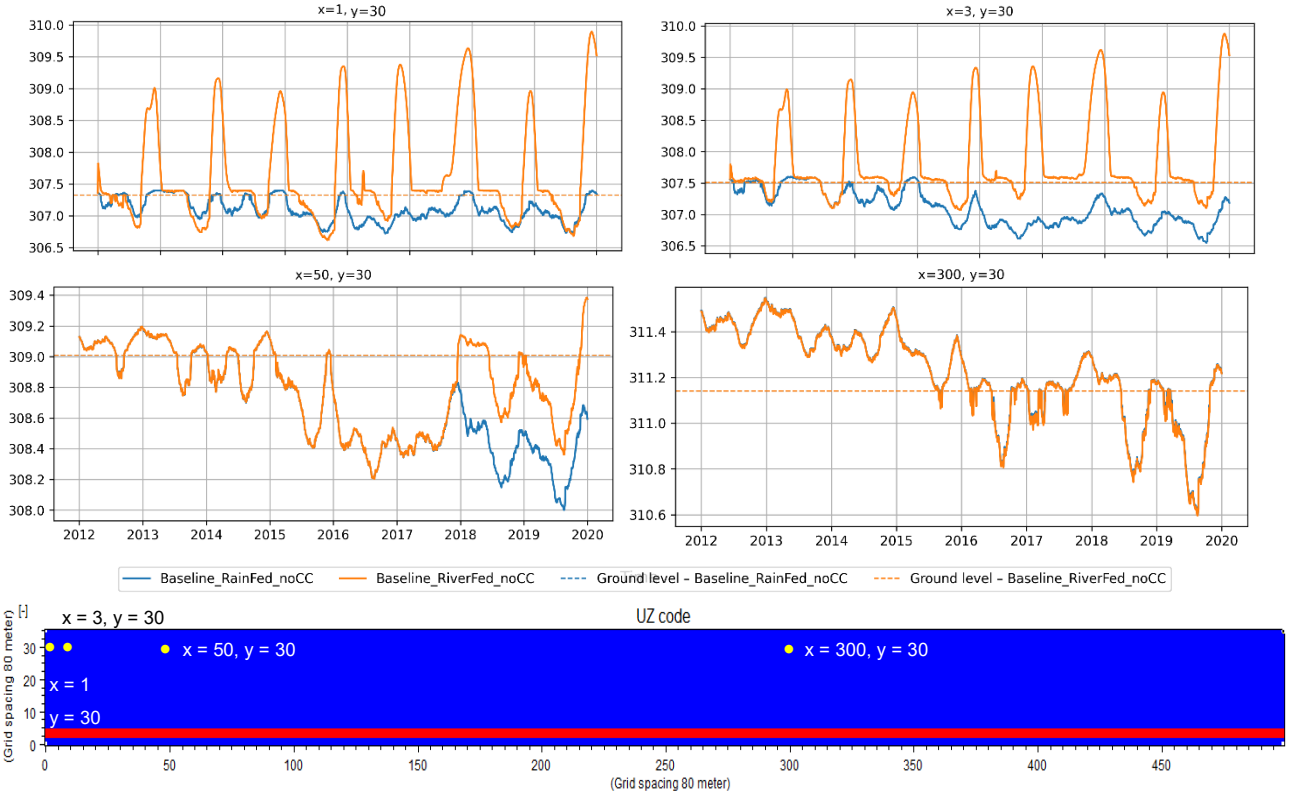

Figure 3.18 Water levels at three given locations within the model area¸ Scenario A.1.2 (Baseline_RiverFed_noCC)

Overland water depths in the boundary zones gradually rise throughout the simulation period. These depths are compared in Figure 3.19 for two river flooding events: one at the beginning of the simulation in 2012 (top) and another at the end in 2019 (bottom). At the peak of the first annual flood in 2012, the inundated area extends 2.2 km inland in the west and 2.6 km in the east, covering 12% of the peat dome. By contrast, during the 2019 flood, the simulated inundated area extends 4.2 km inland in the west and 6.3 km in the east, covering a quarter of the peat dome.

As river inflows replenish the unsaturated zone, the flooded area gradually expands from year to year. The simulation period considered here is not long enough to determine whether the flooded area will eventually reach equilibrium. Within the current period, the water table at the centre of the peat dome is not affected by river flooding (see lower right graph in Figure 3.19). However, the entire dome could eventually be influenced by river flooding, since Oubangui River levels regularly exceed the elevation of the dome peak. To generate the initial water levels for this simulation, the rainfall driven baseline model was run from 2000 to 2012. As a result, the peatland is likely drier than it should be at the start of the simulation and gradually reaches equilibrium over time. However, since the initial conditions are the same for all interventions, the results can be directly compared with the river-fed baseline scenario.

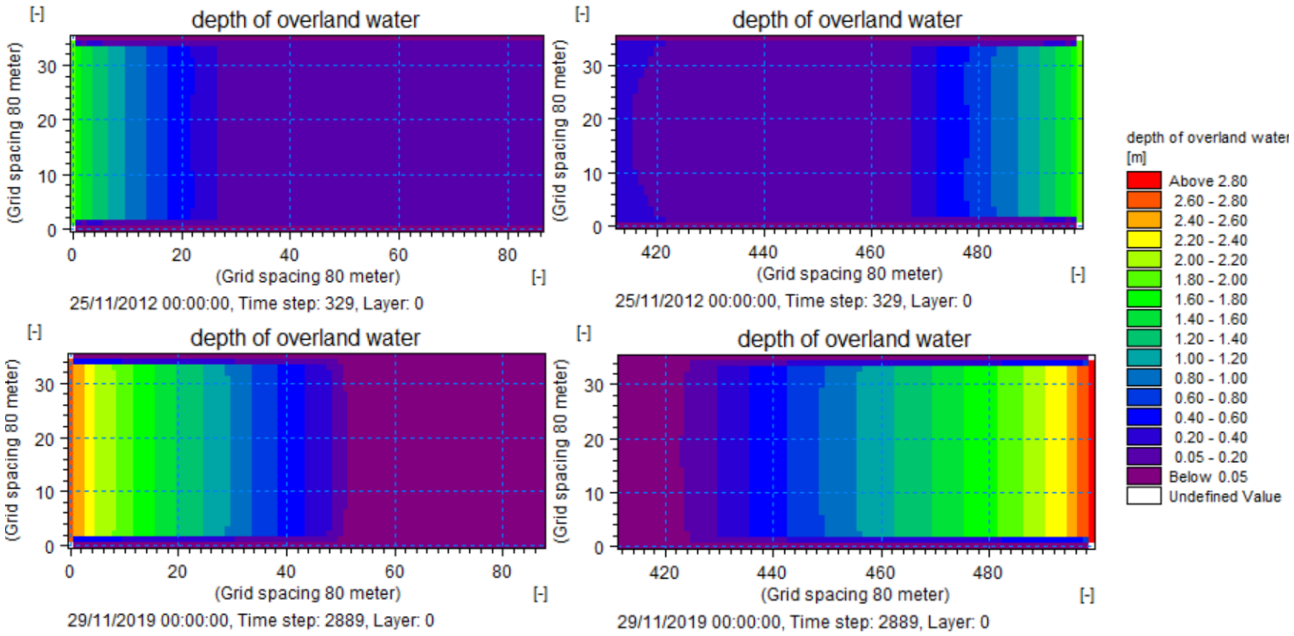

Figure 3.19 Overland water depths in the boundary zones of the model at the peak of two river flood events

3.3.4 Water Balance

The various components of the total water balance during the simulation period are represented in Figure 3.20 for the baseline rain-fed scenario. Evapotranspiration slightly exceeds precipitation (+2%) and the volume stored in the saturated zone decreases, which is coherent giving the drying trend in the Congo Basin. Boundary flows are very small compared to the total precipitated amount. This stems from the very flat topography of the dome, which prevents important overland flow. Inflow from the river to the saturated zone is also very small, which highlights that the simulated peatland is rainfall driven.

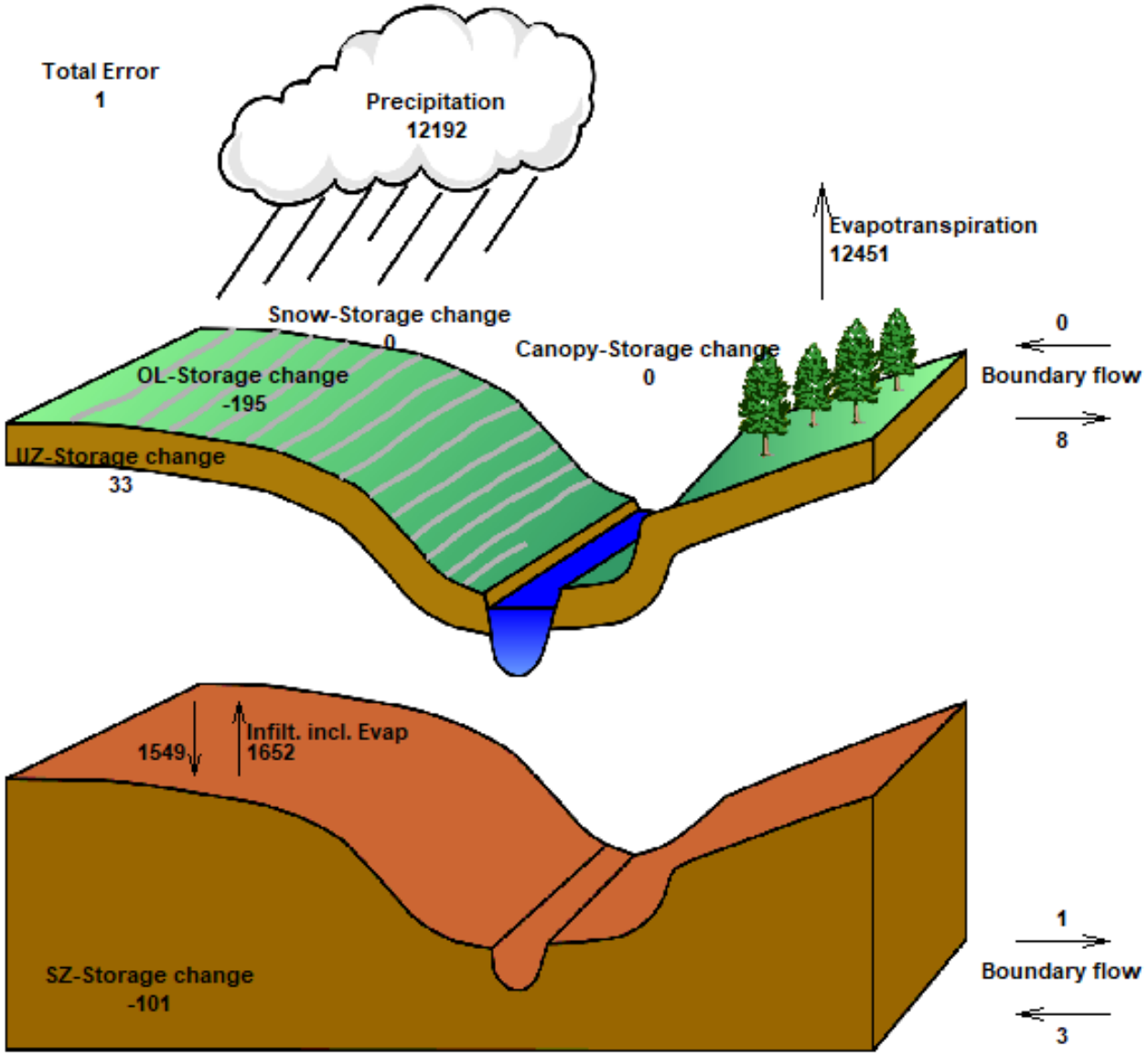

Figure 3.20 Water Balance
Period 2012-2019

3.3.5 Calibration Runs and Sensitivity Analysis

The model parameters were adjusted to better represent physical reality and better reproduce the observations (see Table 3-3). The calibrated parameters are explained in detail in the previous sections.

Table 3-3 Calibrated parameters

Parameter	Initial value	Calibrated value / relative change	Comment
Evapotranspiration			
Reference Evapotranspiration		+ 5%	Decrease in the water table level
Leaf Area Index	7	Fluctuating before 3 and 5 (MODIS dataset)	Better representation of seasonal fluctuations
Root Depth	250 mm	1000 mm	More accurate for a forest
Unsaturated Zone			
Hydraulic conductivity at saturation K_s	2 x 10^{-6} m/s	6 x 10^{-5} m/s	See Apers et al.
α shape parameter of the retention curve	0.12	0.2	Decreases water table fluctuations below ground
Saturated Zone			
Vertical Hydraulic conductivity K_v	10^{-4} m/s in the first meter below ground, 10^{-6} m/s below	10^{-5} m/s	Simplification + Coherence with the Unsaturated Zone
Horizontal Hydraulic conductivity K_h	10^{-3} m/s in the first meter below ground, 5x10^{-5} m/s below	10^{-4} m/s	Simplification + Coherence with the Unsaturated Zone

The calibration runs provided a better understanding of the sensitivity of the various parameters. Reference Evapotranspiration is a key driver of the mean water table depth. Small increases in reference evapotranspiration lead to rapid decreases of the water table level. In contrast, changes in the actual evapotranspiration parameters such as root depth and LAI have very little impacts on the water table. Indeed, the leaf area and root depth are high enough that they don't constrain actual evapotranspiration, which equals the reference evapotranspiration.

The sensitivity to the hydraulic conductivity at saturation of the unsaturated zone (K_{sat}) was also examined. Lower Ksat values caused a delay in the water table response, due to reduced vertical water movement. Higher Ksat values resulted in no significant changes, indicating that beyond a certain threshold, Ksat is not a limiting factor in the system's response.

An alternative soil water retention curve with a lower specific yield was implemented using parameterization from Apert et al. This modification led to notably lower water tables during dry periods, as the soil drained more rapidly. Another simulation with higher specific yields resulted in lower fluctuations below ground, which matched better the field observations from Dargie and Crezee.

3.4 Conclusion

A conceptual hydrological model was developed using MIKE SHE to describe the water cycle in the peatlands of the Cuvette Centrale. The model reproduces a slice of an interfluvial peat dome. All major hydrological processes are simulated: precipitation and interception by the canopy, evapotranspiration, infiltration through the unsaturated zone, groundwater and overland flow.

The model is setup for the period 2000-2020. Simulated water table levels are compared with observations made during two measurements campaigns as documented in literature, one in 2013-2014 in peatlands of the Republic of Congo and one in 2018-2019 in the Democratic Republic of Congo. Given the scarcity of measurements and the fact that the conceptual hydrological model isn't developed for a specific location, it wasn't possible to carry out a complete calibration of the model parameters against observed data. However, the model results are considered satisfactory for the following reasons:

- Like in most measurement locations, simulated mean water levels range between 0 and -20 cm in most of the model area.
- Water levels vary spatially with increasing distance from the river.
- The water table fluctuates seasonally according to the rainfall patterns. Seasonal trends are the same as in the measurements made by Crezee in the Democratic Republic of Congo.

Accurately estimating water table levels is key as those levels determine the carbon dynamics in the peatland. The carbon stock in the soil gets mostly depleted under oxic conditions, i.e. in the soil zone located above the groundwater level. Peat decays slowly under fully anoxic conditions when the whole soil column is saturated. The biodegradation and carbon dynamics model developed as part of this project uses groundwater table level and soil saturation data to estimate the carbon budget. This method is explained in the next chapter.

4 Biodegradation Model

To simulate carbon accumulation and biodegradation in the peatlands of the Cuvette Centrale, a model is developed following by large the modelling approach used in DigiBog as described in the two papers written by the authors behind DigiBog (Young et al., 2017) and (Young et al., 2023). The peat domes in the Congo peatlands form part of wetlands with general slow degradation under mainly anoxic conditions. When the peat becomes exposed to oxic conditions the rate of degradation can increase dramatically. To model the exposure, we use the distributed hydrological model result described in section 3, and estimate the oxic depth from modelled soil saturation in the peat dome. The hydraulic model is spatially distributed in the horizontal plane (x and y) and vertically (depth from surface) to give a full spatial representation of the soil saturation in the peat dome.

We consider soil conditions oxic at air-filled porosity above 10% and use this as a proxy for the depth of aerobic decomposition in the soil profile. For each cell in the horizontal plane, we estimate the depth of oxic degradation in the soil profile by calculating the time evolution of the maximum depth where air-filled porosity is at or above 10%.

The peat degradation is estimated using a dual exponential decay function to represent a rapid initial phase dominated by the breakdown of labile compounds, followed by a slower phase involving more recalcitrant materials:

$$M(t+1) = M_1(t) \cdot e^{\{-k_1 \cdot f_Q \cdot dt\}} + M_2(t) \cdot e^{\{-k_2 \cdot f_Q \cdot dt\}} \quad (1)$$

Where M(t) is total remaining mass of organic material at time t, M_1 and M_2 is initial amount of labile and recalcitrant material and k_1 and k_2 decay rate constants for labile fraction and recalcitrant fraction. f_Q is temperature modification factor representing an increase in degradation rate with increasing temperature:

$$f_Q = Q_{10}^{\left(\frac{t-tbc}{10}\right)} \quad (2)$$

Where Q10 is the temperature sensitivity, t is the mean temperature and tbc is the baseline reference temperature. In (Young et al., 2017) t is a weekly mean temperature but, in this study, t is the average temperature over the simulation period, resulting in a constant adjustment of the degradation rate compared to the baseline period where we assume the degradation rate was measured. Setting t to tbc removes sensitivity to temperature from the equation. t is adjusted under climate change scenarios (see section 5.2).

Sensitivity to soil saturation could also be included similarly to temperature sensitivity as a modification to the degradation rate but it would be difficult to estimate the parameters, and we consider either oxic or anoxic degradation depending on the 10% threshold of air-filled porosity.

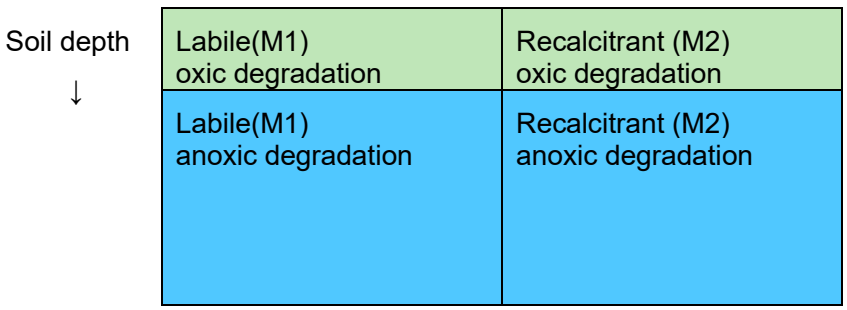

Figure 4.1 Illustration of decomposition of vertically integrated soil profile into Labile (M1) and Recalcitrant (M2) material and oxic and anoxic degradation with soil depth.

Figure 4.1 illustrates the decomposition of the soil in the vertically integrated soil profile into 4 peat masses. Labile and Recalcitrant material is accounted for separately and degradation is calculated

using the dual exponential decay function. We furthermore calculate the fraction between oxic and anoxic soil depths at each time step because both labile and recalcitrant material degrade at different speed under oxic and anoxic conditions which gives a total of 4 different degradation rates and masses as illustrated in the figure. At each timestep the labile and recalcitrant material is individually split into oxic and anoxic decomposition with different degradation rates. For the labile material we assume that oxic depth lower than root zone depth means all labile material is degrading under oxic conditions instead of considering labile material fully mixed in the entire soil profile.

The current model does not consider changes to peat depth due to degradation of peat which can cause alteration to the drainage of the peat-dome rather it is decoupled from the hydrological model and is a post computational step after the hydrological simulation.

The model includes a simple method to compute carbon accumulation. Litter material generated by plant growth is computed by adding a constant fraction of new material to the peat once per year divided into leaves, wood and roots. The composition for each litter type into labile and recalcitrant material is also defined.

Multiple plant functional types can be defined as input parameters and used in the simulation of peat degradation and accumulation.

4.1 Accumulation and Bio Degradation Parameters

The input parameters to the bio degradation and accumulation are presented in Table 4-1, “ParameterID” is the name of the parameter, and “Parameter_description” has a short description. We use two plant functional types (PFT) namely Palm trees (“Palm_PFT”) and hardwood (“Hardwood_PFT”) with 50% of the litter production assigned to each as seen in the parameter “plant_type_prop”. Parameters used in the model are the same as in (Young et al., 2023) where parameters were measured from oxic and anoxic peat samples taken in a peat dome in the Congo peatlands. The column “Parameter_type” shows the different types of parameters. The litter types leaves, wood and roots are assigned separate oxic and anoxic degradation rates for their respective labile and recalcitrant parts. As the study (Young et al., 2023) found that recalcitrant material decomposed at much the same rate as labile material once exposed to oxic conditions we assign the same decay rate to labile and recalcitrant material under oxic conditions.

Table 4-1 Input parameters for the bio. degradation model.

Parameter_type	Parameter_desciption	ParameterID	Palm_PFT	Hardwood_PFT	Units
Oxic decay (labile and recalcitrant litter pools)	Leaves oxic decay: labile and recalcitrant	decay_oxic_leaves	0.180000	0.280000	prop. year−1
Oxic decay (labile and recalcitrant litter pools)	Wood oxic decay: labile and recalcitrant	decay_oxic_wood	0.390000	0.200000	prop. year−1
Oxic decay (labile and recalcitrant litter pools)	Roots oxic decay: labile and recalcitrant	decay_oxic_roots	0.350000	0.260000	prop. year−1
Anoxic decay (labile litter pool)	Leaves anoxic decay: labile	decay_anoxic_labile_leaves	0.050000	0.080000	prop. year−1
Anoxic decay (labile litter pool)	Wood anoxic decay: labile	decay_anoxic_labile_wood	0.110000	0.030000	prop. year−1
Anoxic decay (labile litter pool)	Roots anoxic decay: labile	decay_anoxic_labile_roots	0.070000	0.120000	prop. year−1
Anoxic decay (recalcitrant litter pool)	Anoxic decay recalcitrant: all fractions	decay_anoxic	0.000100	0.000100	prop. year−1
Proportion of recalcitrant material (all litter fractions)	Leaves prop. of recalcitrant material	prop_recal_leaves	0.120000	0.120000	prop.
Proportion of recalcitrant material (all litter fractions)	Wood prop. of recalcitrant material	prop_recal_wood	0.400000	0.400000	prop.
Proportion of recalcitrant material (all litter fractions)	Roots prop. of recalcitrant material	prop_recal_roots	0.650000	0.650000	prop.
Litter addition	Leaves new mass	litter_leaves	10.000000	819.000000	g m−2 year−1
Litter addition	Wood new mass	litter_wood	275.000000	283.000000	g m−2 year−1
Litter addition	Roots new mass	litter_roots	556.000000	406.000000	g m−2 year−1
Shared PFT parameters	Dry bulk density (all litter fractions)	bulk_density	0.170000	0.170000	g cm−3
Shared PFT parameters	Maximum root depth	root_depth	0.300000	0.300000	m
Shared PFT parameters	PFT proportion	plant_type_prop	0.500000	0.500000	prop.

4.2 Initial Mass

The initial decomposition of the peat mass at the start of simulation is set to the fraction of the recalcitrant material in the litter for each FPT. Initial fraction of palm tree roots for example is calculated as:

$$fraction\ palm\ roots\ = \frac{root\ litter\ \cdot\ recalcitrant\ fraction}{total\ recalcitrant\ mass\ of\ palm\ tree} \cdot FPT\ fraction$$

We assume that recalcitrant material, when exposed to oxic conditions, decays with the same rate as labile material where degradation rates vary between the litter types. The initial composition therefore matters but we cannot easily replicate the composition of different layers in the peat. As we are interested in the impact of future scenarios, we consider this approach fit for purpose.

4.3 Change in soil carbon stock

The change in soil carbon stock, resulting from peat degradation and accumulation over time is estimated by the following formula:

$$\Delta_C = m_{peat} \cdot f_C$$

Where Δ_C is the change in soil carbon stock expressed in kg C m^{-2} yr^{-1}, m_{peat} the difference between initial and final peat mass at end of simulation and f_C carbon fraction in peat. We assume that the carbon fraction is 0.55.

Under oxic conditions, peat carbon decays mostly through CO_2 emissions, whereas anoxic peat decomposition results in a mixture of CO_2 and CH_4 fluxes to the atmosphere and dissolved carbon flux to waters (Rieley et al., 2008). Under oxic conditions, cumulative net CO_2 emissions can therefore be approximated by the following formula:

$$m_{CO_2} = \Delta_C \cdot \frac{M_{CO_2}}{M_C}$$

Where M_{CO^2} is the molecular weight of CO_2 (44 g/mol) and M_C the molecular weight of Carbon (12 g/mol).

4.4 Simulation Results

4.4.1 Carbon stock balance

Results are presented here for the baseline hydrological models (see section 3). Carbon uptake by the vegetation is constant in space and time and amounts to 0.65 kg C m^{-2} yr^{-1}. Carbon degradation varies in time and space. Average oxic and anoxic degradation amount to 5.05 kg C m^{-2} yr^{-1} in the rain-fed model and 3.26 kg C m^{-2} yr^{-1} in the river-fed scenario. Carbon loss is lower in the rain- and riverfed model as seasonal river inflow increases water levels along the western and eastern boundaries. Oxic decay vastly outweighs anoxic decay in both peatland models as 97-98% of the decayed carbon mass is degraded under oxic conditions. As oxic decay is preponderant, it can be assumed that the soil carbon decays through CO_2 emissions, amounting to 18.51 kg CO_2-C m^{-2} yr^{-1} in the rain-fed model and 11.94 kg CO_2-C m^{-2} yr^{-1} in the rain- and river-fed scenario.

Carbon uptake is thus much lower than degradation, which results in a negative carbon balance for both baseline models: -5.05 kg C m^{-2} yr^{-1} in the rain-fed model and -3.26 kg C m^{-2} yr^{-1} in the river-fed scenario.

These carbon balance figures contrast sharply with the peat accumulation rates Dargie et al. (2017) and Crezee et al. (2022) computed based on field measurements in the Cuvette Centrale. The former estimated a peat accumulation rate of 18.4 to 69.4 g C m^{-2} yr^{-1} depending on the core location over the

last 2000-9000 years whereas the latter found a rate of 11.8 to 36.8 g C m^{-2} yr^{-1} C, with core age ranging between 10000 and 42000 years before present.

Simulated yearly net carbon dioxide emissions are in the same order of magnitude as measurements made in the region. Mander et al. (2025) measured greenhouse gas fluxes in hardwood peat swamp forest and peaty savanna in Epena, Republic of Congo. They measured CO_2 emissions amounting to 50-90 kg CO_2-C m^{-2} (13-25 kg C m^{-2} yr^{-1}) in the dry season (March 2024) and 17-26 kg CO_2-C m^{-2} (4-7 kg C m^{-2} yr^{-1}) in the wet season (November 2024). The authors report that the emissions in the dry season, greater than the yearly net carbon dioxide emissions simulated in the present study, are high because of the severe heat and dryness which occurred in March 2024.

Ribeiro et al. (2021) compiled in a meta-study measurements of carbon stocks, carbon accumulation rates and CO_2 and CH_4 emissions across tropical peatlands in Asia, America and Africa. Measured values are in the range of 20-200 g C m^{-2} yr^{-1} for carbon accumulation and 7-15 kg CO_2-C m^{-2} (2-4 kg C m^{-2} yr^{-1}) for CO_2 emissions in untouched peatlands. The CO_2 emissions estimated in the present study are in the same range as those measurements.

Several factors could explain the discrepancy in carbon balance between the current approach and literature values, even though CO2 emissions are consistent with measurements.

Carbon uptake, based on field data collected in the Cuvette Centrale between 2019 and 2021 (Young et al., 2023), lies at the lower end of the range reported for tropical peatlands. Moore et al. (2018) measured, in evergreen forests in Ghana, a net primary production (NPP)—that is, the amount of carbon produced by primary producers per unit area and time—of 1.31 kg C m^{-2} yr^{-1}, which is twice the carbon uptake used here. A similar study in Indonesia reports a NPP of 0.97 kg C m^{-2} yr^{-1} (Kurnianto et al., 2015). Even though the carbon uptake values used here are lower than those reported in these studies, they are measurement-based and can therefore be considered quite reliable, it might thus only partly explain the observed discrepancy in carbon balance.

Carbon accumulation values gathered from peat core measurements are long-term rates of carbon accumulation over thousands of years whereas only the period 2012-2019 is simulated in this study. The negative carbon balance modelled here might be explained by the current dry climate conditions (see section 3.2.3).

4.4.2 Oxic and anoxic decay

In Figure 4.2 is shown the time-depth result of soil saturation from the baseline rain-fed model for a single cell in the center of the peat dome. The soil is considered oxic when saturation falls below 90%, i.e., when more than 10% of the pore space is filled with air. The plot shows significant variability over the years - the drought in later years shows significant increase of the oxic depth and exposure of the peat to oxic degradation.

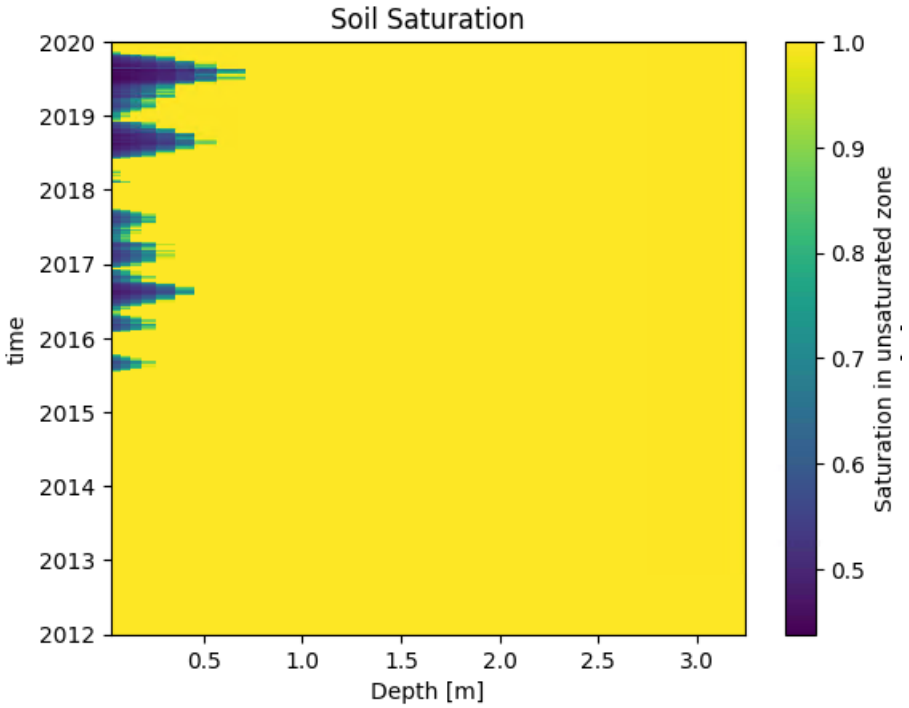

Figure 4.2 Soil saturation with depth in a central cell in the peat dome for the baseline rain-fed model.

The soil saturation profile for the baseline scenario, shown in Figure 4.2, is used as input to the simulation results found in Figure 4.3 together with the parameters presented in section 4.1. In the figure, the plant function types and different litter compositions are grouped into the four groups from Figure 4.1. The blue line is the oxic depth and represents depth from the surface where soil conditions are oxic and deeper in the soil the decomposition is considered anoxic. The mass of “Labile oxic” and “Recalcitrant oxic” are seen to increase when the oxic depth increase and “Labile anoxic” and “Recalcitrant Anoxic” becomes correspondingly smaller as peat mass is shifted from anoxic to oxic.

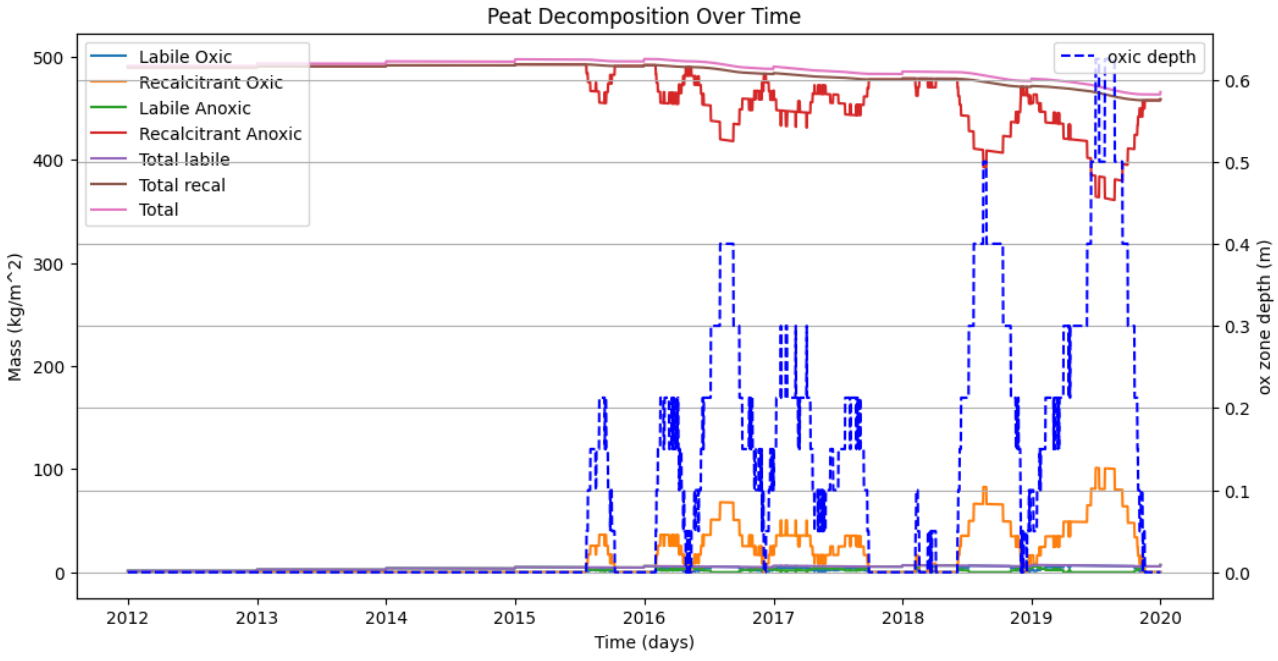

Figure 4.3 Simulation of peat degradation and peat mass divided into the 4 categories as shown in Figure 4.1, labile and recalcitrant mass further in oxic and anoxic decomposition. Blue line is the oxic depth.

The sensitivity of the peat degradation when it is exposed to oxic conditions is clearly seen as the dry years from around 2016 result in loss of peat mass but in the first years up to 2015-2016 with anoxic conditions through the whole soil profile “Total” peat mass is increasing.

4.4.3 Spatial repartition of peat decay

The spatial repartition of the change in soil carbon stock for the baseline rain-fed scenario is juxtaposed to the mean groundwater table depth in Figure 4.4. A negative mean groundwater level indicates that the water table is mostly above ground. Both variables are logically correlated: peat decay occurs mostly near the model boundaries where the groundwater table is deep. Peat decay is limited near the centre of the dome where the water table is most of the times above ground.

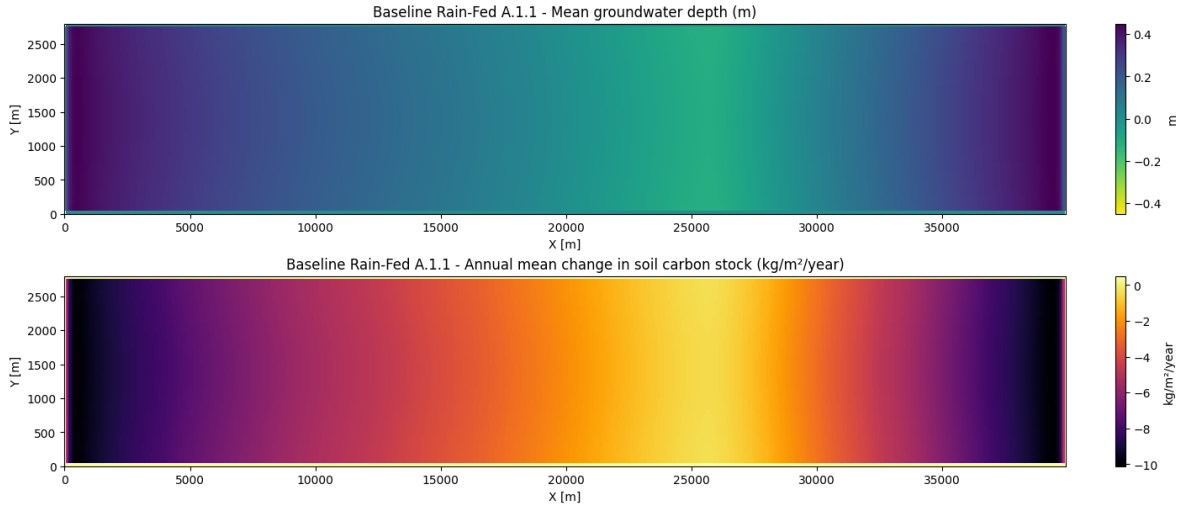

Figure 4.4 Mean groundwater table depth and change in soil carbon stock throughout the model domain for the baseline rainfall driven model (A.1.1). A negative groundwater depth indicates that the mean water level is above ground.

In the river-fed scenario, peat decays more than in the rainfall driven baseline scenario as water tables are higher in the boundary zones. There is even peat accumulation near the eastern river (**Error! R eference source not found.**). The highest soil carbon losses are now located at the periphery of the river-flooded area. The centre of the dome is not affected by flooding, and the change in soil carbon stock there remains similar in both scenarios.

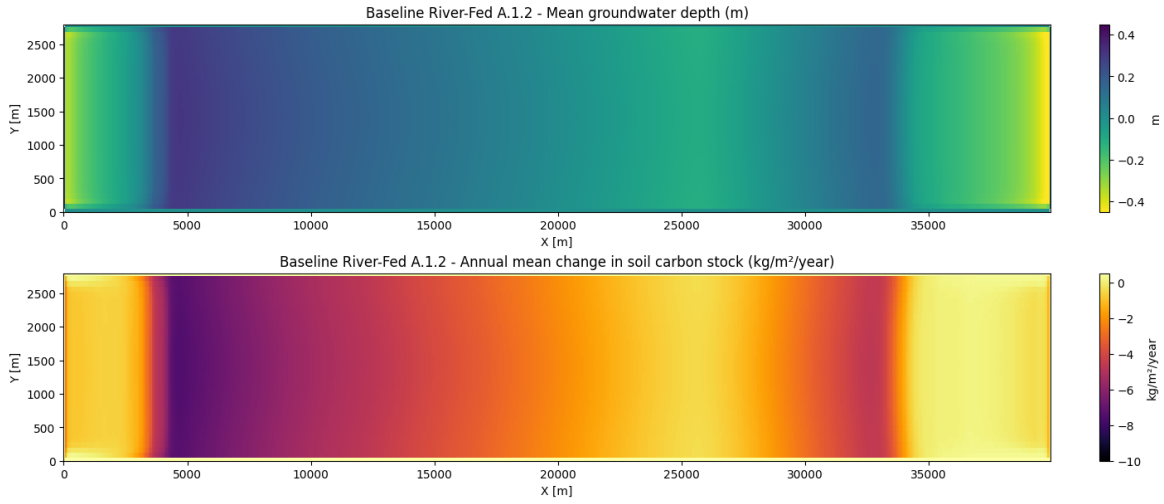

Figure 4.5 Mean groundwater table depth and change in soil carbon stock throughout the model domain for the baseline rainfall driven model (A.1.2). A negative groundwater depth indicates that the mean water level is above ground.

5 Scenario Definitions and Evaluation Method

Scenarios are representations of answers to questions of the type "What happens if…?". For each scenario models are developed. These represent the questions. The respective simulation results of the models represent the answer to the question.

The "if" part in the question that defines a scenario has the following aspects:

- **Development intervention**: What happens if infrastructure is developed, or what happens under agricultural development conditions? The development interventions investigated in the analyses are derived from stakeholder consultations.
- **Climate**: What happens under current climatic conditions and under specific climate change conditions?
- **Hydrological region**: Are the hydrological processes in the peatlands only driven by rainfall and evapotranspiration (this is mostly the case in the northern parts of the region)? Or are the hydrological processes in the peatlands driven by rainfall and evapotranspiration, as well as fluctuating water levels in bordering water bodies (e.g., river reaches), as this is mostly the case in central parts that are adjacent to the main rivers in the region.

5.1 Development Interventions

The generalized development interventions derived from the stakeholder consultations are the following:

Code	Name	Description
A	Baseline without Intervention	Vegetation and topography of the peatlands are according to the current conditions - between 2010 and 2020
B	Road Built and Operational	(a) A raised impervious road is built 1 meter above the natural surface. It is finished and operational. (b) Vegetation is removed, and the soil surface is flattened. (c) The road embankment is filled with permeable gravel. (d) The underlying peat is compressed due to the road's weight.
C	Road during Construction	(a) A raised impervious road is being built 1 meter above the natural surface. (b) Vegetation is removed, and the soil surface is flattened. (c) The road embankment is filled with permeable gravel. (d) The underlying peat is compressed due to the road's weight. (e) During construction, drainage is installed 2 meters below the ground, i.e., 1 meter below the surrounding surface.
D	Settlements Developed	(a) A settlement is developed in the peatland forest. (b) The topography is raised by 50 cm to prevent flooding. (c) Vegetation is cleared, and the soil surface is partially paved. (d) The peat is compressed under the load of buildings.
E	Forest Fire – Deforestation	(a) A forest fire completely clears the vegetation. (b) As a result, soil properties change: bulk density increases, and specific yield decreases.
F	Palm Plantation replaces Forest	Deforestation and Conversion to Oil Palm Plantations: (a) Natural vegetation is cleared to establish additional oil palm plantations. (b) Oil palms thrive with a mean water level 40 cm to 60 cm below ground. There is drainage at 50 cm depth. (c) Vegetation properties are altered according to 15-year-old mature oil palm plantation. (d) The microtopography is smoothed due to clearing. (e) Soil properties change by drainage:

Code	Name	Description
		increased bulk density, reduced specific yield, and reduced hydraulic conductivity at saturation. (f) The topography is lowered by 50 cm due to soil subsidence induced by drainage.
G	Rice Cultivation replaces Forest	Deforestation and Conversion to Rice Cultivation: (a) Natural vegetation is removed and replaced with rice paddies. Rice is the most common seasonally flooded crop in the Cuvette Centrale. (b) There are two harvests per year. Vegetation and surface properties/roughness vary with crop stage.

All interventions take place within a given area of the conceptual model. This zone is a 240m-wide horizontal stripe extending along the entire length of the model area (see Figure 5.1). Both the effects of the intervention on the intervention zone and on the area around are studied here.

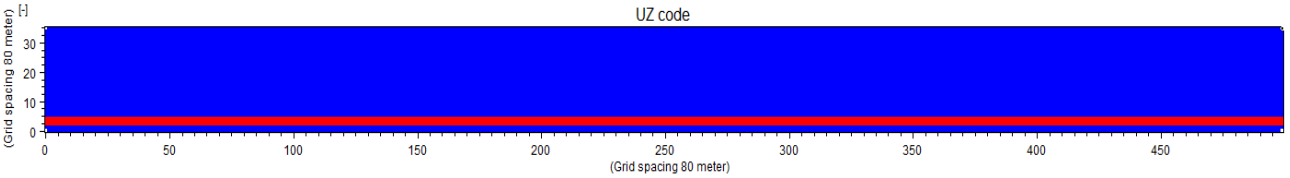

Figure 5.1 Intervention zone (in red) and area around the intervention zone (in blue)

In each model that represents the respective development intervention model parameters are adjusted as such that the impacted hydrological processes can be simulated adequately. The changes carried out to the baseline model (see description section 3.2) are detailed below.

5.1.1 Intervention A – Baseline

See section 3.2.

5.1.2 Intervention B – Road Built and Operational

Given that the peatland surface is regularly flooded, the road is raised by 1 m compared to the surrounding terrain. Vegetation on the road surface is removed. As the leaf area index and rooting depth are set to 0, there will be no transpiration from the intervention zone. Evaporation can still occur from the ground.

With their smooth surface, roads act as primary overland flow routes. The Manning-Strickler roughness coefficient, set to 10 $m^{1/3}/s$ in the baseline model, is thus raised to 20 $m^{1/3}/s$ on the road. The detention storage, set to 65 mm in the baseline model, is reduced to 1 mm as vegetation is removed, and water can't accumulate in surface depressions like in untouched peatlands.

The modelled soil profile is represented Figure 5.2. A paved area modelling the impervious superficial layer is added over the road to prevent infiltration into the soil column. The road embankment is composed of two horizontal soil horizons. Beneath the paved area and extending to 1 m below the surface is a layer of compacted gravel, which stabilizes the road embankment. It has a horizontal hydraulic conductivity (K_h) of 3 x 10^{-4} m/s and a vertical hydraulic conductivity (K_v) of 3 x 10^{-5} m/s. Beneath this lies a more permeable gravel layer, 1 m thick.

The peat layer below the gravel embankment, compressed by the weight of the road, has a low hydraulic conductivity. The conductivity values for all soil horizons are given Table 5-1. Specific yield and specific storage values for gravel are taken from literature. Compressed peat is assumed to have hydraulic conductivities 10 times lower than those of unaltered peat and a specific yield of 0.15, reflecting its reduced macropore volume. Since the compressed peat layer lies more than 2 m below ground, it is always beneath the phreatic surface. It is therefore unnecessary to include compressed peat in the unsaturated zone layers.

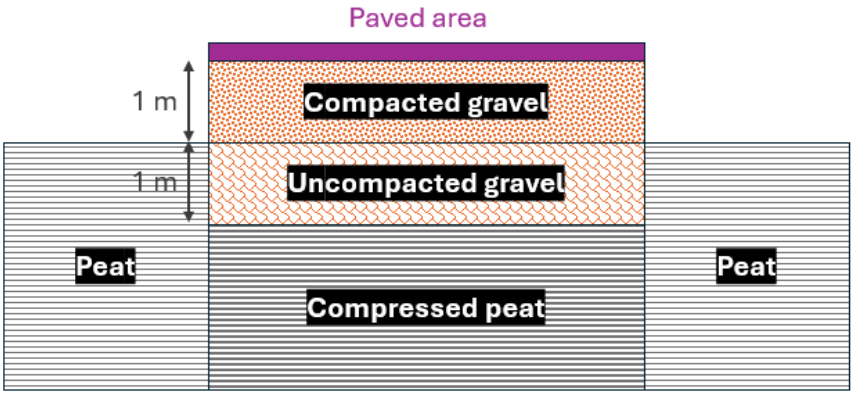

Figure 5.2 Structure of the soil profile for the road intervention

Table 5-1 Hydraulic properties of the soil horizons in the unsaturated and saturated zones.
K_{sat} = hydraulic conductivity at saturation, K_v = vertical hydraulic conductivity, K_h = horizontal hydraulic conductivity, S_y = specific yield

Soil horizon	Road	Baseline
Unsaturated Zone		
Compacted gravel	K_{sat} = 3.27 x 10^{-5} m/s S_y = 0.37*	K_{sat} = 6 x 10^{-5} m/s S_y = 0.47*
Uncompacted gravel	K_{sat} = 3.27 x 10^{-4} m/s S_y = 0.39*	(Peat)
Saturated Zone		
Compacted gravel	K_v = 3.27 x 10^{-5} m/s K_h = 3.27 x 10^{-4} m/s S_y = 0.37	K_v = 10^{-5} m/s K_h = 10^{-4} m/s S_y = 0.47
Uncompacted gravel	K_v = 3.27 x 10^{-4} m/s K_h = 3.27 x 10^{-3} m/s S_y = 0.39	(Peat)
Compressed peat	K_v = 10^{-6} m/s K_h = 10^{-5} m/s S_y = 0.28	
Weighted Average gravel & peat	$10^{-6} < K_v < 7 \times 10^{-6}$ m/s $7 \times 10^{-4} < K_h < 2 \times 10^{-3}$ m/s $0.32 < S_y < 0.38$	

**In the unsaturated zone, specific yield is defined here as the difference between total water content and water content at field capacity.*

In the saturated zone, the gravel and peat layers are combined into a single computational layer. The horizontal conductivity is calculated as a thickness-weighted arithmetic mean, while a thickness-weighted harmonic mean is used for vertical conductivity. Because conductivity values can span several orders of magnitude, a simple weighted mean would be dominated by the higher values. This approach is appropriate for horizontal conductivity, as horizontal flow is controlled by the most transmissive layers. For vertical conductivity, however, a harmonic mean is more suitable, since vertical

flow is largely limited by the least permeable layer. Specific yield is interpolated using a simple weighted mean. The averaged ranges are highlighted in red in Table 5-1. The averaged hydraulic properties vary with the thickness of the peat layer, which is greatest at the centre of the peat dome.

Peat decay and carbon emissions within the road footprint are simulated in the same way as in the baseline case. Litter production is deactivated within the road footprint.

5.1.3 Intervention C – Road during Construction

Intervention C is based on Intervention B but includes a drain to remove water from the road embankment. The road structure and characteristics are the same as in Intervention B. The drain is located at a depth of 2 metres, beneath the uncompacted gravel layer. Flow through the drain is regulated in MIKE SHE by the time constant, which in this case is set to 1.16 /s, placing it at the upper end of the typical range.

Peat decay and carbon emissions within the road footprint are simulated in the same way as in the baseline case. Litter production is deactivated within the road footprint.

5.1.4 Intervention D – Settlements developed

The effects of building a settlement in the peatland are modelled. The settlement's topography is raised by 50 cm to ensure the ground remains unflooded throughout the simulation period. As in the road intervention, vegetation on the road surface is removed. With the leaf area index and rooting depth set to zero, there is no transpiration from the intervention zone; however, evaporation can still occur from the ground. The overland flow parameters are identical to those in the road scenario: the Manning-Strickler roughness coefficient is raised to 20 $m^{1/3}/s$ on the road and the detention storage is reduced to 1 mm as vegetation is removed.

As in the road intervention, a paved area is placed above the soil column. However, as settlements usually include unpaved areas such as gardens, parks, and sports facilities, where water can infiltrate, the paved area included here only covers a third of the footprint area. The pressure exerted by buildings compresses peat and alters its hydraulic properties (see, e.g., Li et al., 2020). There are few scientific studies examining these effects. Among these, laboratory experiments by Jelisic (2005) showed that relative peat compression can reach up to 60%. In this study, it is assumed that compression affects peat to a depth of one metre below ground.

In a small settlement with mostly single-storey buildings, the load exerted is lower than beneath a road. Roads apply a more uniform load across the entire surface and are also subject to traffic loads. Furthermore, settlements may use piles driven through the peat to more stable layers, bypassing much of the compression in the peat itself. For these reasons, the hydraulic properties selected for compressed peat in this scenario represent a middle ground between those of unaltered peat and those of compressed peat used in the road intervention (see Table 5-2). Compressed peat is less porous and less permeable in the saturated zone than in the unsaturated zone, reflecting the increase in peat density with depth.

Table 5-2 Hydraulic properties of the compressed peat in the unsaturated and saturated zones.

Soil horizon	Urbanization	Road (Interventions B & C)	Baseline
Unsaturated Zone			
K_{sat} - Saturated Hydraulic Conductivity (m/s)	10^{-5}	/	6×10^{-5}
θ_s - Saturated Water Content (-)	0.6	/	0.8
Saturated Zone			
K_v - Vertical Hydraulic Conductivity (m/s)	5×10^{-6}	10^{-6}	10^{-5}

Soil horizon	Urbanization	Road (Interventions B & C)	Baseline
K_h - Horizontal Hydraulic Conductivity (m/s)	5×10^{-5}	10^{-5}	10^{-4}
S_y - Specific Yield (-)	0.3	0.28	0.47

The compressed and regular peat layers are merged into a single computational layer in the saturated zone. Hydraulic conductivity and specific yield are higher at the centre of the dome, as the regular peat layer is thicker than at the edges of the model.

The retention curves used as inputs in the MIKE SHE models (see Figure 5.3) describe the water-holding capacity of untouched peat and peat beneath the settlement at different suction pressures. Compressed peat has a lower macroporosity and therefore retains less water at saturation. Compression affects the whole retention curve, as in for a given suction pressure, the moisture content is lower in compressed peat.

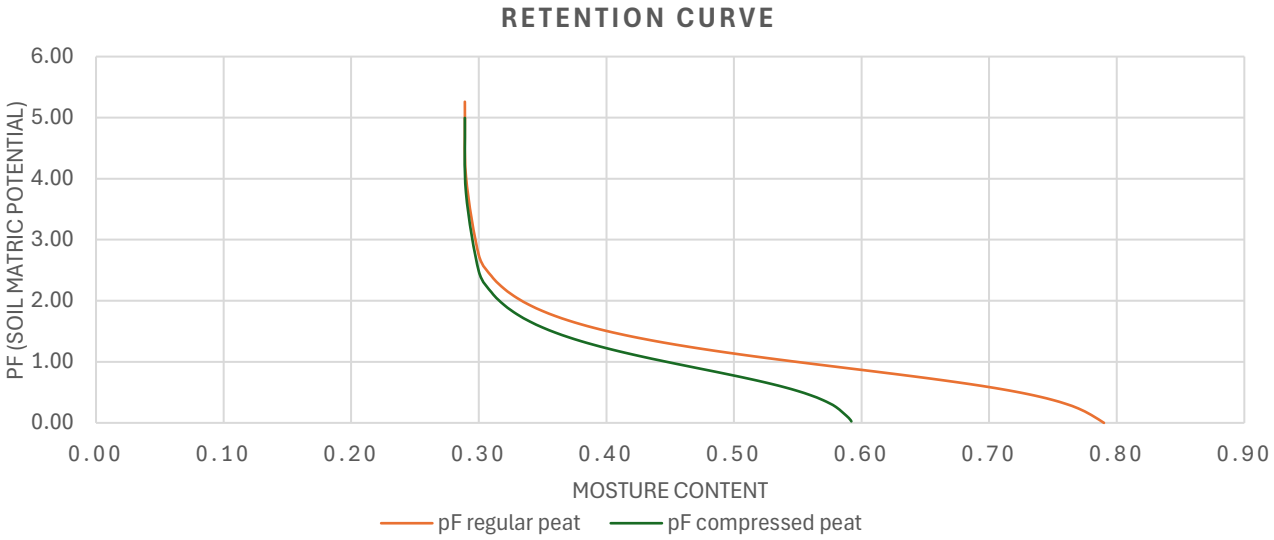

Figure 5.3 Retention curves of regular peat and peat compressed by a settlement

Peat decay and carbon emissions within the settlement footprint are simulated in the same way as in the baseline case. Litter production is deactivated within the settlement footprint.

5.1.5 Intervention E – Forest Fire / Deforestation

In this intervention, vegetation is cleared after a forest fire. With the leaf area index and rooting depth set to zero, there is no transpiration from the intervention zone; however, evaporation can still occur from the ground. Ground roughness decreases after vegetation removal, so the Manning–Strickler coefficient is increased from 10 to 15 $m^{1/3}/s$ and detention storage is reduced from 65 to 32 mm to reflect the loss of hollows and hummocks caused by peat smouldering.

In typical tropical forests, fires consume aboveground biomass but rarely penetrate deep into the soil. By contrast, peatland fires can smoulder into the peat, burn root systems, and alter soil structure. Although peatland fires are widespread and frequent in Southeast Asia, relatively little is known about their impacts on peat hydraulic properties. Sinclair et al. (2020) measured peat bulk density in degraded and intact peatlands in Central Kalimantan, Indonesia. They compared five intact sites with nine degraded sites subject to frequent annual fires and found that the bulk density of the upper 50 cm was on average 20% higher in sites that had experienced three fires over the past two decades than in unburnt sites (0.155 vs 0.130 g/cm^3).

Liu et al. (2020) compiled hydrophysical data from 39 published studies on temperate and boreal peatlands and showed that bulk density is negatively correlated with porosity, saturated hydraulic conductivity, and specific yield. Using the average bulk densities of untouched and burnt peat reported by Sinclair et al. and the polynomial regression equations linking bulk density to hydrophysical parameters from Liu et al., it is possible to estimate changes in the main soil hydraulic parameters for the IKI Congo MIKE SHE models. Saturated hydraulic conductivity is reduced by 80% and specific yield, defined in the article as the difference between total water content and water content at pF = 1, is reduced by 20% (see Table 5-3 and Figure 5.4). The decrease in total porosity due to fire, which is less than 2%, is not considered here.

The hydraulic properties of the saturated zone (see Table 5-3) are derived from those of the unsaturated zone. Like in the baseline scenario, the vertical hydraulic conductivity is higher than the saturated hydraulic conductivity to account for peat compression with depth. The burnt and unburnt peat layers are merged into a single computational layer in the saturated zone. Hydraulic conductivity and specific yield are higher at the centre of the dome, as the untouched peat layer is thicker than at the edges of the model.

Table 5-3 Hydraulic properties of the burnt peat in the unsaturated and saturated zones.

Soil horizon	Fire	Baseline
Unsaturated Zone		
K_{sat} - Saturated Hydraulic Conductivity (m/s)	1.31×10^{-5}	6×10^{-5}
S_y – Modified Specific Yield*	0.2	0.25
Saturated Zone		
K_v - Vertical Hydraulic Conductivity (m/s)	5×10^{-6}	10^{-5}
K_h - Horizontal Hydraulic Conductivity (m/s)	5×10^{-5}	10^{-4}
S_y - Specific Yield (-)	0.45	0.47

**Liu et al. use the term "specific yield" to refer to the difference between total water content and water content at pF = 1.*

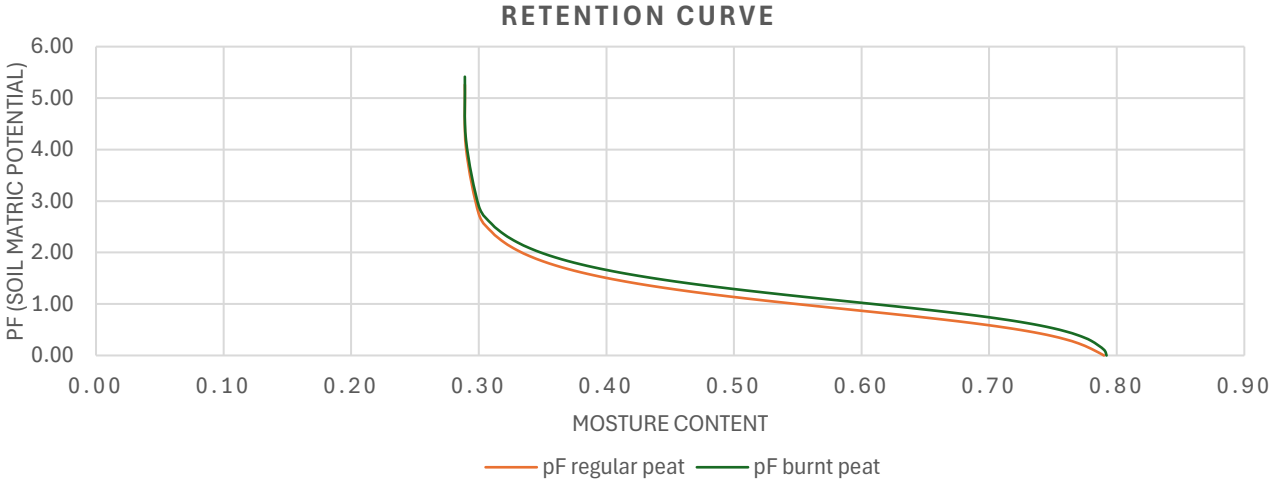

Figure 5.4 Retention curves of regular peat and peat burned by fire

Peat decay and carbon emissions within the burnt area are simulated in the same way as in the baseline case. Litter production is deactivated within the burnt area.

5.1.6 Intervention F – Forest replaced by Oil Palm Plantations

Intervention F involves the conversion of forested peatland to oil palm plantations. Oil palm cultivation has existed in the region for more than a century, and further expansion of plantations is planned[6]. Natural vegetation is cleared to establish new oil palm stands. The leaf area index (LAI) of oil palm plantations has been measured in numerous studies, and it typically increases with plantation age, reaching a value of about 4 in 15-year-old mature plantations (see Awal et al., 2008; Rusli et al., 2014). Accordingly, an LAI of 4 is used in this intervention (see comparison with the baseline intervention in Figure 5.5). A constant rooting depth of 1 m, as in the baseline intervention, is also applied here (see Safitri et al., 2018).

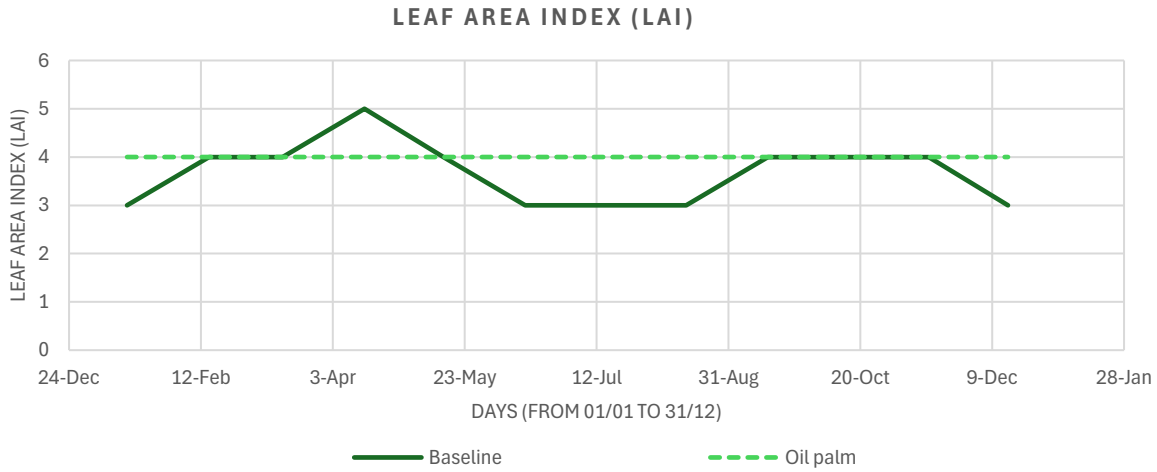

Figure 5.5 Annual variations of the Leaf Area Index (LAI) used in the model – Baseline vs Oil Palm

Oil palm thrives when the mean water level is maintained 40–60 cm below ground (see Ginting et al., 2016). A drain is therefore introduced in the model at 50 cm depth. Drainage induces major changes in soil properties. Apers et al. (2022) compiled data from literature on peatlands in Southeast Asia to derive average soil retention and conductivity curves for untouched and drained tropical peatlands. The changes in soil hydraulic parameters reported by Apers et al. were used here to define the hydraulic parameters of drained peat in the present study (see Table 5-4). Draining peat leads to a reduction in porosity (saturated water content), specific yield, and hydraulic conductivity. Microporosity, however, is not affected by drainage: the retention curves of untouched and drained peat are nearly identical above pF = 1 (see Figure 5.6).

Table 5-4 Hydraulic properties of the drained peat in the unsaturated and saturated zones.

Soil horizon	Oil Palm (drained peatland)	Baseline
Unsaturated Zone		
K_{sat} - Saturated Hydraulic Conductivity (m/s)	2×10^{-6}	6×10^{-5}
θ_s - Saturated Water Content (-)	0.62	0.8
Saturated Zone		
K_v - Vertical Hydraulic Conductivity (m/s)	10^{-6}	10^{-5}
K_h - Horizontal Hydraulic Conductivity (m/s)	10^{-5}	10^{-4}
S_y - Specific Yield (-)	0.28	0.47

[6] De Augustinis, F., & Kambale, J. (2025, April 22). *DRC's plans to dramatically increase palm oil production*. Pulitzer Center.

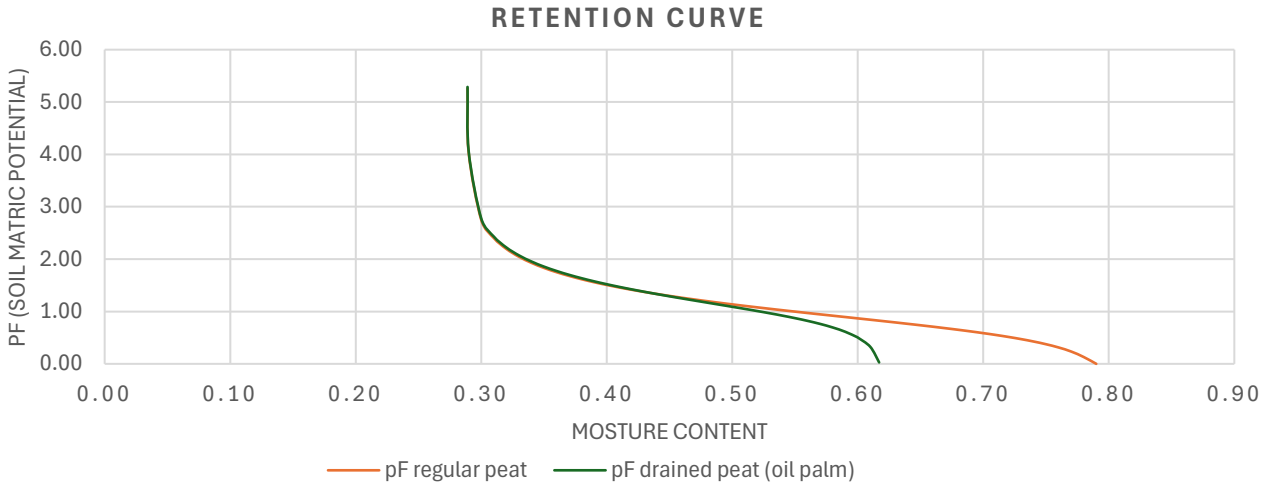

Figure 5.6 Retention curves of regular peat and drained peat

The drained and undrained peat layers are merged into a single computational layer in the saturated zone. Hydraulic conductivity and specific yield are higher at the centre of the dome, as the undrained peat layer is thicker than at the edges of the model.

In tropical peatlands, ground topography is characterised by elevated areas, or hummocks, and local depressions, or hollows. Lampela et al. (2016, 2017) carried out thousands of surface elevation measurements across two sites representing, respectively, untouched and drained peatlands in Indonesia. Using these data, Apers et al. (2022) derived microtopographic distributions for both conditions (see section 3.2.6). Drainage smooths the peatland microtopography: based on Apers' results, detention storage is set to 50 mm in this intervention, compared to 65 mm in the baseline scenario. Ground roughness decreases after the oil palm plantation, so the Manning–Strickler coefficient is increased from 10 to 15 $m^{1/3}/s$.

Drainage of tropical peatlands also leads to carbon loss through oxidation, resulting in land subsidence. Numerous studies in Southeast Asia have quantified subsidence rates in drained peatlands, synthesised in Hooijer et al. (2012) and Evans et al. (2019). These findings show that drained oil palm plantations initially experience very high subsidence rates, which stabilise at 3–5 cm/yr. Subsidence rates increase substantially with drainage depth. As MIKE SHE does not allow ground levels to vary over time, the ground surface in the oil palm plantation is lowered by 50 cm, representing conditions a few years after initial drainage. A higher subsidence should be applied when modelling plantations in their second or third rotation. Evans et al. (2019) found that intact forested peatlands located near drained oil palm plantations were also subject to subsidence, with rates exceeding 2 cm/yr at distances of 3 km from the forest–plantation boundary. This effect, however, is not included in the present models.

Peat decay, litter production and carbon emissions within the oil palm plantation are simulated in the same way as in the baseline case.

5.1.7 Intervention G – Forest replaced by Rice Plantations

Like Intervention F, Intervention G examines the conversion of forest to crops, in this case rice paddies. Rice is well adapted to seasonally flooded areas and has traditionally been cultivated in the region, particularly around Lake Tumba. It is also considered a suitable option for degraded, drained peatlands (see Surahman et al., 2018).

Rice paddies are typically flooded during the later stages of crop growth. Following the two main wet seasons, there are two cultivation cycles per year in the Cuvette Centrale: the first from March–April to July–August, and the second from August–September to December–January (Food Security Cluster,

2024; Mayengo et al., 2005). The leaf area index (LAI) and rooting depth—parameters used in MIKE SHE to compute transpiration—vary over the crop growth cycle.

The LAI of rice gradually increases during crop growth and reaches a plateau during the ripening stage (see Figure 5.7). Because no LAI data for rice are available from Central Africa, values measured in Indian rice paddies are used here (Mahajan et al., 2012; Prabhakar et al., 2024). Rice roots extend deeper during the early growth stages and then tend to spread horizontally during the heading and ripening stages. The rooting depth time series used in the model are adapted to African varieties (Samejima et al., 2016).

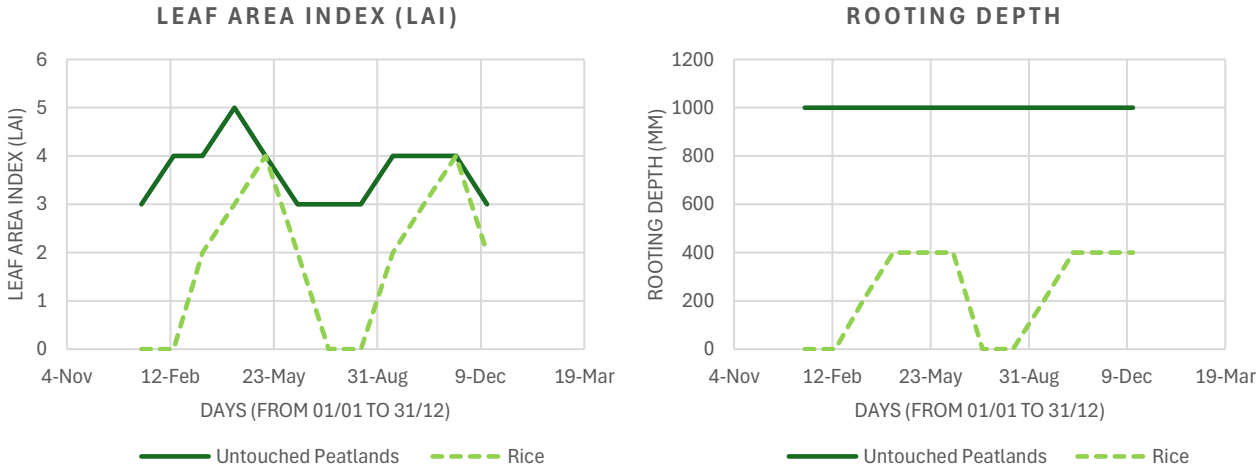

Figure 5.7 Annual variations of the Leaf Area Index (LAI) and rooting depth used in the model – Baseline vs Rice

To allow for rice cultivation, the microtopography is levelled in the model and detention storage is reduced from 65 mm to 2 mm. Ground roughness varies with the crop stage (see Figure 5.8): it increases when rice is mature and decreases when the ground is bare between two cultivation cycles. Soil properties are assumed to be the same as in the baseline intervention.

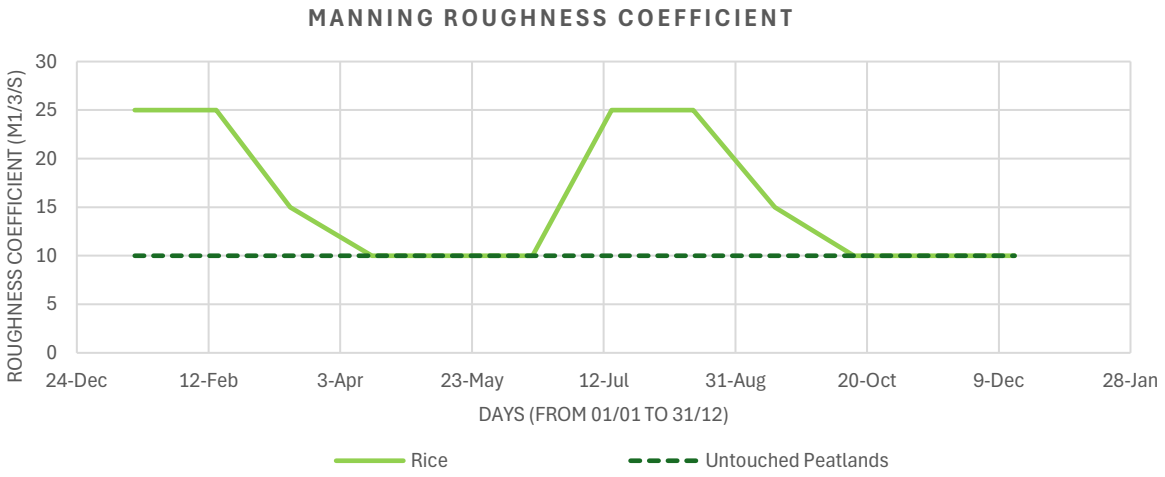

Figure 5.8 Annual variations of the Manning-Strickler roughness coefficient used in the model – Baseline vs Rice

As in the other interventions, the area affected by the land use change is represented in the model as a stripe extending across the entire length of the conceptual peat slice. Shallow peat, being more fertile, is better suited for rice cultivation than deep peat. It is therefore unlikely that rice would be cultivated on the deep peat located at the centre of the dome.

Rice paddies aren't drained in this model. As water levels in the paddies exceeding 10 cm are detrimental for rice growth, drainage might be necessary in areas with high water levels near the centre of the dome.

Peat decay and carbon emissions in the rice paddies are simulated in the same way as in the baseline case. Litter production is deactivated within the rice plantation.

5.2 Climate Scenarios

The Intergovernmental Panel on Climate Change (IPCC) Sixth Assessment Report (AR6), (IPCC,2021) climate change scenarios were used to assess the impact of climate change. The basis of the IPCC AR6 results are the Coupled Model Intercomparison Project Phase 6 (CMIP6) in which multiple climate modelling groups around the world run Global Climate Models (GCMs) with agreed input parameters to simulate different scenarios.

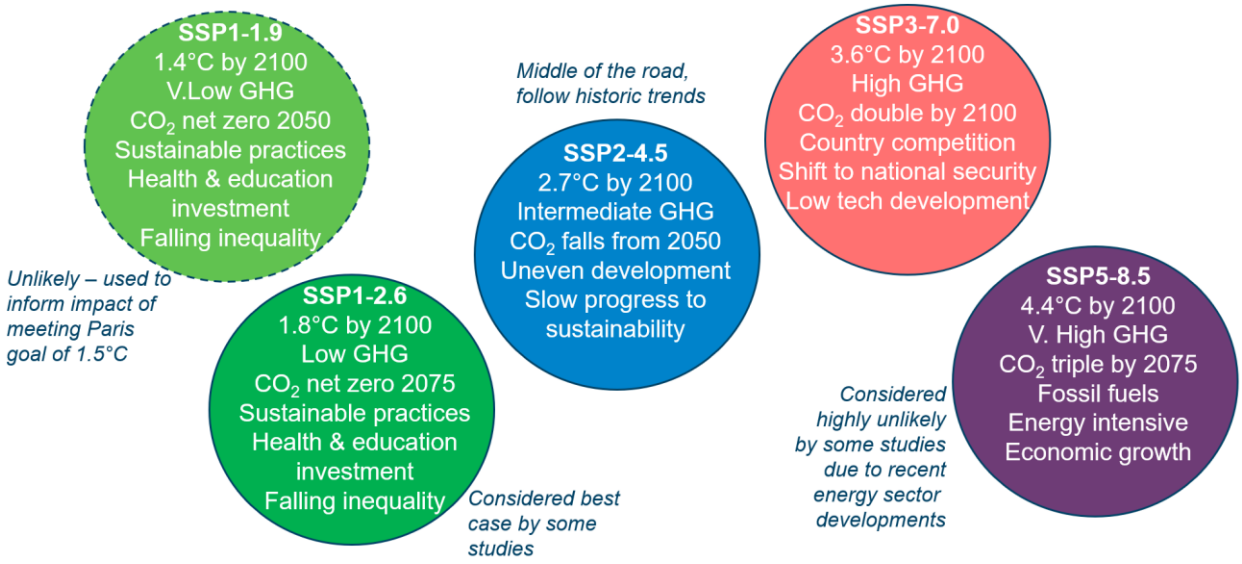

Figure 5.9 Summary of the five emissions' scenarios that inform the latest IPCC AR6 report

From the IPCC AR6 emission scenarios we choose the following to form part of our scenario definitions:

Code	Name	Description
1	Current Climate	Rainfall, temperature and evapotranspiration between 2010 and 2020 are chosen to represent the current climate conditions.
2	CC Sustainable Growth	SSP1-2.6: (a) Global warming is limited to around 1.5°C-2°C above pre-industrial levels. (b) This scenario is in line with the objectives of the Paris Agreement and represents an optimistic future with sustainable economic growth and minimal impact on climate change.
3	CC Severe Impact	SSP3-7.0: (a) Projected warming: 3°C-4°C by 2100, with severe climatic consequences. (b) This scenario represents a high-risk future, characterized by significant climate change, social inequalities and environmental degradation.

Climates are represented with timeseries of rainfall and evapotranspiration used as forcings to the hydrological model as described in chapters 3.2.2 and 3.2.2. The effect of projected temperature change is included indirectly as input for projected reference evapotranspiration and directly as a temperature modification parameter in the biodegradation model described in chapter 4. The biodegradation rates are modified by a constant factor, f_Q using the difference between average

temperature (tbc) in the baseline period and the climate change scenario (t). Reference evapotranspiration is calculated using the Priestley-Taylor equation, see 3.2.2.

GCMs simulate large scale climate changes and are not calibrated to specific regions. They typically show significant biases which makes the model results unsuitable as forcings to local hydrological models. We assume, that the bias and other sources of deviance present in the climate model baseline are also found in the projection period and that the relative change between baseline and projection is suitable to describe the broad climate change for our location. The relative climate change is used to modify our model baseline forcings to generate climate projected model forcings using the commonly used statistical method, the delta change method. We therefore use the model baseline forcing data as described in section 3.2 but rescale them in the projection period to account for climate change.

5.2.1 Projection period

This section explains the CMIP6 GCM's baseline and projection period and the model baseline (simulation period of the hydrological model of this study). Baselines represent the period we consider represent the current climate. The projection period is the future climate, and we chose the period 2041-2060 (20 years) with the centre year in 2050. The climate model baseline period is 1990-2014 (25 years) and our model baseline is 2012-2019 (7 years).

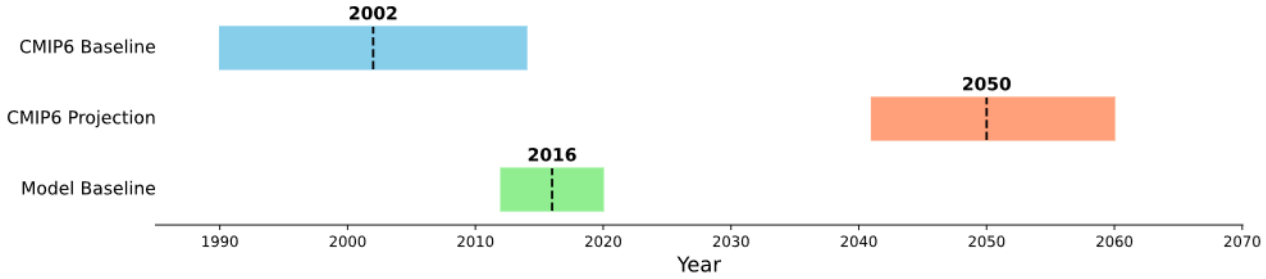

Figure 5.10 CMIP6 projection and baseline period and model baseline (simulation period). Centre year is marked with a dotted line.

By comparing CMIP6 GCMs baseline and projection period we can estimate how the climate variables rainfall and temperature have changed between the two periods. Our model baseline does not coincide with the CMIP6 baseline period and we calculate a reduction we call BRF (baseline reduction factor), used in the delta change method.

$$BRF = \frac{X_{GCM,projection} - X_{Model,baseline}}{X_{GCM,projection} - X_{GCM,baseline}} = \frac{2050-2016}{2050-2002} = 0.708$$

Where X stands for the centre year of each period. Because our simulation period comes after the CMIP6 baseline period we reduce the climate change with a corresponding factor to reflect that part of the climate change has already taken place in our model baseline period.

5.2.2 Delta change method

The delta change method consists of applying a fixed scaling that we derive from CMIP6 GCM simulations to the model forcing variables precipitation, reference evapotranspiration and temperature. The scaling factors are derived by comparing the average for a scenario baseline period to the average in the projection period for each of the forcing variables. We furthermore divide the periods into the 12 months of the year using 12 monthly scaling factors instead of 1 to include seasonal variations. Scaling factors are multiplicative for precipitation and evaporation, and additive for temperature:

Precipitation and evaporation:

$$y^f_{i+T,m} = x^p_{obs,i} * \frac{\overline{y^f_{mod,m}}}{\overline{x^p_{mod,m}}} * BRF$$

Temperature:

$$y^f_{i+T,m} = x^p_{obs,i} + \left(\overline{y^f_{mod,m}} - \overline{x^p_{mod,m}}\right) * \mathrm{BRF}$$

Where m is the calendar month, $y^f_{i+T,m}$ is the corrected variable in the future at time i, $\overline{y^f_{mod,m}}$ the model output average for month m in the future period, $\overline{x^p_{mod,m}}$ the model output average for month m in the baseline period and $x^p_{obs,i}$ the observed variable at time i. BRF is a reduction factor introduced because the model baseline comes after the CMIP6 baselines, see “projection period” above for further explanation.

Using the delta change method we get the following scaling factors for precipitation, temperature and reference evapotranspiration for the chosen scenarios. The scaling factor for temperature is additive. Data is extracted for Lac Télé – Lac Tumba area.

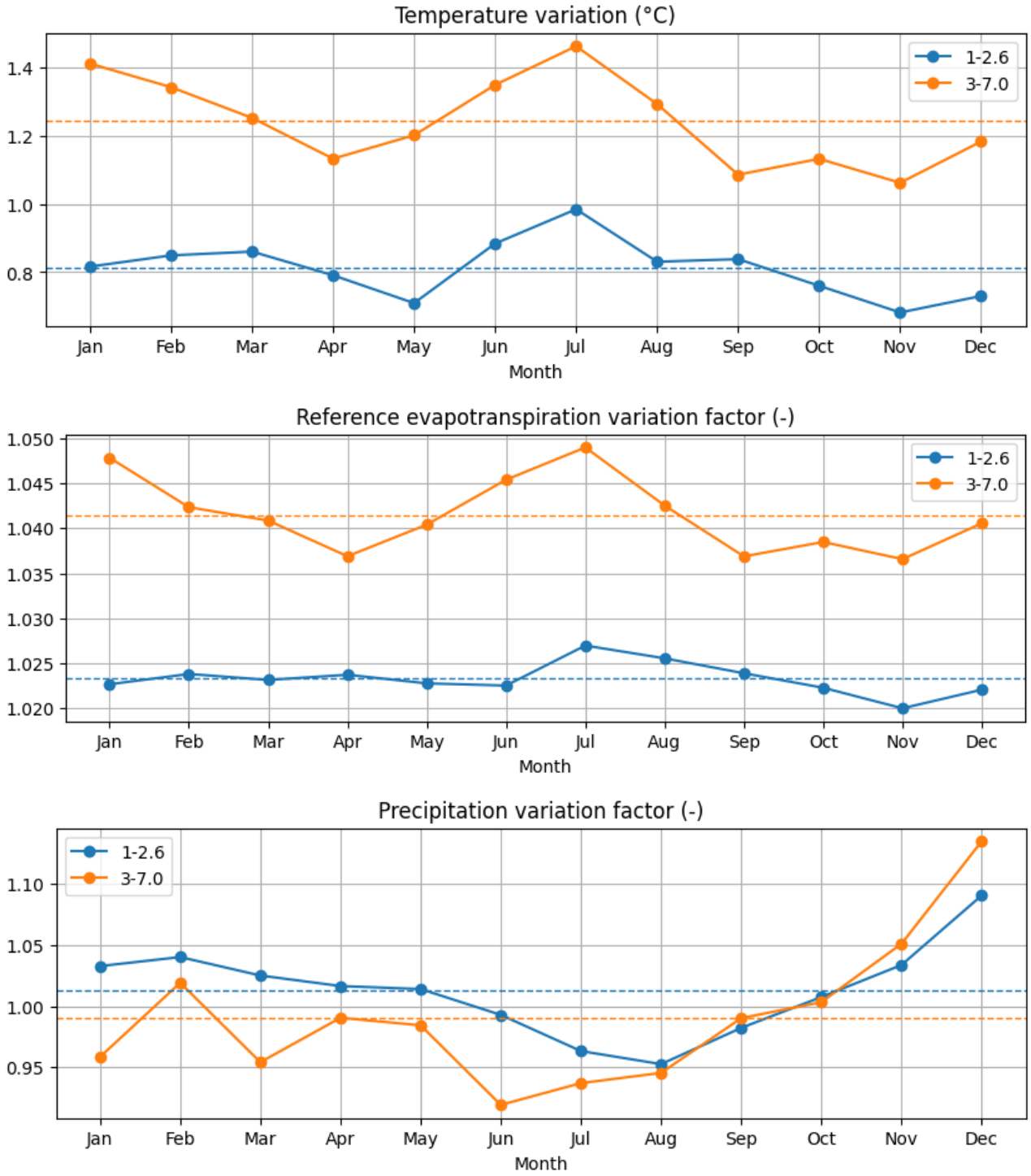

Figure 5.11 Climate change scaling factors for precipitation, temperature and reference evapotranspiration

Scaling factors are multiplicative for precipitation and reference evapotranspiration and additive for temperature. The dashed lines represent the average values of the monthly factors.

Temperatures are projected to increase under both scenarios, with a mean annual rise of 0.8 °C under SSP1-2.6 and 1.2 °C under SSP3-7.0 by 2050, compared with the simulation period 2012–2019. The increases are more pronounced during the dry season. Reference evapotranspiration increases as a result of rising temperatures, by 2.3% per year under SSP1-2.6 and 4.1% per year under SSP3-7.0.

Annual average precipitation should increase by 0.8% under SSP1-2.6 and decrease by 0.8% under SSP3-7.0. In both cases, rainfall should increase during the main wet season in October-November and decrease during the main wet season from June to August. Between January and May, precipitation should rise under SSP1-2.6 and drop under SSP3-7.0.

After rescaling the model forcings we can apply them to the hydrological and biological models to simulate the effect of climate change by comparing the simulated future projections for the climate change scenarios to the model baseline simulation. The temperature used in the peat decay equation (equation 2 in section 4) is increased by 0.92°C under SSP1-2.6 and 1.25°C under SSP3-7.0.

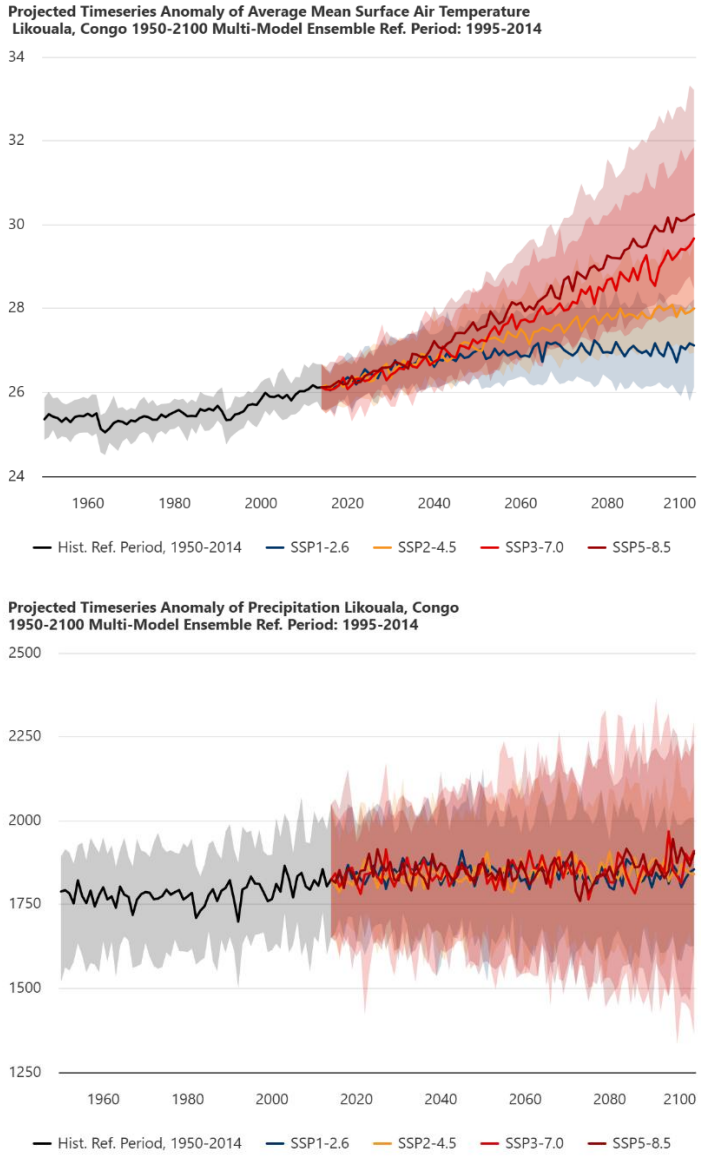

Figure 5.12 Projected changes in temperature (top) and precipitation (bottom) and uncertainties related (Source: Climate Change Knowledge Portal, Word Bank)
The p10 and p90 shading indicate the 10th and 90th percentile ranges among the different climate models in the ensemble, providing insight into the uncertainty or spread of projections.

In Figure 5.12, the p10 and p90 shading provide insight on the uncertainty of CMIP6 projections in the Likouala province in the Republic of Congo. While temperatures show a clear warming trend, the models of the multi-ensemble show very different results for precipitation. The significant uncertainties associated with the precipitation predictions in the region mean that the results of the climate change scenarios (section 8) should be interpreted with caution.

5.3 Hydrological Regions

The following hydrological regions are parts of the scenario definition:

Code	Name	Description
1	Rain-fed	Rainfall and Evapotranspiration only: The hydrological processes in the peatlands are only driven by rainfall and evapotranspiration. This is mostly the case in interfluvial peat domes, mostly located in the Republic of Congo.
2	River-fed	Rainfall and Evapotranspiration plus River Water Levels: The hydrological processes in the peatlands are driven by rainfall and evapotranspiration, as well as fluctuating water levels in bordering water bodies (e.g., river reaches). This is mostly the case in the riparian peatlands, mostly located in the Democratic Republic of Congo.

The hydrological regions are represented in the models as model boundary conditions: in the rainfall driven configuration, the western and eastern boundaries have a constant head set at surface level. These water levels fluctuate in the river-fed models. Boundary conditions are model drivers like the climate model drivers.

5.3.1 Rainfall driven conditions only

See section 3.2.

5.3.2 Rain- and river-fed conditions

See section 3.2.

Time varying river water levels are used as boundaries in the peat dome simulation to account for the seasonal variation of the water level, described in section 3.2.7. Climate change might lead to changing river flows which would affect the simulation results. Estimating the change in water level under a climate change scenario would require comprehensive modelling of the upstream catchment area under altered climatic conditions. This would entail substantial effort in terms of data acquisition, scenario development, and hydrological modelling. A simpler approach based on a literature review in the region is thus preferred here.

Using CORDEX regional downscaled climate change projections based on CMIP5, Karam et al. (2023) estimated that discharge in the Sangha, Oubangui and Likoula aux Herbes river is expected to decrease by 5% by 2041-2070 under RCP 4.5 (see Figure 5.13). This contrasts with a previous study from Tshimanga and Hughes (2012), who estimated decreases in discharge of 8% and 13% for the Sangha and Oubangui rivers respectively under IPCC scenario A2 using downscaled and bias corrected GCMs. Aloysius and Saiers (2017) forced a hydrological model of the Congo basin with climate projections from 25 global climate models and found that total runoff in the equatorial region of the basin is projected to increase by 7% by mid-century under RCP 4.5 and 8.5.

The important discrepancies between the studies mentioned above lead us to believe that it is reasonable to use the current water level timeseries at the model boundaries in the climate change scenarios without modifications. Besides, water discharge results can't be converted to water levels without evaluating river cross sections.

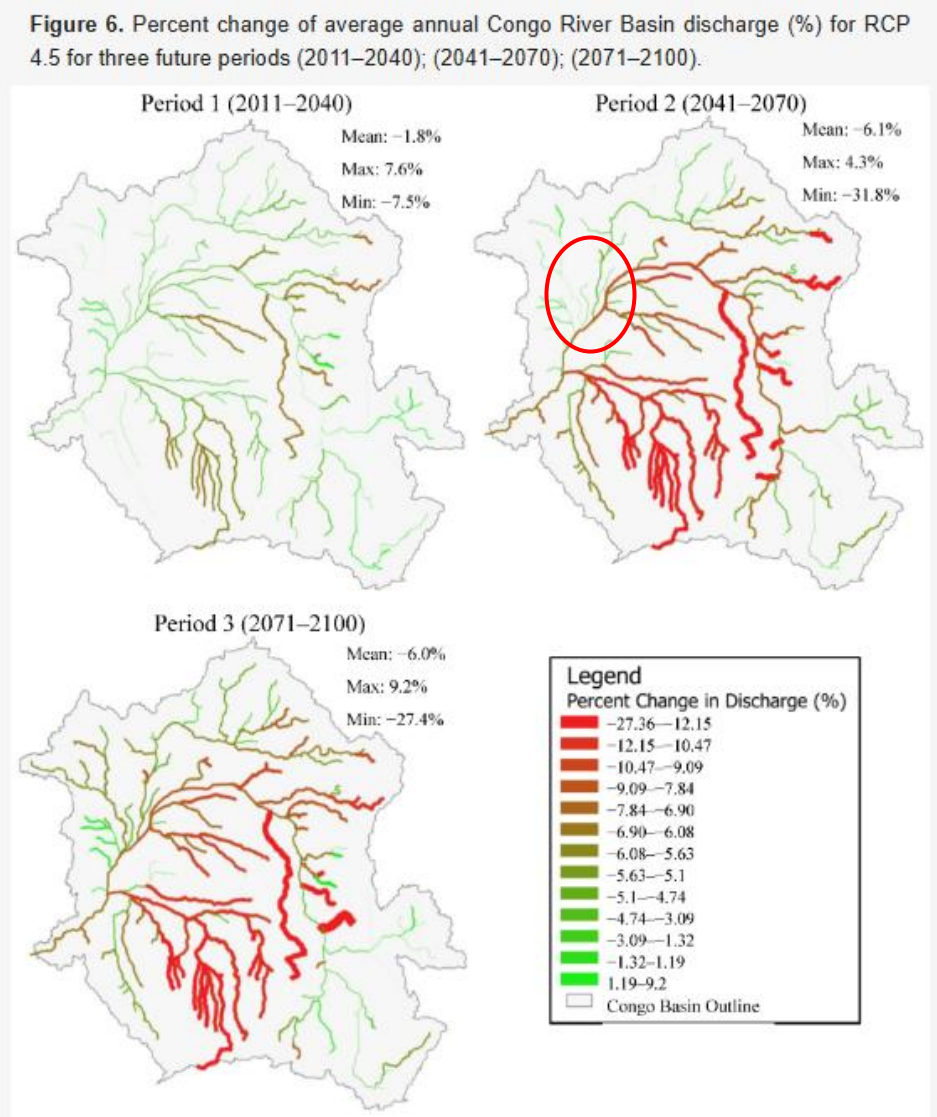

Figure 5.13 Climate change effects on discharges in the Congo basin taken from Karam, et al., 2023

5.4 Resulting Set of Scenarios

With 7 development interventions, 3 climate scenarios and 2 hydrological regions, the number of scenarios investigated is 42 = 7 x 3 x 2.

For example, scenario **B.3.2** is the representation of the following: What would happen in the peatlands under the following circumstances?

Development Intervention	**B**: Road Built and Operational: (a) A raised impervious road is built 1 meter above the natural surface. It is finished and operational. (b) Vegetation is removed, and the soil surface is flattened. (c) The road embankment is filled with permeable gravel. (d) The underlying peat is compressed due to the road's weight.
Climate	**3**: SSP3-7.0: (a) Projected warming: 3°C-4°C by 2100, with severe climatic consequences. (b) This scenario represents a high-risk future, characterized by significant climate change, social inequalities and environmental degradation.
Hydrological Region	**2**: Rainfall and Evapotranspiration plus River Water Levels: The hydrological processes in the peatlands are driven by rainfall and evapotranspiration, as well as fluctuating water levels in bordering water bodies (e.g., river reaches). This is the

mostly case in the riparian peatlands, mostly located in the Democratic Republic of Congo.

5.5 Scenario Evaluation Method with Indicators

Behind each scenario definition is a comprehensive model with its input parameters and simulation results. The evaluation of scenarios makes use of indicators that are derived from the detailed simulation results. The following indicators are defined to allow simplified evaluation of scenarios and comparisons:

CO2 emissions depend on the oxic depth, which itself is related to groundwater depth. When the mean water level is below ground, the oxic depth is lower than the depth of the groundwater table. At the groundwater table, the soil is fully saturated. The soil is considered oxic when saturation falls below 90%, i.e., when more than 10% of the pore space is filled with air. Capillary rise causes water to move upward in the soil column, so water content gradually decreases above the groundwater table until the oxic depth is reached. Oxic depth values are however higher than groundwater depth values when mean water levels are above ground. In this case, oxic depth is indeed set to 0 whereas groundwater depth is negative. Details to this topic are explained in detail in section 4.

Name	Indicator Description
Carbon Flux Inside	Carbon stock change in kg per m2 per year inside the footprint of the intervention
Carbon Flux Outside	Carbon stock change in kg per m2 per year outside the footprint of the intervention
Oxic Depth Inside	Average oxic depth inside the footprint of the intervention: Depth in the soil where oxygen is still present, affecting nutrient cycling, i.e., carbon transformations. This influences the rate of organic matter decomposition and thus carbon sequestration.
Oxic Depth Outside	Average oxic depth outside the footprint of the intervention: Depth in the soil where oxygen is still present, affecting nutrient cycling, i.e., carbon transformations. This influences the rate of organic matter decomposition and thus carbon sequestration.
GWT Depth Inside	Average ground water table depth inside the footprint of the intervention - in meters below the surface
GWT Depth Outside	Average ground water table depth outside the footprint of the intervention - in meters below the surface

Note to the indicator “Carbon stock change in kg per m2 per year” inside and outside the footprint of the intervention”:

The indicator is a normalized value per square meter which characterizes the impact on a unit area. Hence, for specific sizes of interventions, the decision maker needs to multiply the respective indicator values with the significant areas of the concrete interventions.

Example with assumptions: For a peatland area of 20 km x 20 km the decision maker wants to compare the following:

- Scenario A: the current situation (no intervention); reference area = 4 x 10^8 m^2 (400 km^2)
- Scenario B: Road Built and Operational, let one assume that the road is 30 m wide and traverses the peatland: road footprint area = 30 m x 20 x 10^3 m = 6 x 10^5 m^2; outside footprint area = 4 x 10^8 m^2 - 6 x 10^5 m^2 = 399.4 km^2

- Scenario F: Palm Plantation replaces Forest: let one assume that the plantation area is 10 km x 10 km: plantation footprint area = 10^8 m^2 (100 km^2); outside footprint area = 4 x 10^8 m^2 - 10^8 m^2 = 3 x 10^8 m^2 (300.0 km^2)

If we take for example the results for scenarios A.1.1, B.1.1 and F.1.1 (see chapters 6.1.3, 6.2.3 and 6.6.3 respectively) the carbon stock changes would be as follows:

- Scenario A: -4.716 kg/m^2/yea
- Scenario B: -17.975 kg/m^2/year inside the footprint and -2.905 kg/m^2/year outside the footprint
- Scenario F: -15.639 kg/m^2/year inside the footprint and -15.010 kg/m^2/year outside the footprint

Hence for the above example the carbon stock changes would be as follows

- Scenario A: -1.89 million tons/year
- Scenario B: -1.17 million tons/year if area of impact outside footprint is overestimated, -1.89 million tons/year (same as baseline) if impact outside footprint is neglected
- Scenario F: -6.09 million tons/year

6 Scenario Analyses for the current climate under rainfall driven conditions only

This section examines how various interventions affect groundwater depth and, consequently, carbon fluxes in the peatland. The focus is on the situation under current climate under rainfall driven conditions only (with fixed boundary water levels). The section is organised as follows: for each intervention, hydrological results are presented first, followed by carbon fluxes. Finally, recommendations are provided for policy makers and peatland managers.

6.1 Scenario A.1.1

6.1.1 Definition

What would happen in the peatlands under the following circumstances?

Development Intervention Vegetation and topography of the peatlands are according to the current conditions - between 2010 and 2020

Climate Rainfall, temperature and evapotranspiration between 2010 and 2020 are chosen to represent the current climate conditions.

Hydrological Region The hydrological processes in the peatlands are only driven by rainfall and evapotranspiration. This is the mostly case in the northern parts of the region.

6.1.2 Hydrological results

See section 3.3.

6.1.3 Indicators

See details in section 4.

Indicator Short Name	Indicator Value	Unit
Oxic Depth Inside/Outside	0.20	m
Groundwater Depth Inside/Outside	0.15	m
Carbon Flux Inside/Outside	-4.72	kg/m^2/year

6.1.4 Key Effects

(a) This baseline scenario reveals seasonal fluctuations in groundwater levels with a decreasing trend in groundwater levels as observed between 2012 and 2019. (b) Water levels range between 1 meter below ground and 50 centimetres above ground. (c) Spatial variability: Shallow groundwater tables are observed in flat central areas, while deeper groundwater tables are found at the steep edges of the dome.

6.1.5 Recommendations

Key threats to the peatlands are the following: (1) accelerated peat decomposition and carbon release, leading to the loss of millennia-old carbon stocks, (2) increased greenhouse gas emissions, and (3) the degradation of a globally significant carbon sink. These threats would be triggered by the following: (a) lowering of water tables, (b) climatic drying, (c) increased dry-season intensity and duration, (d)

enhanced overland water loss due to growing peat domes, (e) drainage (e.g., with canals and ditches) that would increase subsurface water loss.

Fostering development while preserving the peatlands needs to consider the following: (a) avoid activities that lower the water table (e.g., drainage, excessive water extraction), (b) protect against climate-induced drying by integrating peatland conservation into climate adaptation and mitigation strategies, (c) minimize land-use conversion, (d) regulate canal and ditch construction in peatland areas.

6.2 Scenario B.1.1

6.2.1 Definition

What would happen in the peatlands under the following circumstances?

Development Intervention	(a) A raised impervious road that requires 80 m width is built 1 meter above the natural surface. It is finished and operational. (b) Vegetation is removed, and the soil surface is flattened. (c) The road embankment is filled with permeable gravel. (d) The underlying peat is compressed due to the road's weight.
Climate	Rainfall, temperature and evapotranspiration between 2010 and 2020 are chosen to represent the current climate conditions.
Hydrological Region	The hydrological processes in the peatlands are only driven by rainfall and evapotranspiration. This is the mostly case in the northern parts of the region.

6.2.2 Hydrological results

Water levels in and around the intervention area are shown in Figure 6.1. In the intervention area (upper graphs), fluctuations are dampened compared to the baseline scenario. This is because the soil is sheltered by the paved surface, seepage and plant transpiration are disabled, and the aquifer is replenished only by lateral groundwater flow. Rainfall on the road runs off rapidly towards the lower neighbouring cells. This additional inflow explains why water levels in those cells are, on average, higher than in the baseline scenario (middle graphs). The effect diminishes further away from the road (lower graphs).

The road impacts the centre of the peat dome differently from the areas near the western and eastern boundaries. In the dome centre, water tables remain mostly above ground during the simulation period, whereas near the boundaries they are mostly below ground. Due to the specific yield characteristics of peat - where water table rises depends on pore space and hydraulic conductivity - a similar inflow from the road produces greater changes in the water table below the peat surface than above it (see middle left vs. middle right graphs). Near the boundaries, the water table drops quickly with distance from the road as water drains towards the boundary (lower left). In contrast, at the dome centre, the road's impact remains visible even 2 km away, with the water table up to 10 cm higher than in the baseline scenario (lower right).

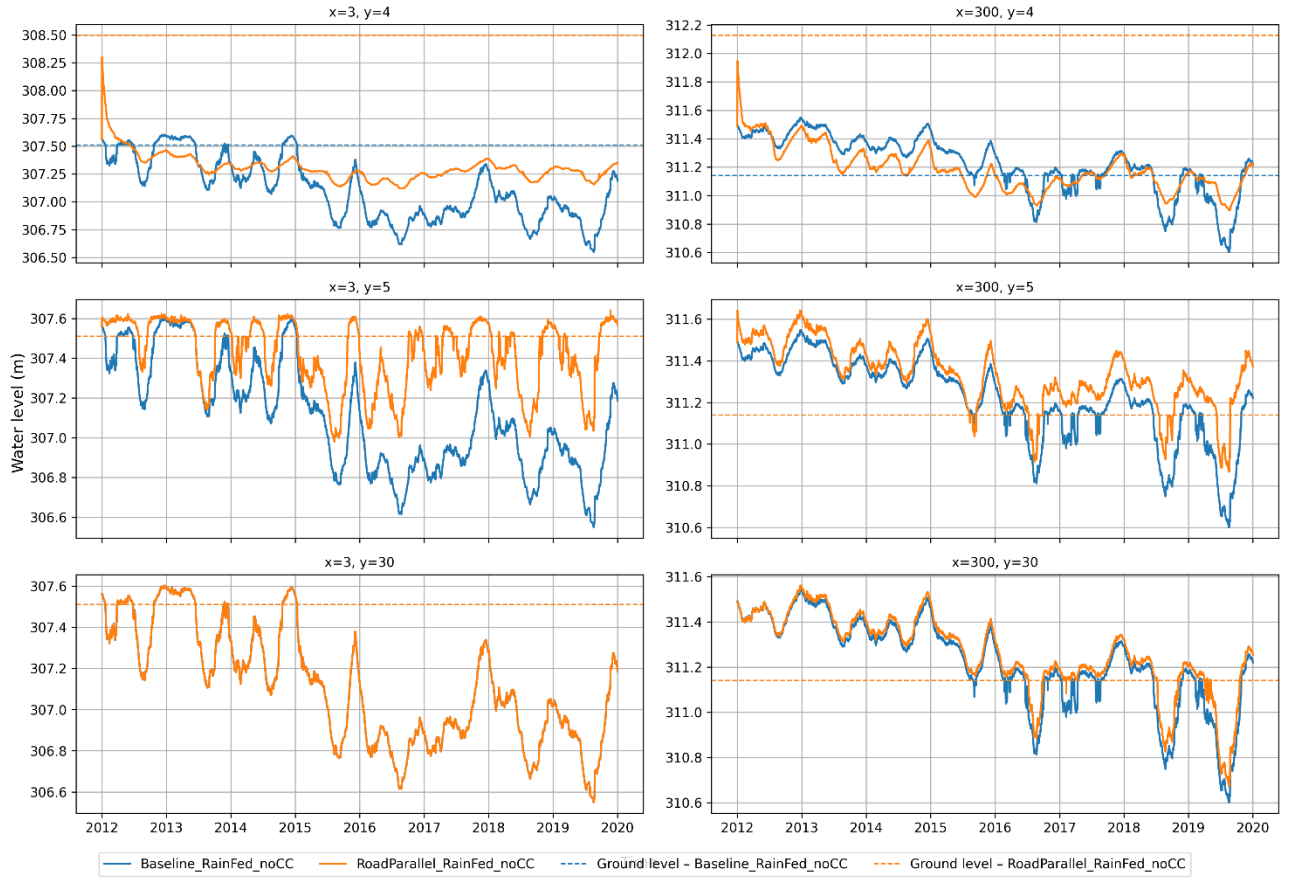

Figure 6.1 Water levels at six given locations within the model area: Scenario B.1.1 (RoadParallel_RainFed_noCC)

Figure 6.2 shows a y-directional water level profile at the centre of the peat dome at a given time. It illustrates the effect of the road on the local water table. Without seepage, the water level drops beneath the road but is elevated in the neighbouring cells due to overland inflow from the road surface. This effect gradually diminishes with distance from the road.

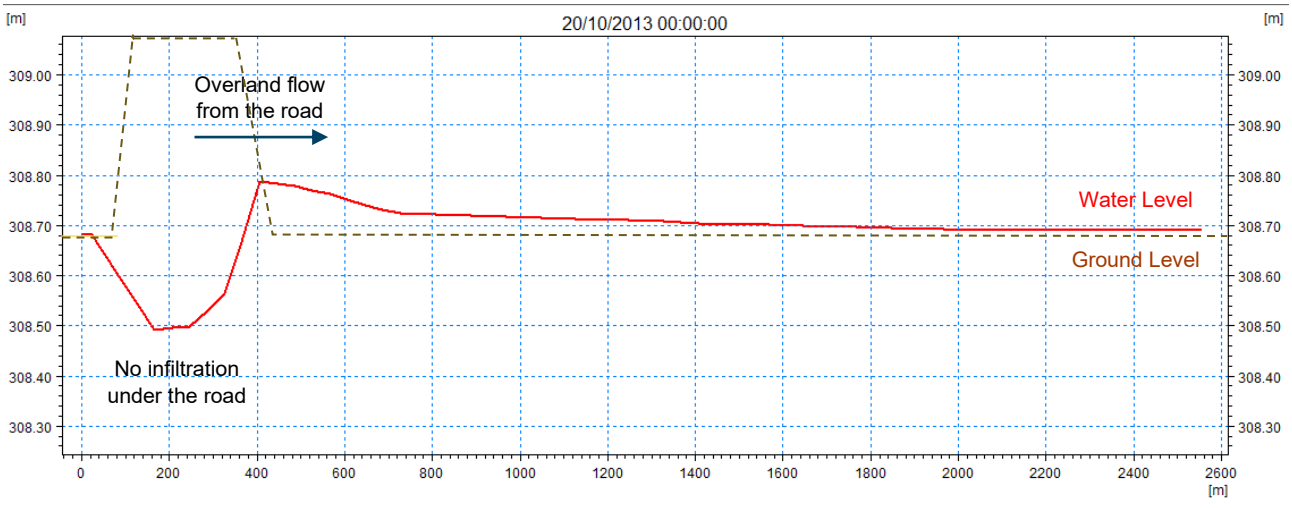

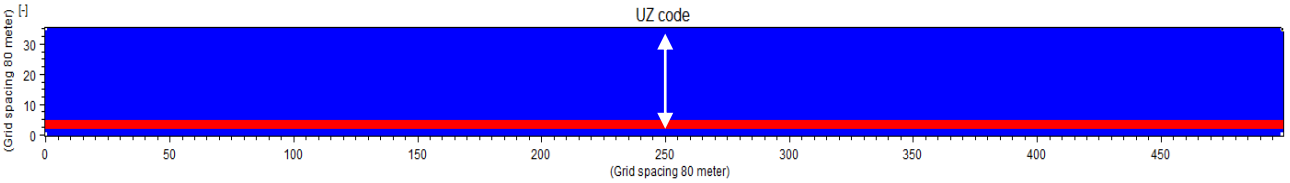

Figure 6.2 Y-directional Water level profile

6.2.3 Indicators

Indicator values are displayed in the table below. Oxic depth and groundwater table depth beneath the road are high because the road was raised by 1 m. This, however, does not appear to result in significant CO_2 emissions. Groundwater depths never exceed 2 m, which corresponds to the depth of the gravel embankment beneath the road. The underlying peat is therefore subject only to slow anoxic decay throughout the simulation.

Outside the road area, the mean groundwater table is shallower than in the baseline scenario (see hydrological results above). Here, the oxic depth exceeds the groundwater depth because the mean water table is above ground across much of the model's footprint, although it remains lower than in the baseline scenario. This lower oxic depth explains why the carbon flux outside the road is about half the flux in scenario A.1.1.

Indicator Short Name	**Indicator Value B.1.1**	*Indicator Value A.1.1*	**Unit**
Oxic Depth Inside	0.92	*0.20*	m
Groundwater Depth Inside	1.06	*0.15*	m
Carbon Flux Inside	0.00	*-4.72*	kg/m^2/year
Oxic Depth Outside	0.13	*0.20*	m
Groundwater Depth Outside	0.05	*0.15*	m
Carbon Flux Outside	-2.90	*-4.72*	kg/m^2/year

A spatial representation of carbon fluxes (see Figure 6.3) shows that building an undrained road reduces peat decay in the surrounding cells, although it is still significant near the western and eastern boundaries.

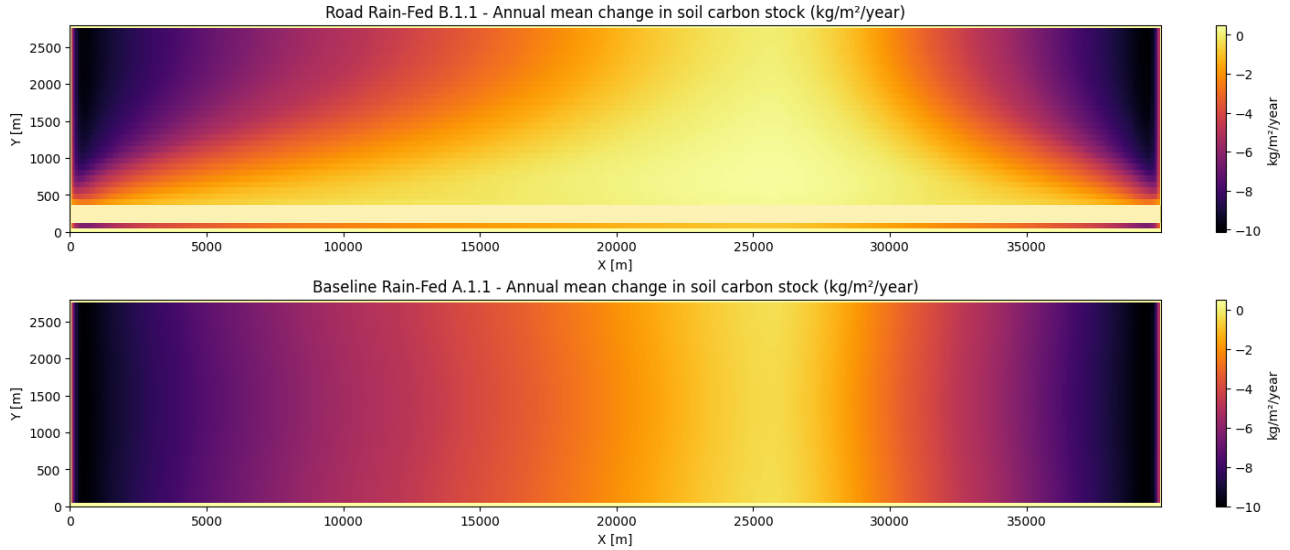

Figure 6.3 Annual mean soil carbon fluxes – Road (B.1.1) vs Baseline (A.1.1)

6.2.4 Key Effects

(a) Infiltration does not occur directly on the road; precipitation flows over the surface to adjacent lower-lying areas, where it infiltrates and recharges the aquifer. (b) The raised road increases the depth to groundwater beneath it. (c) Water levels increase near the road, with influence decreasing with distance from the road. (d) As a result, peat decay is reduced compared to current conditions (baseline).

6.2.5 Recommendations

The influence of the road generally extends as far as 2 km from its edge. The slope of the surface near the road would be altered, and hence the infiltration and surface flow patterns would change. This may lead to long-term and irreversible drying of the soil along the road.

Recommended measures to mitigate these effects are the following: In a buffer zone along the road, maintain the moisture of the peatlands by: (1) rewetting - block drainage canals and ditches to raise the water table and restore natural hydrology; and (2) vegetation management - promote native, water-retaining vegetation (like swamp forest species) that helps shade the peat and reduce evaporation.

6.3 Scenario C.1.1

6.3.1 Definition

What would happen in the peatlands under the following circumstances?

Development Intervention	(a) A raised impervious road that requires 80 m width is being built 1 meter above the natural surface. (b) Vegetation is removed, and the soil surface is flattened. (c) The road embankment is filled with permeable gravel. (d) The underlying peat is compressed due to the road's weight. (e) During construction drainage is installed 2 meters below the ground, i.e., 1 meter below the surrounding surface.
Climate	Rainfall, temperature and evapotranspiration between 2010 and 2020 are chosen to represent the current climate conditions.
Hydrological Region	The hydrological processes in the peatlands are only driven by rainfall and evapotranspiration. This is the mostly case in the northern parts of the region.

6.3.2 Hydrological results

Water levels in and around the intervention area are shown in Figure 6.4. Within one month, water levels beneath the road drop to the drain level, 2 m below ground (upper graphs). Drainage also affects neighbouring cells, where the water table is deeper than in the baseline scenario near the centre of the dome despite the inflow of runoff from the road surface (middle right). The impact of drainage remains significant even 2 km away from the road, where water levels near the dome centre are 1 m lower than in the baseline scenario at the end of the simulation (lower right). Differences between the two scenarios are less pronounced near the western and eastern boundaries, as the groundwater table in those areas is already deep in the baseline scenario (left).

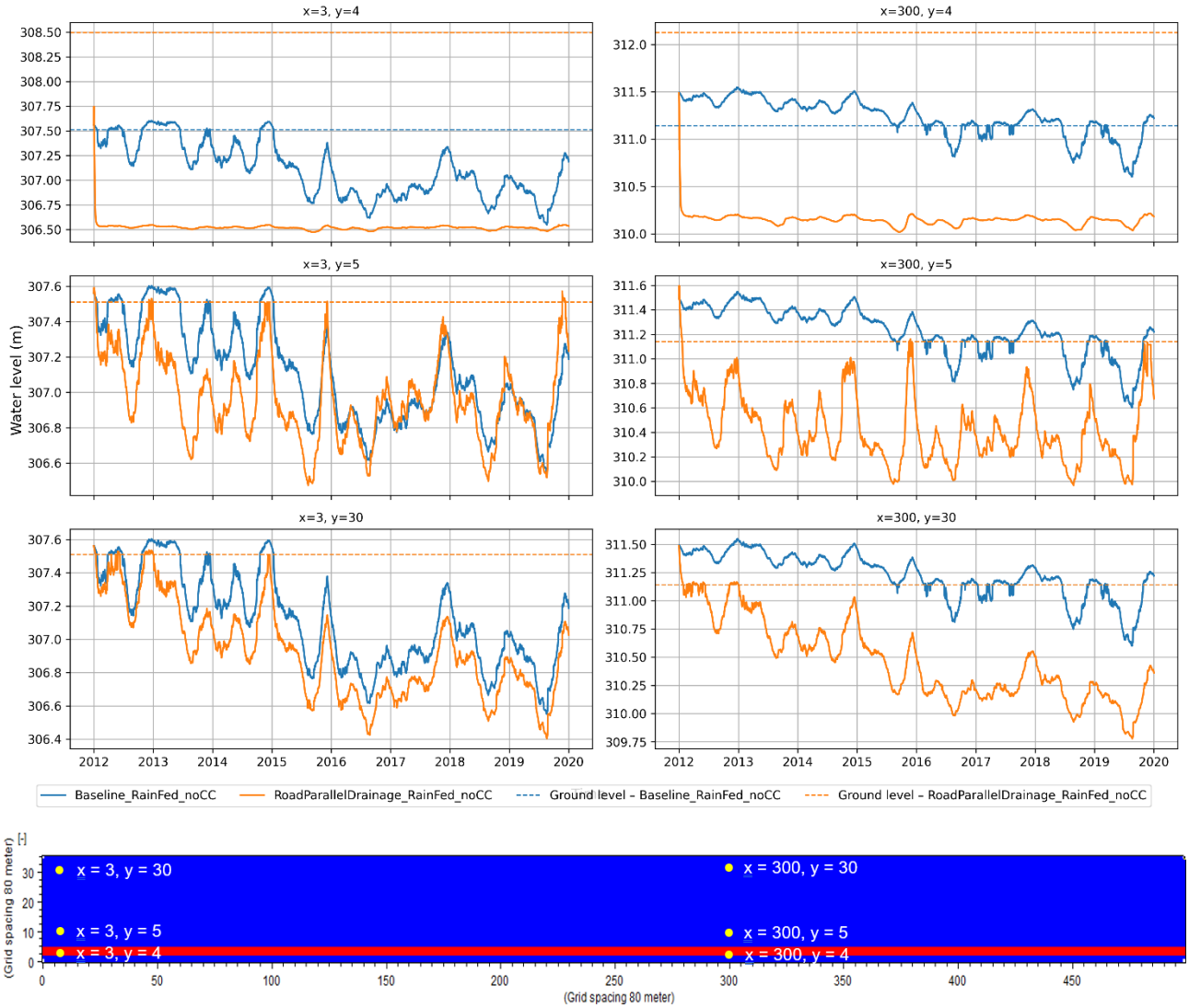

Figure 6.4 Water levels at six given locations within the model area, Scenario C.1.1 (RoadParallelDrainage_RainFed_noCC)

6.3.3 Indicators

Indicator values are displayed in the table below. Like in scenario B.1.1, oxic depth and groundwater table depth beneath the road are high because the road was raised by 1 m. This does not result in significant peat decay as groundwater depths rarely exceed 2 m, which corresponds to the depth of the gravel embankment beneath the road. The underlying peat is therefore subject only to slow anoxic decay throughout the simulation.

Indicator Short Name	Indicator Value C.1.1	*Indicator Value A.1.1*	Unit
Oxic Depth Inside	2.12	*0.20*	m
Groundwater Depth Inside	2.00	*0.15*	m
Carbon Flux Inside	0.00	*-4.72*	kg/m^2/year
Oxic Depth Outside	0.68	*0.20*	m
Groundwater Depth Outside	0.68	*0.15*	m
Carbon Flux Outside	-14.26	*-4.72*	kg/m^2/year

Unlike in the baseline scenario A.1.1, peat decay is very high throughout the whole model domain, showing the major influence drainage has on water levels (see Figure 6.5).

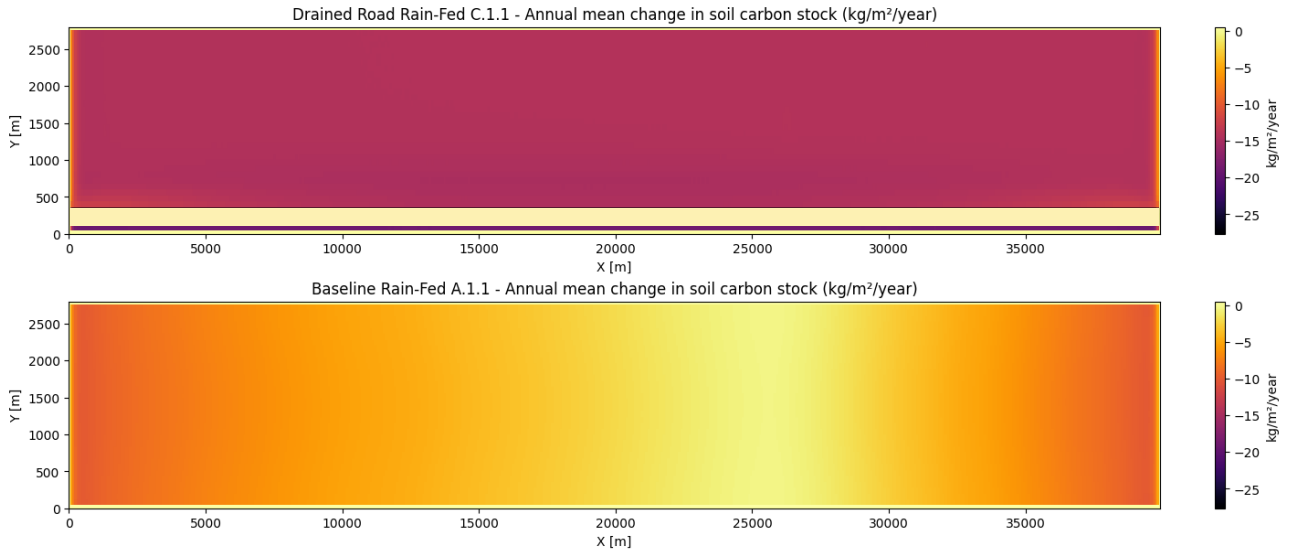

Figure 6.5 Annual mean change in soil carbon stock – Drained Road (C.1.1) vs Baseline (A.1.1)

6.3.4 Key Effects

(a) Groundwater levels stabilize at 2 meters depth under the road. (b) Drainage influence extends beyond the intervention area, reducing groundwater levels in adjacent zones. (c) Peat decay is increased because of the low water levels in the adjacent zones.

6.3.5 Recommendations

The effects of drainage during construction are substantial. The aim therefore is to limit their impact as far as possible.

During construction the following needs to be considered: (1) temporary drainage systems - design drainage that minimizes water table drawdown and is easy to remove or block after construction; (2) install silt fences and sediment traps; (3) limit drainage duration; (4) rewet immediately after construction - block temporary ditches and allow natural water levels to return quickly; (5) use low-impact construction techniques - employ raised roads, geotextiles, or matting to reduce soil compaction and water flow disruption; (6) restore vegetation promptly - plant native wetland species to stabilize soil and help retain moisture.

6.4 Scenario D.1.1

6.4.1 Definition

What would happen in the peatlands under the following circumstances?

Development Intervention	(a) A settlement is developed in the peatland forest. (b) The topography is raised by 50 cm to prevent flooding. (c) Vegetation is cleared, and the soil surface is partially paved. (d) The peat is compressed under the load of buildings.
Climate	Rainfall, temperature and evapotranspiration between 2010 and 2020 are chosen to represent the current climate conditions.
Hydrological Region	The hydrological processes in the peatlands are only driven by rainfall and evapotranspiration. This is the mostly case in the northern parts of the region.

6.4.2 Hydrological results

Water levels in and around the intervention area are shown in Figure 6.6. In the elevated settlement (upper graphs), water table levels are higher than in the baseline scenario, especially along the western and eastern boundaries. The water table rises in the soil column because peat has a strong capillary potential. Besides, since vegetation is cleared in scenario D.1.1, there is no transpiration. During wet periods, transpiration is compensated by evaporation from the soil surface, so the total evaporated volume is the same as in scenario A.1.1. The total water content and the specific yield of the peat are reduced due to compression by the settlement. This reduction in storable volume means that there is less water available for evaporation from the topsoil layer during dry times.

Thus, because of capillary rise under the elevated settlement and as evapotranspiration is lower than in the baseline scenario, the water table does not show the same gradual decline observed in the baseline simulation. The influence of the settlement is also visible in the neighbouring cells where the water table is shallower than the baseline (middle graphs). Water table depths in the settlement are initially much higher than in the baseline scenario but gradually converge toward it over time.

Due to the specific yield characteristics of peat - where water table rise depends on pore space and hydraulic conductivity - the water table fluctuates more below the peat surface than above it (see middle left vs. middle right graphs). Near the boundaries, the water table drops quickly with distance from the settlement as water drains towards the boundary (lower left). Around the centre of the peat dome, water levels fluctuate much more under the settlement than in the baseline scenario during the first half of the simulation, given that the topography was raised by 50 cm and the water table is below ground instead of above ground (upper right).

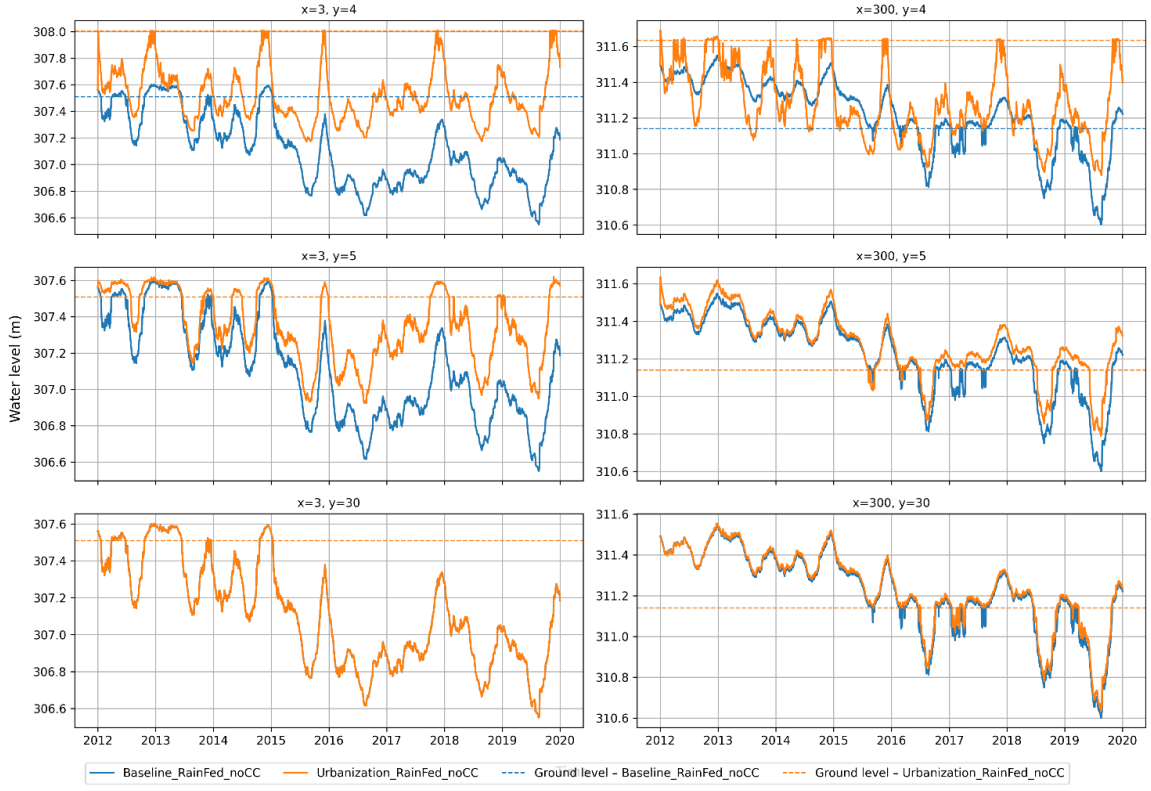

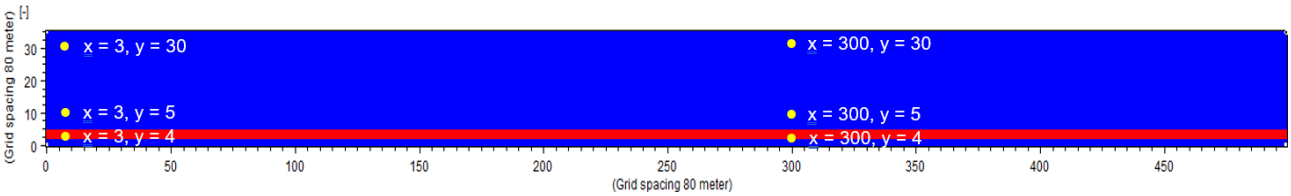

Figure 6.6 Water levels at six given locations within the model area, Scenario D.1.1 (Urbanization_RainFed_noCC)

6.4.3 Indicators

Indicator values are displayed in the table below. Oxic depth and groundwater table depth beneath the urbanized area are higher than the baseline scenario because the settlement was raised by 50 cm. This results in a significant loss of soil carbon stock. Outside the settlement area, the mean groundwater table is shallower than in the baseline scenario (see hydrological results above). Oxic depth is reduced, leading to lower peat decay than in scenario A.1.1.

Indicator Short Name	Indicator Value D.1.1	*Indicator Value A.1.1*	Unit
Oxic Depth Inside	0.37	*0.20*	m
Groundwater Depth Inside	0.40	*0.15*	m
Carbon Flux Inside	-8.77	*-4.72*	kg/m^2/year
Oxic Depth Outside	0.16	*0.20*	m
Groundwater Depth Outside	0.10	*0.15*	m
Carbon Flux Outside	-3.80	*-4.72*	kg/m^2/year

A spatial representation of the mean change in soil carbon stock (see Figure 6.7) shows that building a settlement increases sharply peat decay in the settlement footprint and reduces it in the surrounding cells, although it is still significant near the western and eastern boundaries.

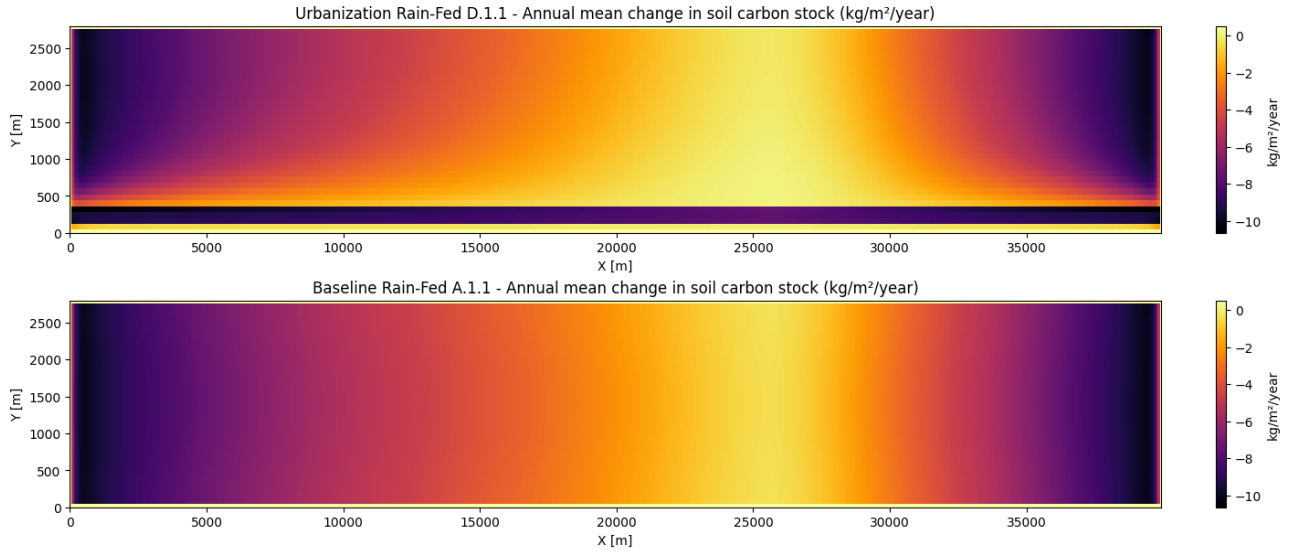

Figure 6.7 Annual mean change in peat carbon stock – Settlement (D.1.1) vs Baseline (A.1.1)

6.4.4 Key Effects

(a) Raising the settlement ground results in deeper groundwater tables. (b) Mean water levels rise outside the urban footprint, but the effect fades with distance. (c) Peat decay outside the intervention zone is reduced due to higher mean water levels.

6.4.5 Recommendations

Building a settlement in the peatlands would have serious environmental consequences, such as (1) lower water table, (2) as a result, increased peat decay, (3) land subsidence, and (4) increased fire risk.

Mitigation measures to consider are: (a) zoning - use land-use planning to steer development elsewhere; (b) minimal drainage design - use raised foundations or boardwalks to reduce the need for drainage and soil disturbance; (c) hydrological buffer zones - maintain surrounding wetland areas to preserve natural water flow and moisture; (d) fire prevention plans - implement fire breaks, community awareness, and emergency response systems.

6.5 Scenario E.1.1

6.5.1 Definition

What would happen in the peatlands under the following circumstances?

Development Intervention	(a) A forest fire completely clears the vegetation. (b) As a result, soil properties change: bulk density increases, and specific yield decreases.
Climate	Rainfall, temperature and evapotranspiration between 2010 and 2020 are chosen to represent the current climate conditions.
Hydrological Region	The hydrological processes in the peatlands are only driven by rainfall and evapotranspiration. This is the mostly case in the northern parts of the region.

6.5.2 Hydrological results

Water levels in and around the intervention area are shown in Figure 6.8. Near the western and eastern boundaries, water table levels in the burnt area are higher than in the A.1.1 baseline scenario during the second half of the simulation period (see upper left graph). Since no vegetation remains in scenario E.1.1, there is no transpiration. During wet periods, transpiration is compensated by evaporation from the soil surface, so the total evaporated volume is the same as in scenario A.1.1. From 2015 onwards, however, moisture content in the topsoil layer drops below field capacity, meaning that less water is available for evaporation. As a result, the water table gradually rises above the baseline scenario. This increase in water table level is also noticeable just outside the burnt area (middle left).

At the centre of the peat dome (upper right), the water table is shallower than near the boundaries, which prevents the topsoil moisture content from dropping below field capacity, even during dry periods. Evapotranspiration is therefore the same as in the baseline scenario. However, the water table falls deeper during dry seasons because the field capacity of burnt peat is reduced compared to untouched peat. For a given evaporated volume, a lower field capacity results in a greater drop in water level.

Given that the fire smoothed the terrain microtopography, the burnt area acts as a preferential flow path which is why the overland water depth is reduced compared to the baseline (upper left). The overland outflow may also explain why water tables below ground are also lower during the first half of the simulation period (upper and middle left).

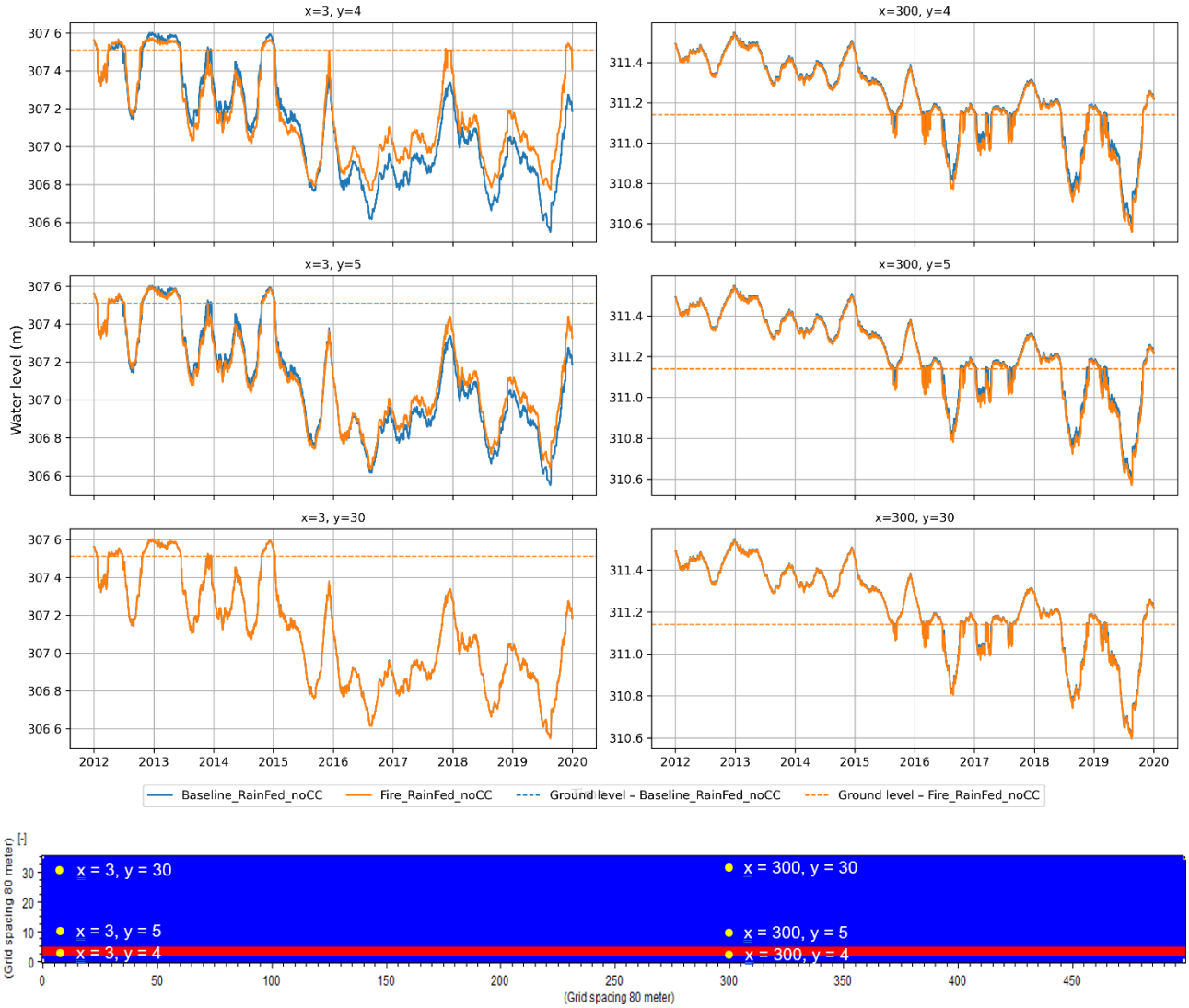

Figure 6.8 Water levels at six given locations within the model area, Scenario E.1.1 (Fire_RainFed_noCC)

6.5.3 Indicators

Indicator values are displayed in the table below. Reduced evapotranspiration in the burnt zone results in higher soil moisture contents and therefore lower mean oxic depths. Lower oxic depths don't translate here into a lower net carbon outflow from the burnt zone. Indeed, this effect is offset by the absence of litter production/carbon storage in the burnt area. Outside of the intervention area, differences between scenarios E.1.1 and A.1.1 are small.

Indicator Short Name	Indicator Value E.1.1	*Indicator Value A.1.1*	Unit
Oxic Depth Inside	0.18	*0.20*	m
Groundwater Depth Inside	0.14	*0.15*	m
Carbon Flux Inside	-4.67	*-4.72*	kg/m^2/year
Oxic Depth Outside	0.20	*0.20*	m
Groundwater Depth Outside	0.16	*0.15*	m
Carbon Flux Outside	-4.78	*-4.72*	kg/m^2/year

The spatial distribution of the mean change in carbon stock within the model area shows that similar average fluxes in both scenarios conceal spatial differences: in the burnt area, there is slightly more peat decay than in the baseline scenario near the centre of the peat dome and less near the western and eastern boundaries (Figure 6.9).

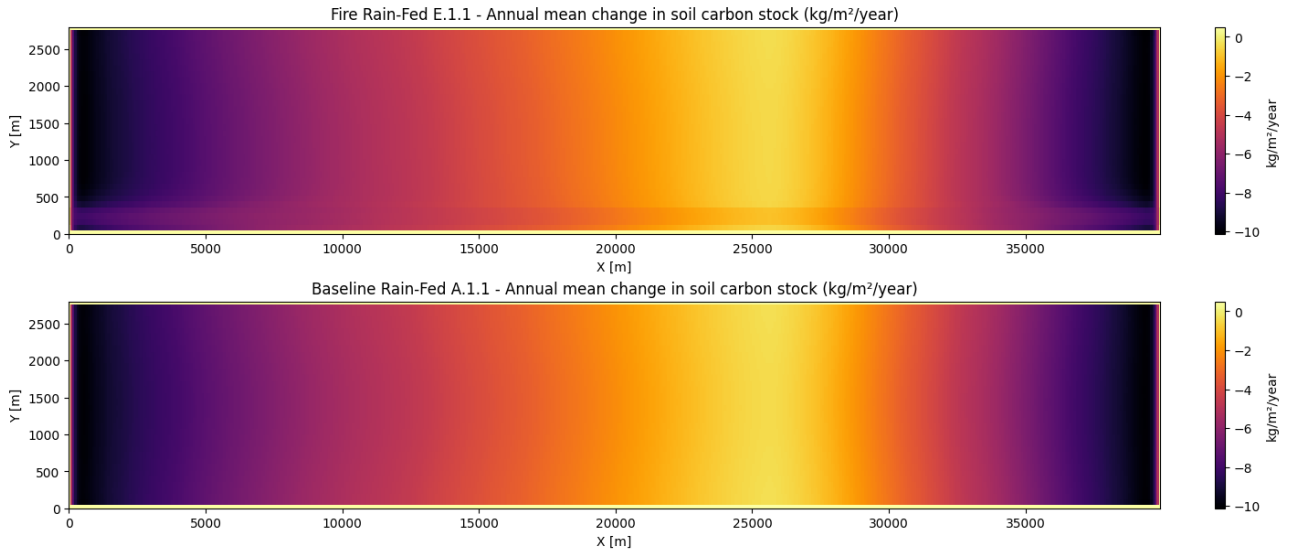

Figure 6.9 Annual mean change in soil carbon stock – Fire (E.1.1) vs Baseline (A.1.1)

As oxic decay is preponderant, it can be assumed that the soil carbon decays through CO_2 emissions, amounting to 17.11 kg CO_2-C m^{-2} yr^{-1} in the footprint. Hirano et al. (2012) compared CO2 emissions across untouched peatlands and burnt swamp forest in Kalimantan, Indonesia and found that they are much higher in burnt forests (18.30 +- 2.64 kg CO2/m²/yr) than in untouched peatlands (6.38 +- 7.47 kg CO2/m²/yr). This important difference in carbon fluxes between both peatlands contrasts with the simulated results presented above.

6.5.4 Key Effects

(a) Compared to baseline conditions, groundwater levels increase in dry seasons along the boundaries but decrease in the rest of the dome. (b) Outside the fire footprint, water levels are like those of the baseline scenario. (c) Within the intervention zone, the mean change in soil carbon stock is similar to the baseline as the decrease in emissions due to shallower oxic depths is offset by the absence of carbon storage by the burnt vegetation. No significant change in carbon fluxes outside the intervention area.

6.5.5 Recommendations

Recommendations to mitigate forest fire effects: (1) vegetation loss prevention with firebreaks and controlled burns; (2) water tables maintaining or restoring by rewetting (block drainage channels and restore natural hydrology to keep peat moist and reduce fire risk) and by building water retention structures (use bunds or small dams to retain water during dry seasons); (3) post-fire restoration with revegetation (replant native peatland species to stabilize soil and restore evapotranspiration) and soil amendment (use organic mulches or biochar to improve soil structure and water retention).

6.6 Scenario F.1.1

6.6.1 Definition

What would happen in the peatlands under the following circumstances?

Development Intervention	Deforestation and Conversion to Oil Palm Plantations: (a) Natural vegetation is cleared to establish additional oil palm plantations. (b) Oil palms thrive with a mean water level 40 cm to 60 cm below ground. There is drainage at 50 cm depth. (c) Vegetation properties are altered according to 15-year-old mature oil palm plantation. (d) The microtopography is smoothed due to clearing. (e) Soil properties change by drainage: increased bulk density, reduced specific yield, and reduced hydraulic conductivity at saturation. (f) The topography is lowered by 50 cm due to soil subsidence induced by drainage.
Climate	Rainfall, temperature and evapotranspiration between 2010 and 2020 are chosen to represent the current climate conditions.
Hydrological Region	The hydrological processes in the peatlands are only driven by rainfall and evapotranspiration. This is the mostly case in the northern parts of the region.

6.6.2 Hydrological results

Water levels in and around the intervention area are shown in Figure 6.10. Within one month, water levels near the centre of the peat dome beneath the plantation drop to the drain level, 50 cm below ground (upper right). As in the baseline scenario, the water table follows a downward trend throughout the simulation and falls below the drain level. Drainage and soil subsidence under the plantation also affect the neighbouring cells, where the water table is 1 to 1.5 m deeper than in the baseline scenario (middle right). Even 2 km away from the oil palm plantation, the water table remains much lower than in the baseline scenario (lower right).

Differences between the two scenarios are less pronounced near the western and eastern boundaries, since the groundwater table in those areas is already deep in the baseline scenario (left). In the cells near the boundaries, the ground surface under the plantation lies up to 50 cm below the water level at the boundary. As a result, the plantation cells near the boundary receive overland runoff from the boundary, which explains why the water table beneath the plantation remains shallower than the drain level during the first half of the simulation period (upper left).

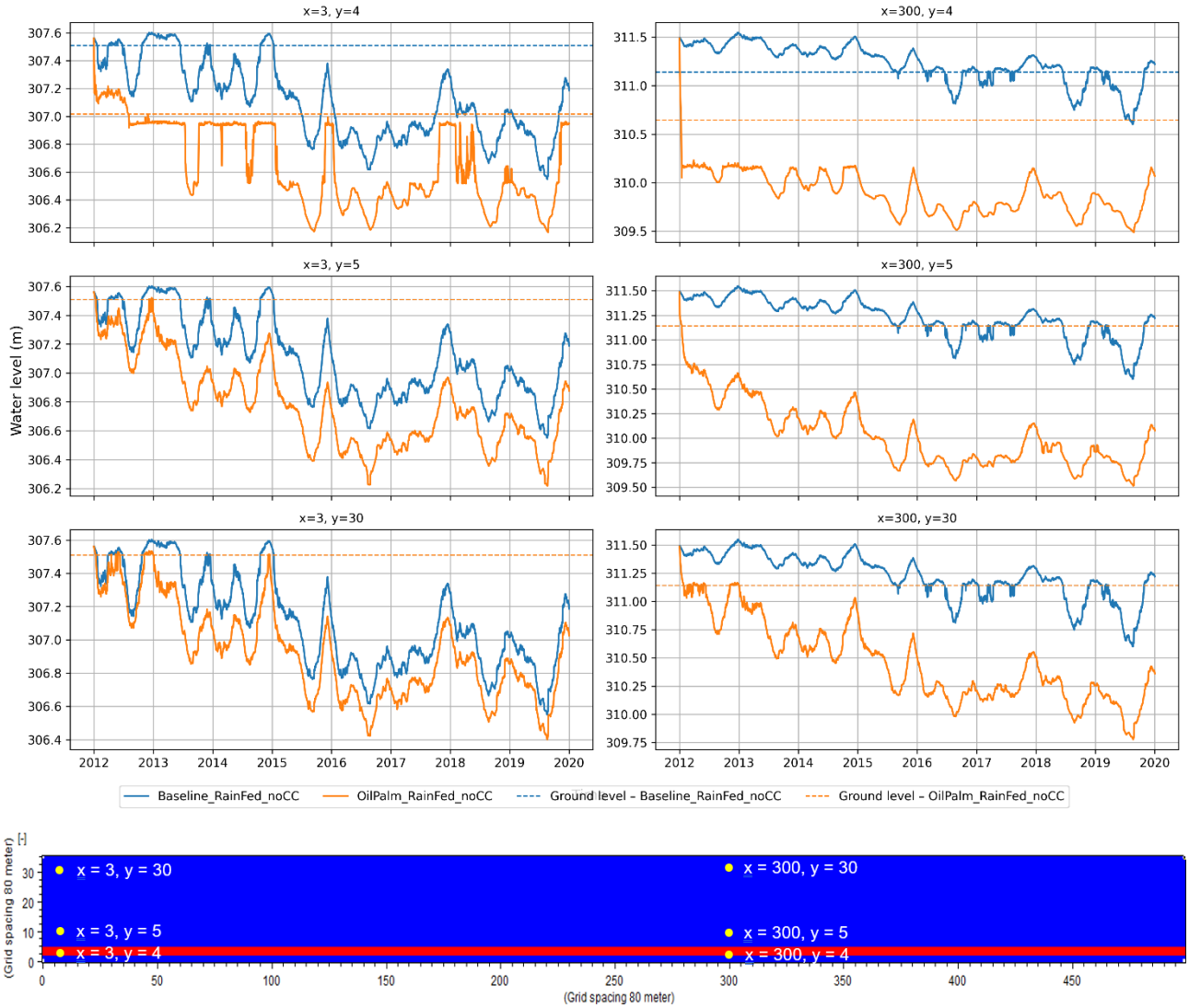

Figure 6.10 Water levels at six given locations within the model area, Scenario F.1.1 (OilPalm_RainFed_noCC)

6.6.3 Indicators

Indicators are displayed in the table below. The groundwater table in and around the plantation is lower than in the baseline scenario (see hydrological results above), which results in 3 times more carbon outflow.

Indicator Short Name	Indicator Value F.1.1	*Indicator Value A.1.1*	Unit
Oxic Depth Inside	0.77	*0.20*	m
Groundwater Depth Inside	0.79	*0.15*	m
Carbon Flux Inside	-15.64	*-4.72*	kg/m^2/year
Oxic Depth Outside	0.73	*0.20*	m
Groundwater Depth Outside	0.73	*0.15*	m
Carbon Flux Outside	-15.01	*-4.72*	kg/m^2/year

A spatial representation of the annual change in soil carbon stock reveals that the carbon stock is more depleted near the plantation footprint than in the footprint itself (see Figure 6.11). Indeed, although water levels in and around the plantation footprint are close, the ground surface has subsided under the plantation, resulting in a shallower oxic zone. As in the drained road scenario, peat decay is very high across the entire model domain, highlighting the strong influence of drainage on water levels.

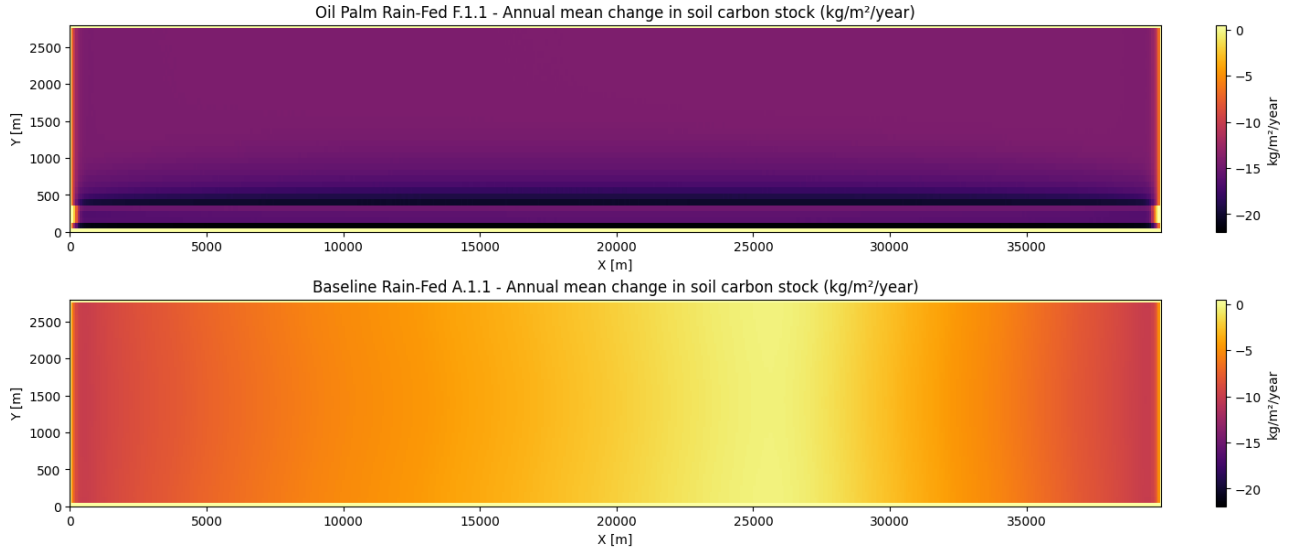

Figure 6.11 Annual mean change in soil carbon stock – Oil Palm Plantation (F.1.1) vs Baseline (A.1.1)

As oxic decay is preponderant, it can be assumed that the soil carbon decays through CO_2 emissions, amounting to 57.34 kg CO_2-C m^{-2} yr^{-1} in the footprint. Simulated net CO2 emissions can be compared to measurements from Indonesia.

McCalmont et al. (2021) measured net emissions of 13.8 kg CO2/m²/yr in peatlands newly converted to drained oil palm plantations and 1.75 kg CO2/m²/yr in mature oil palm peatlands. These measurements are lower than the net emissions simulated here in oil palm plantations. The authors suggested that their estimates may be a conservative estimate for mature plantations as the mean water table depth is shallower (0.26 m) than a typical target of 0.6 m, whereas it was more typical (0.54 m) in the newly converted plantation. The mean water depth in newly converted plantations is still lower than the mean water depth simulated here, which may partly explain the lower net CO2 emissions.

Hirano et al. (2012) measured for 4 years net CO2 exchange in untouched peatlands and peatlands drained for agriculture. They found out that CO2 emissions in drained agricultural peatlands (12.0 +- 7.48 kg CO2/m²/yr) were twice higher than in untouched peatland (6.38 +- 7.47 kg CO2/m²/yr). Both studies may indicate that the carbon emissions simulated here in scenario F.1.1 are overestimated. Nevertheless, Hirano et al. (2012) analyzed the CO2 emissions timeseries and found out that the lowering of annual-mean groundwater level by 0.1 m increases annual net CO2 emissions by 8.73 and 5.90 kg CO2/m², respectively, for the untouched and drained peatland. These figures indicate that a quick drop in groundwater level due to drainage may have drastic consequences on CO2 emissions and are in line with our estimates.

Hooijer et al. (2006) derived a relation between CO_2 emissions and water table depth in peatlands from gas flux measurements found in literature (see Figure 6.12). The indicator results presented above feat well with the trendline for the tropics. For the baseline model, CO_2 emissions of 17.29 kg CO2/m²/yr are estimated for an average groundwater depth of 15cm, whereas a value of 14 kg CO2/m²/yr is found applying the relation of Hooijer et al. to a similar water table depth. For the oil palm intervention with an estimated average water table depth of 73 cm, results are also quite similar, with estimated CO_2 emissions of 57.34 kg CO2/m²/yr in the present study vs 66 kg CO2/m²/yr applying the relation of Hooijer et al..

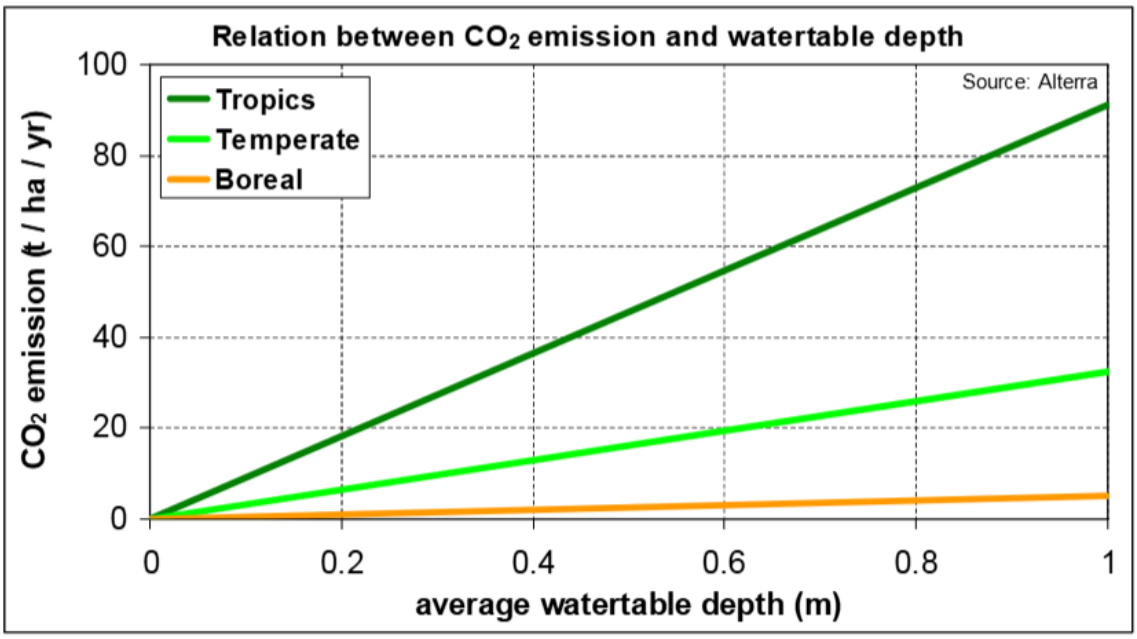

Figure 6.12 Empirical relation between CO2 emissions and water table depth
Source: Hooijer et al, 2006

6.6.4 Key Effects

(a) Groundwater levels under the plantation are lower than in the baseline situation, driven by drainage and soil subsidence. (b) A decrease in groundwater levels is observed throughout the area. (c) Peat decay increases due to lower water levels.

6.6.5 Recommendations

Recommendations for mitigation: (1) hydrological management: (a) shallow drainage design by raising drainage depth closer to the surface (e.g., 30–40 cm) to reduce peat oxidation while still supporting oil palm growth, (b) controlled drainage systems by using adjustable weirs or gates to manage seasonal water levels dynamically, (2) soil subsidence reduction: (a) minimize drainage intensity by reducing the duration and depth of drainage to slow peat decomposition and subsidence, (b) use ground covers by planting understory vegetation to reduce evaporation and protect soil structure, (3) vegetation and biodiversity buffers: retain natural vegetation strips by maintaining forested buffer zones along waterways and peat domes to preserve biodiversity and hydrological function, (4) carbon emission mitigation: rewetting of degraded areas by restoring abandoned or marginal plantation zones and reforesting, (5) topography and microtopography restoration: (a) avoid smoothing natural microtopography by preserving hummock-hollow structures to maintain water retention and habitat diversity, (b) rebuild surface layers by using in degraded areas organic mulches or compost to rebuild lost peat and improve water retention.

6.7 Scenario G.1.1

6.7.1 Definition

What would happen in the peatlands under the following circumstances?

Development Intervention Deforestation and Conversion to Rice Cultivation: (a) Natural vegetation is removed and replaced with rice paddies. Rice is the most common seasonally flooded crop in the Cuvette Centrale. (b) There are two harvests per year. Paddies are flooded during the wet season. (c) Vegetation and surface properties/roughness vary with crop stage.

Climate	Rainfall, temperature and evapotranspiration between 2010 and 2020 are chosen to represent the current climate conditions.
Hydrological Region	The hydrological processes in the peatlands are only driven by rainfall and evapotranspiration. This is the mostly case in the northern parts of the region.

6.7.2 Hydrological results

Water levels in and around the intervention area are shown in Figure 6.13. Near the western and eastern boundaries, water table levels in the rice paddies are higher than in the A.1.1 baseline scenario during the second half of the simulation period (see upper left graph). During the growth and ripening stages, the Leaf Area Index (LAI) and root depth are lower in scenario E.1.1 than in the baseline scenario (see Section 5.1.1), and transpiration is therefore reduced. At these times, the decrease in transpiration is only partially offset by evaporation from the soil surface, so total evapotranspiration is lower than in scenario A.1.1. When the water level drops during these crop phases, moisture content in the topsoil falls below field capacity, meaning less water is available for evaporation. As a result, the water table gradually rises above the baseline scenario once the climate becomes drier from 2015 onwards. This increase in water table level is also visible just outside the rice paddies (middle left).

At the centre of the peat dome (upper right), the water table is shallower than near the boundaries, which prevents the topsoil moisture content from dropping below field capacity, even during dry periods. Evaporation is therefore the same as in the baseline scenario. However, transpiration is slightly lower during the rice growth and ripening phases, which explains why the water table is shallower at the end of the simulation.

Given that the conversion to rice crops smoothens the terrain microtopography, the paddies act as a preferential flow path which is why the overland water depth is reduced compared to the baseline (upper left). The overland outflow explains why water tables are lower below ground during the first half of the simulation period (upper and middle left).

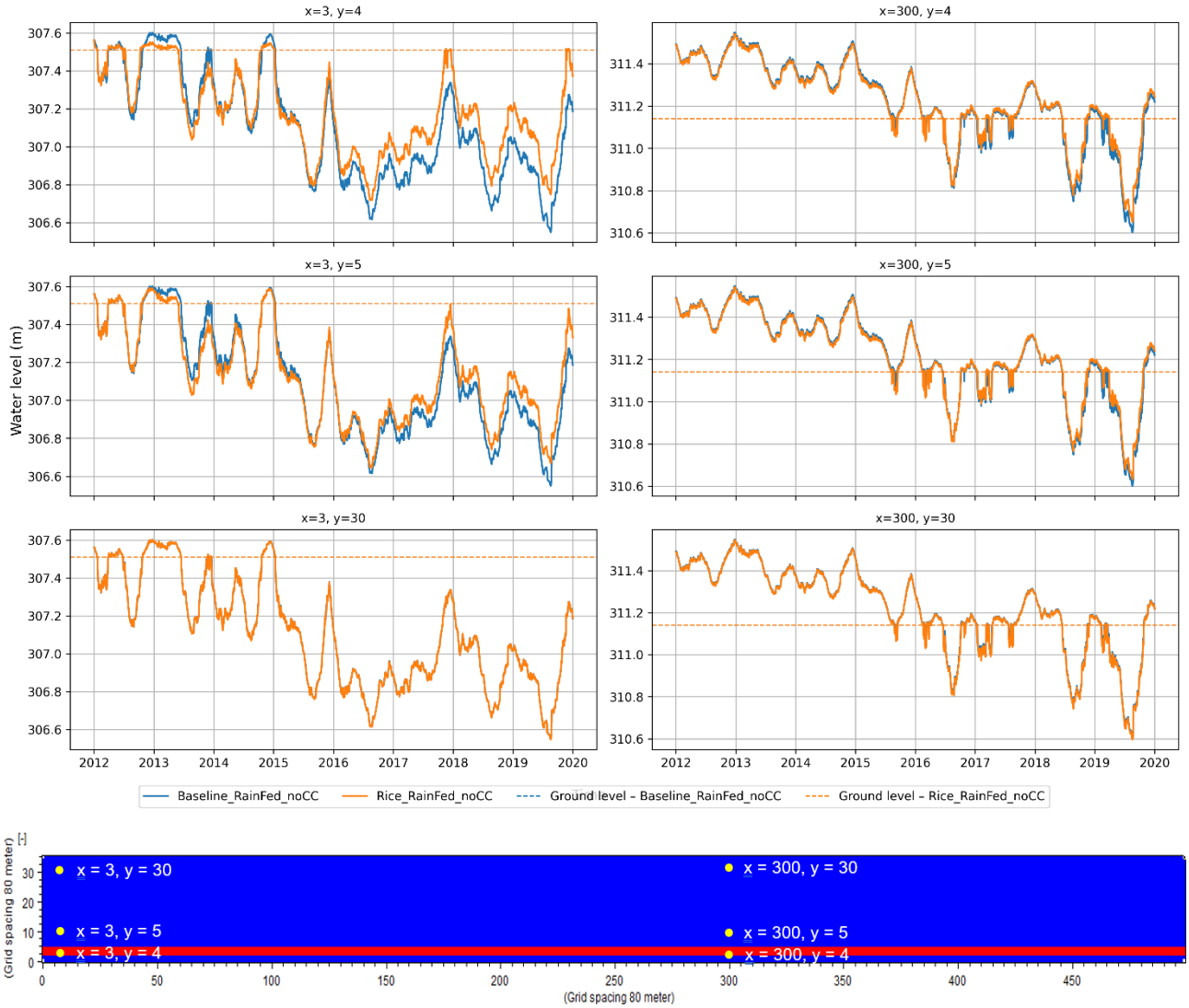

Figure 6.13 Water levels at six given locations within the model area, Scenario G.1.1 (Rice_RainFed_noCC)

6.7.3 Indicators

Indicator values are displayed in the table below. Reduced evapotranspiration in the rice paddies results in higher soil moisture contents and therefore lower mean oxic depths and peat decay. Outside the intervention area, differences between scenarios G.1.1 and A.1.1 are very small.

Indicator Short Name	Indicator Value G.1.1	*Indicator Value A.1.1*	Unit
Oxic Depth Inside	0.14	*0.20*	m
Groundwater Depth Inside	0.10	*0.15*	m
Carbon Flux Inside	-3.77	*-4.72*	kg/m^2/year
Oxic Depth Outside	0.20	*0.20*	m
Groundwater Depth Outside	0.15	*0.15*	m
Carbon Flux Outside	-4.70	*-4.72*	kg/m^2/year

The spatial distribution of mean changes in soil carbon stock within the model area shows that peat in the burnt area decays more than in the baseline scenario over most of the length of the model except near the centre of the peat dome where it decays slightly less (Figure 6.14).

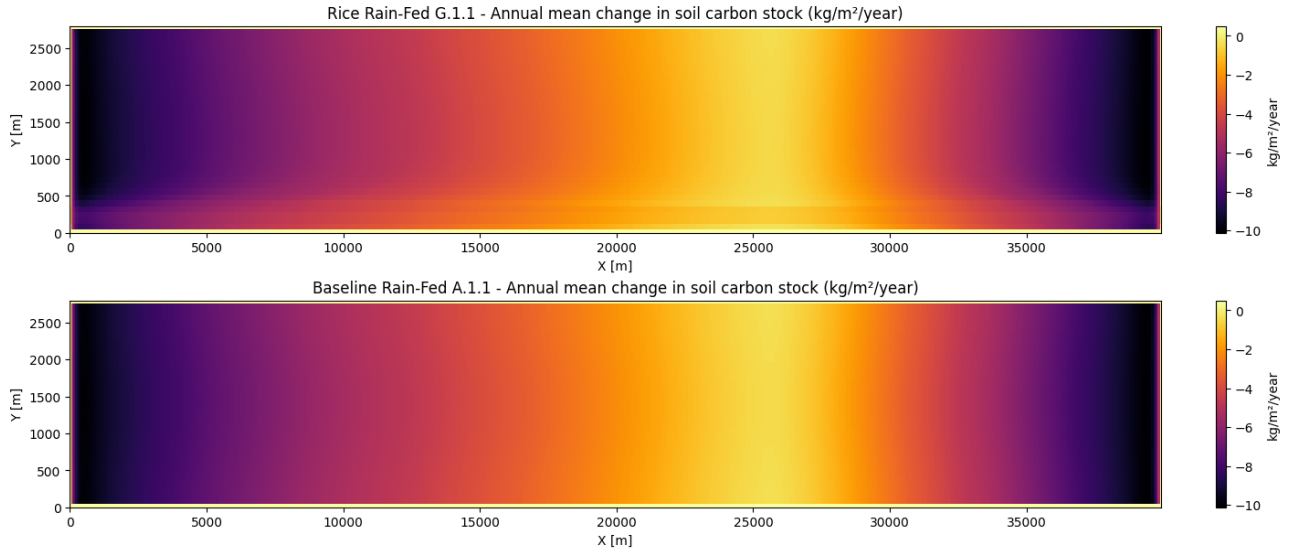

Figure 6.14 Annual mean net change in soil carbon stock – Rice (G.1.1) vs Baseline (A.1.1)

6.7.4 Key Effects

(a) Groundwater table is up to 20 cm shallower than the baseline during dry times due to reduced evapotranspiration. (b) Peat decay is reduced within the intervention zone, no significant change outside the intervention area.

6.7.5 Recommendations

(1) Water table management: Use bunds and controlled irrigation to maintain shallow groundwater levels and reduce peat oxidation. (2) Evapotranspiration balancing: Apply alternate wetting and drying (AWD) to optimize water use and minimize CO_2 and methane emissions. (3) Soil protection: Use organic amendments (e.g. biochar, mulch) to improve soil structure and water retention. (4) Vegetation buffers: Preserve native vegetation strips around paddies to support hydrological stability and biodiversity. (5) Post-conversion restoration: If cultivation ceases, rewet and revegetate to restore peatland function and reduce emissions.

6.8 Summary of Results

Water levels and carbon fluxes across the model area were analysed for various interventions. The model area is hydrologically heterogeneous, with a flat peat dome centre that is nearly permanently waterlogged and rather steep boundary zones where water levels are deep. The 7-year simulation period includes both wet and dry years, allowing the effects of interventions to be assessed under different climate conditions. During dry periods, deep groundwater tables and oxic zones at the western and eastern model boundaries result in significant peat degradation. In the baseline scenario, peat decay in the dome centre is low because the water table is mostly above ground and the oxic depth is therefore very low.

The modelled interventions modify topography, peat hydraulic properties, vegetation, and land use. These changes are represented in a 240-m-wide horizontal stripe extending along the entire length of the model area. The hydrological and carbon emission impacts of the interventions are assessed within and around the intervention footprint. Indicator values are summarised in the table below. Values highlighted in red and green indicate, respectively, high and low soil carbon losses.

Indicator Short Name	Unit	Indicator Values for Scenarios						
		A.1.1	B.1.1	C.1.1	D.1.1	E.1.1	F.1.1	G.1.1
Oxic Depth Inside	m	0.20	0.92	2.12	0.37	0.18	0.73	0.14
Groundwater Depth Inside	m	0.15	1.06	2.00	0.40	0.14	0.73	0.10
Carbon Flux Inside	kg/m^2/year	**-4.72**	0.00	0.00	-8.77	-4.67	-15.64	-3.77
Oxic Depth Outside	m	0.20	0.13	0.68	0.16	0.20	0.77	0.20
Groundwater Depth Outside	m	0.15	0.05	0.68	0.10	0.16	0.79	0.15
Carbon Flux Outside	kg/m^2/year	**-4.72**	-2.90	-14.26	-3.80	-4.78	-15.01	-4.70

Topographic changes significantly affect water levels, with impacts extending beyond the intervention footprint. This is particularly evident in the road, urbanisation, and oil palm scenarios. The ground is raised by 1 m in the road scenario (B.1.1) and by 50 cm in the urbanisation scenario (D.1.1), which leads to higher water levels but also deeper water tables within the footprint. Water levels also rise sharply outside the intervention zone, though the effects diminish with distance from the footprint. In the oil palm scenario (F.1.1), a ground subsidence of 50 cm resulting from peat oxidation has been accounted for. Subsidence causes a substantial increase in water table depth both within and around the footprint, resulting in higher peat carbon losses. In this case, subsidence happens alongside drainage, and both processes together cause the water table to drop.

Drainage has a strong impact on water levels and therefore on soil carbon stocks, as illustrated by the drained road and oil palm scenarios. In the drained road scenario (C.1.1), the soil is drained at 2 m below ground, while in the oil palm scenario (F.1.1) drainage occurs at 50 cm below ground. Because all water above the drain level is emptied, water table depth increases sharply within the footprint. This results in higher carbon losses in the oil palm plantation. This differs from the drained road case, where gravel - not peat - makes up the soil above the drain. Drainage also causes a pronounced lowering of the water table outside the intervention zone, leading to significant peat decay across the entire model area.

Changes in soil properties and vegetation affect water levels to a lesser extent, and typically only within the intervention zone. Actual evapotranspiration is reduced in the fire footprint (E.1.1) and in the rice paddies (G.1.1), leading to a rise in groundwater levels. These effects are noticeable near the boundaries, where the water table is deep, but not at the centre of the dome, where water levels are above ground and evaporation occurs from ponded water. Peat compaction (B.1.1, C.1.1, D.1.1), burning (E.1.1), and oxidation (F.1.1) were represented in the models through decreases in soil porosity, permeability, and/or water storage capacity. The most evident impact of these changes was larger fluctuations in water table levels and deeper water tables during dry seasons. In the fire scenario (E.1.1), which combines changes in both soil properties and vegetation, carbon fluxes are similar than in the baseline within and outside the footprint.

Soil artificialization and vegetation changes lead to reduced carbon uptake by vegetation, resulting in a higher net carbon outflow when peat decay remains constant. This implies that shallower water levels do not necessarily translate into a lower net carbon outflow if the hydrological benefits are offset by reduced litter production. This situation occurs in the fire intervention (E.1.1), where the change in soil carbon stock is comparable to the baseline scenario despite higher average water levels.

The impacts of each intervention differ depending on location within the peatland. The two drained scenarios (C.1.1 and F.1.1) are characterized by a drop in water levels and, consequently, an increase in carbon dioxide emissions across the entire model area - most markedly where water levels are high, i.e. near the center of the dome. All other interventions primarily affect water levels in the boundary zones, where the water table is deep, while water levels in the dome centre remain mostly above ground. The models presented here are configured as domes with steep gradients and constant boundary water levels. This setup produces deep water tables and, therefore, high rates of peat decay near the boundaries. However, the low-lying areas at the dome edges are subject to river flooding. The analysis in the next section will focus on how fluctuating boundary water levels influence groundwater dynamics and carbon fluxes - both at the boundaries and across the entire peat dome.

7 Scenario Analyses for the current climate with seasonal river level fluctuations

This section presents the results of the scenarios with fluctuating water levels at the western and eastern boundaries. It examines how various interventions affect groundwater depth and, consequently, changes in soil carbon stock under current climate conditions in a peatland influenced by river flooding. The section is structured in the same way as the previous one: for each intervention, hydrological results are described first, followed by carbon fluxes. Finally, recommendations are provided for policymakers and peatland managers.

7.1 Scenario A.1.2

7.1.1 Definition

What would happen in the peatlands under the following circumstances?

Development Intervention Vegetation and topography of the peatlands are according to the current conditions - between 2010 and 2020

Climate Rainfall, temperature and evapotranspiration between 2010 and 2020 are chosen to represent the current climate conditions.

Hydrological Region The hydrological processes in the peatlands are driven by rainfall and evapotranspiration, as well as fluctuating water levels in bordering water bodies (e.g., river reaches). This is the mostly case in the riparian peatlands, mostly located in the Democratic Republic of Congo.

7.1.2 Hydrological results

See section 3.3.3.

7.1.3 Indicators

See details in section 4.

Indicator Short Name	Indicator Value A.1.2 River-fed	*Indicator Value A.1.1 Rainfall driven*	Unit
Oxic Depth Inside/Outside	0.12	*0.20*	m
Groundwater Depth Inside/Outside	0.03	*0.15*	m
Carbon Flux Inside/Outside	-2.82	*-4.72*	kg/m^2/year

7.1.4 Key Effects

(a) High river levels cause seasonal flooding over large areas along the western and eastern boundaries. (b) Peat is more saturated at the end of the simulation period due to repeated river flooding. (c) Higher water tables along the boundaries result in a reduced peat decay compared to the rainfall driven configuration.

7.1.5 Recommendations

Key threats to the peatlands are the following: (1) accelerated peat decomposition and carbon release, leading to the loss of millennia-old carbon stocks, (2) increased greenhouse gas emissions, and (3) the degradation of a globally significant carbon sink.

These threats would be triggered by the following: (a) reduced seasonal inundation due to altered river flow, (b) prolonged dry seasons and climatic drying, (c) upstream water regulation or extraction, (d) drainage infrastructure that accelerates water loss, (e) disruption of natural flood pulses.

Fostering development while preserving the peatlands needs to consider the following: (a) maintain seasonal flood connectivity and avoid upstream interventions that reduce flood peaks, (b) protect against climate-induced drying by integrating peatland conservation into water and climate strategies, (c) minimize land-use conversion in flood-prone zones, (d) regulate canal and ditch construction to prevent unintended drainage.

7.2 Scenario B.1.2

7.2.1 Definition

What would happen in the peatlands under the following circumstances?

Development Intervention	(a) A raised impervious road that requires 80 m width is built 1 meter above the natural surface. It is finished and operational. (b) Vegetation is removed, and the soil surface is flattened. (c) The road embankment is filled with permeable gravel. (d) The underlying peat is compressed due to the road's weight.
Climate	Rainfall, temperature and evapotranspiration between 2010 and 2020 are chosen to represent the current climate conditions.
Hydrological Region	The hydrological processes in the peatlands are driven by rainfall and evapotranspiration, as well as fluctuating water levels in bordering water bodies (e.g., river reaches). This is the mostly case in the riparian peatlands, mostly located in the Democratic Republic of Congo.

7.2.2 Hydrological results

Water levels in and around the intervention area are shown in Figure 7.1 for the current scenario (B.1.2) and the river-fed baseline scenario (A.1.2). As in the river-fed baseline simulation, the centre of the dome is not affected by river flooding (right graphs). Differences between scenarios B.1.2 and A.1.2 are therefore the same as in the rainfall driven simulations (see results in section 6.2).

Around the western and eastern boundaries, however, the water table is influenced by river flooding. Flooding peaks in the road footprint are dampened compared to the baseline. Because the road is raised by 1 m, the flood waves propagate mainly below ground. As groundwater flow is much slower than overland flow, the rise in water level during river floods is reduced compared to the baseline. The extent of the flooded area remains similar in both scenarios.

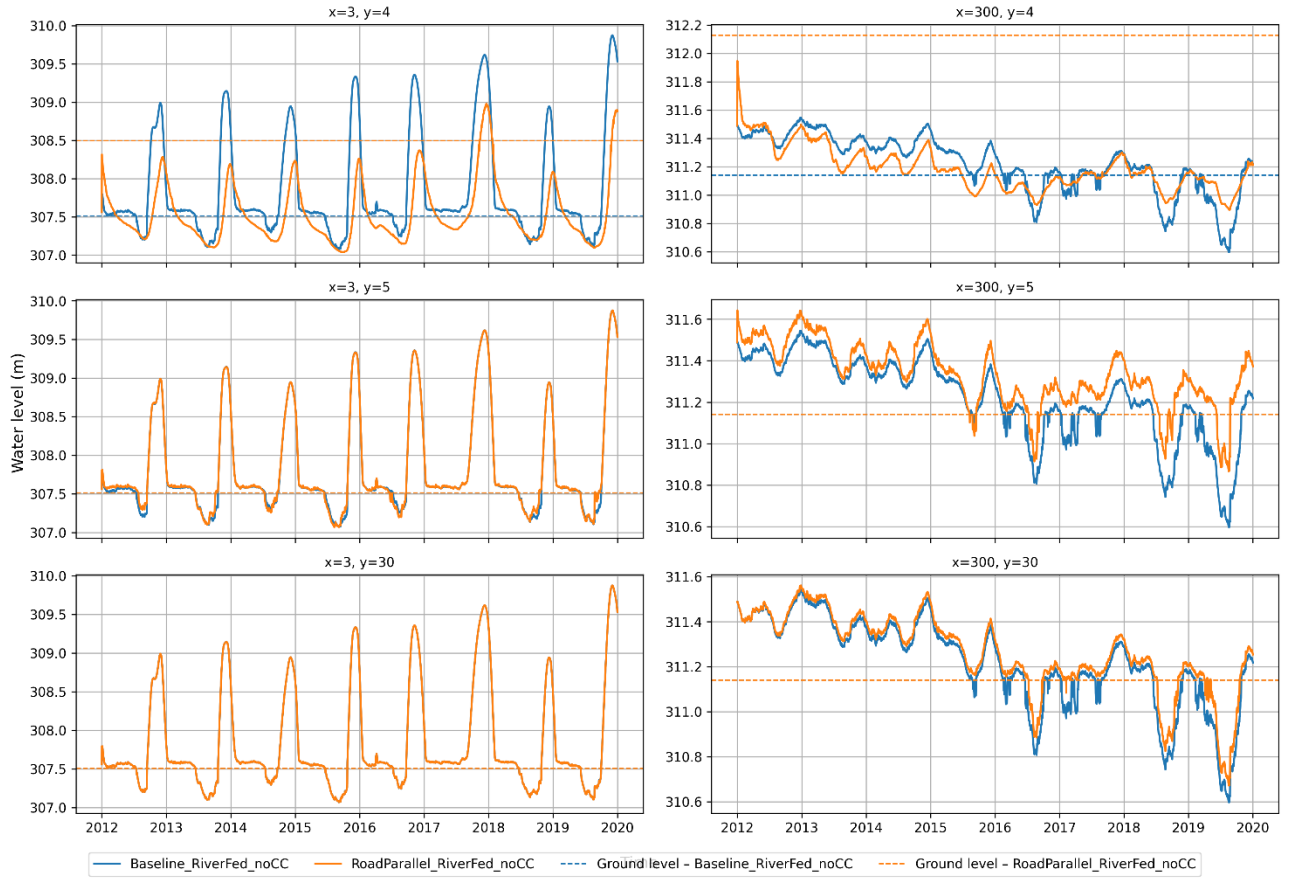

Figure 7.1 Water levels at six given locations within the model area; Scenario B.1.2 (RoadParallel_RiverFed_noCC)

7.2.3 Indicators

Indicator values are displayed in the table below. As in scenario A.1.2, oxic depth and groundwater table depth beneath the road are high because the road was raised by 1 m. This does not result in any CO_2 emissions as the water table is always located within the gravel embankment above the peat layer. Outside the road area, the mean groundwater level is negative, indicating that the water table is mostly above ground. As in the rainfall driven simulation, the oxic depth -computed during periods when the water table is below ground- is lower than in the baseline scenario, which results in lower soil carbon losses.

Indicator Short Name	**Indicator Value B.1.2**	*Indicator Value A.1.2*	**Unit**
Oxic Depth Inside	0.89	*0.12*	m
Groundwater Depth Inside	1.03	*0.03*	m
Carbon Flux Inside	0.00	*-2.82*	kg/m^2/year
Oxic Depth Outside	0.07	*0.12*	m

Indicator Short Name	Indicator Value B.1.2	*Indicator Value A.1.2*	Unit
Groundwater Depth Outside	-0.05	*0.03*	m
Carbon Flux Outside	-1.40	*-2.82*	kg/m²/year

A spatial representation of the change in soil carbon stock (see Figure 6.3) shows that carbon losses are very low in the flooded areas near the rivers. Outside the flooded areas, results are like those of the rainfall driven simulation (see section 6.2).

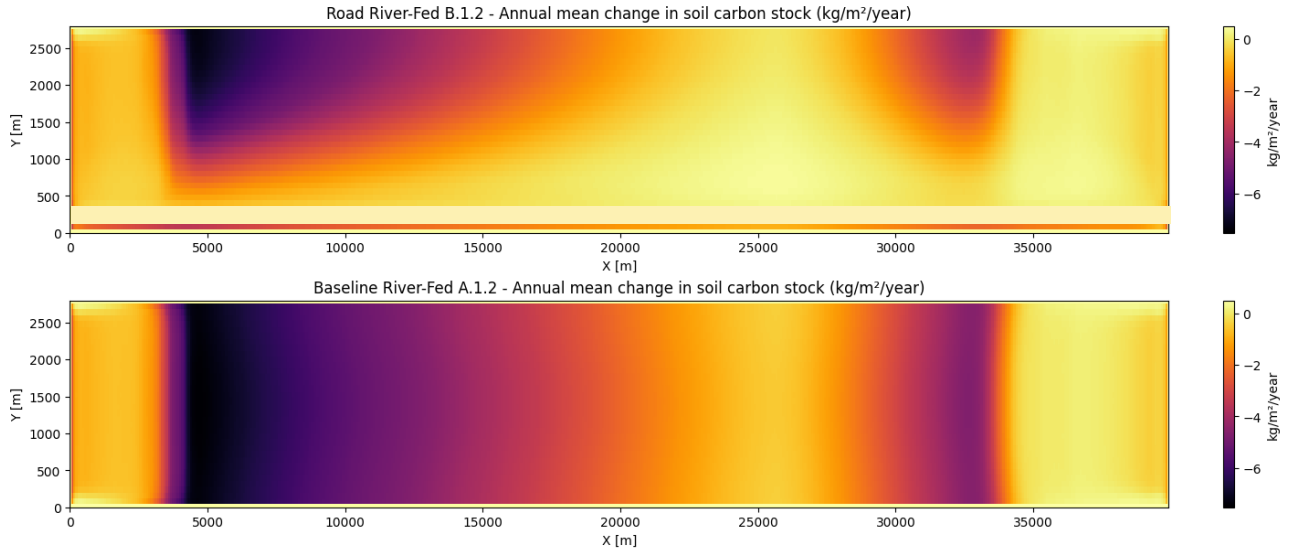

Figure 7.2 Annual mean change in soil carbon stock – Road River-fed (B.1.2) vs Baseline River-fed (A.1.2)

7.2.4 Key Effects

(a) Infiltration does not occur directly on the road; precipitation flows over the surface to adjacent lower-lying areas, where it infiltrates and recharges the aquifer. (b) The raised road increases the depth to groundwater beneath it. (c) In the floodplain, flood peaks under the road are attenuated. (d) Water levels increase near the road, with influence decreasing in distance. (e) As a result, peat decay is reduced compared to current conditions (baseline).

7.2.5 Recommendations

The influence of the road generally extends as far as 2 km from its edge. In river-fed peatlands, seasonal flooding is essential to maintain peat saturation and prevent decomposition. The road may disrupt natural flood pulses and reduce inundation in adjacent areas, especially during prolonged dry seasons.

Recommended measures to mitigate these effects are the following: In a buffer zone along the road, maintain the moisture of the peatlands by: (1) rewetting – block drainage canals and ditches to retain floodwater and restore natural hydrology; and (2) vegetation management – promote native, water-retaining vegetation (like swamp forest species) that helps shade the peat, reduce evaporation, and stabilize water levels during dry periods.

7.3 Scenario C.1.2

7.3.1 Definition

What would happen in the peatlands under the following circumstances?

Development Intervention	(a) A raised impervious road that requires 80 m width is being built 1 meter above the natural surface. (b) Vegetation is removed, and the soil surface is flattened. (c) The road embankment is filled with permeable gravel. (d) The underlying peat is compressed due to the road's weight. (e) During construction drainage is installed 2 meters below the ground, i.e., 1 meter below the surrounding surface.
Climate	Rainfall, temperature and evapotranspiration between 2010 and 2020 are chosen to represent the current climate conditions.
Hydrological Region	The hydrological processes in the peatlands are driven by rainfall and evapotranspiration, as well as fluctuating water levels in bordering water bodies (e.g., river reaches). This is the mostly case in the riparian peatlands, mostly located in the Democratic Republic of Congo.

7.3.2 Hydrological results

Water levels in and around the intervention area are shown in the figure below for the current scenario (C.1.2) and the river-fed baseline scenario (A.1.2). As in the river-fed baseline simulation, the centre of the dome is not affected by river flooding (right graphs). Differences between scenarios C.1.2 and A.1.2 are therefore the same as in the rainfall driven simulations (see results in section 6.3).

Within one month, water levels beneath the road drop to the drain level, 2 m below ground (upper graphs). River flooding only marginally influences the water table beneath the road (upper left). As in the rainfall driven scenario, drainage affects all cells outside the footprint, where the water table is deeper than in the baseline scenario (middle and lower graphs). Water level peaks induced by river flooding are slightly attenuated (middle left graph). Flood waves propagate indeed more slowly than in the baseline, as peat is drier due to drainage. At most, 17% of the dome area is flooded by rivers, compared to 25% in the baseline scenario.

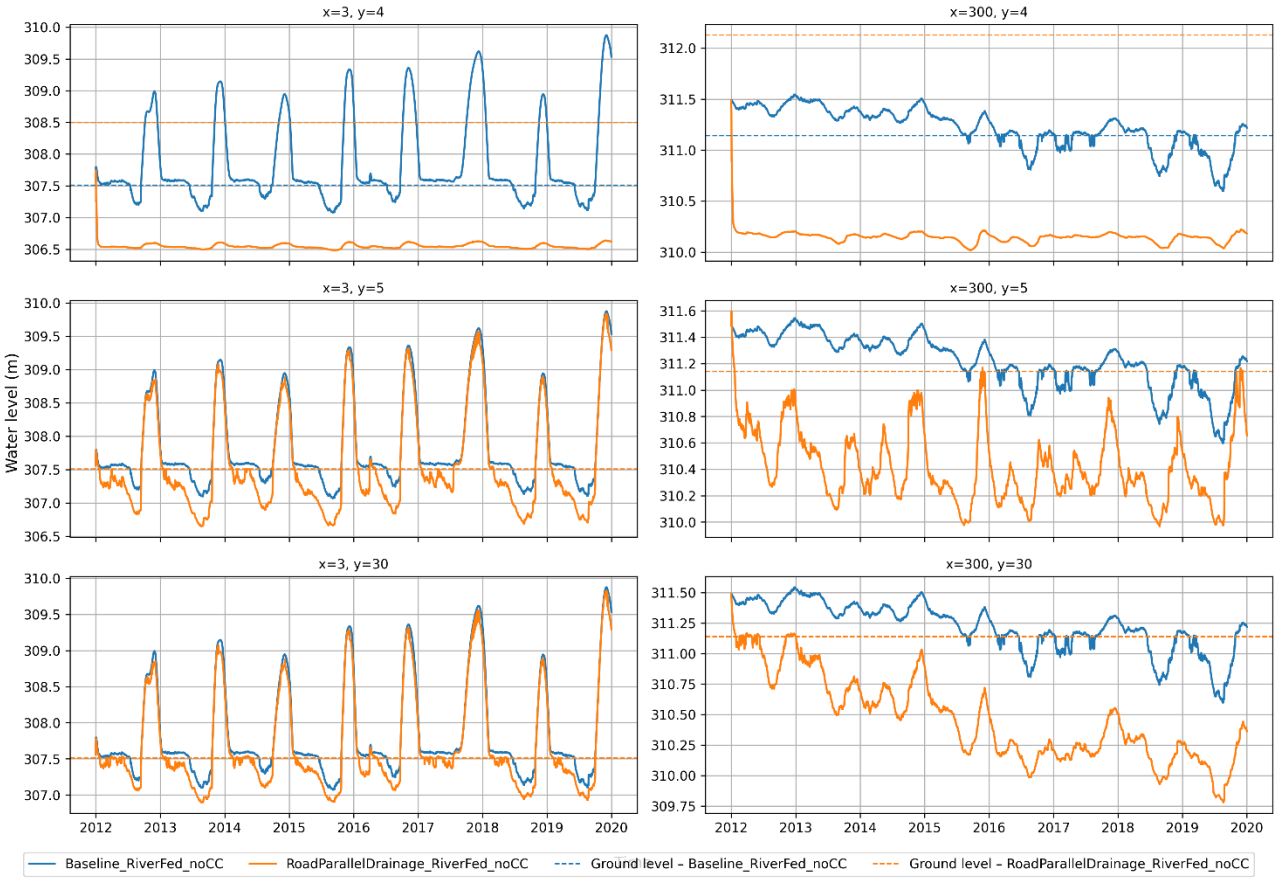

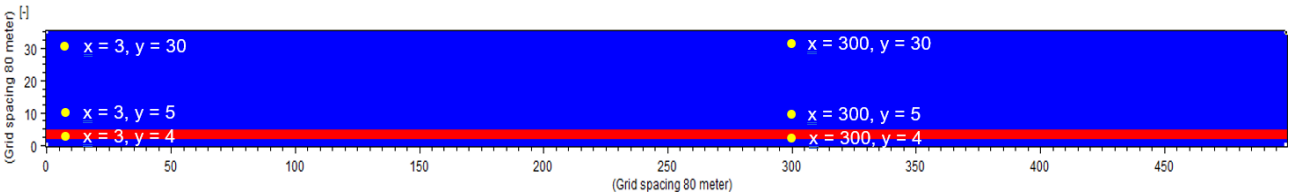

Figure 7.3 Water levels at six given locations within the model area; Scenario C.1.2 (RoadParallelDrainage_RiverFed_noCC)

7.3.3 Indicators

Indicator values are displayed in the table below. Like in scenario B.1.2, oxic depth and groundwater table depth beneath the road are high because the road was raised by 1 m. This does not result in any peat decay as the water table is located within the gravel embankment above the peat layer. Outside the road, soil carbon losses rise sharply as drainage leads to a lowering of the water table.

Indicator Short Name	Indicator Value C.1.2	*Indicator Value A.1.2*	Unit
Oxic Depth Inside	2.12	*0.12*	m
Groundwater Depth Inside	2.01	*0.03*	m
Carbon Flux Inside	0.00	*-2.82*	kg/m^2/year
Oxic Depth Outside	0.61	*0.12*	m
Groundwater Depth Outside	0.59	*0.03*	m
Carbon Flux Outside	-12.88	*-2.82*	kg/m^2/year

Figure 7.4 shows that the area affected by river flooding is smaller than in the baseline scenario, and that carbon losses within this area are higher.

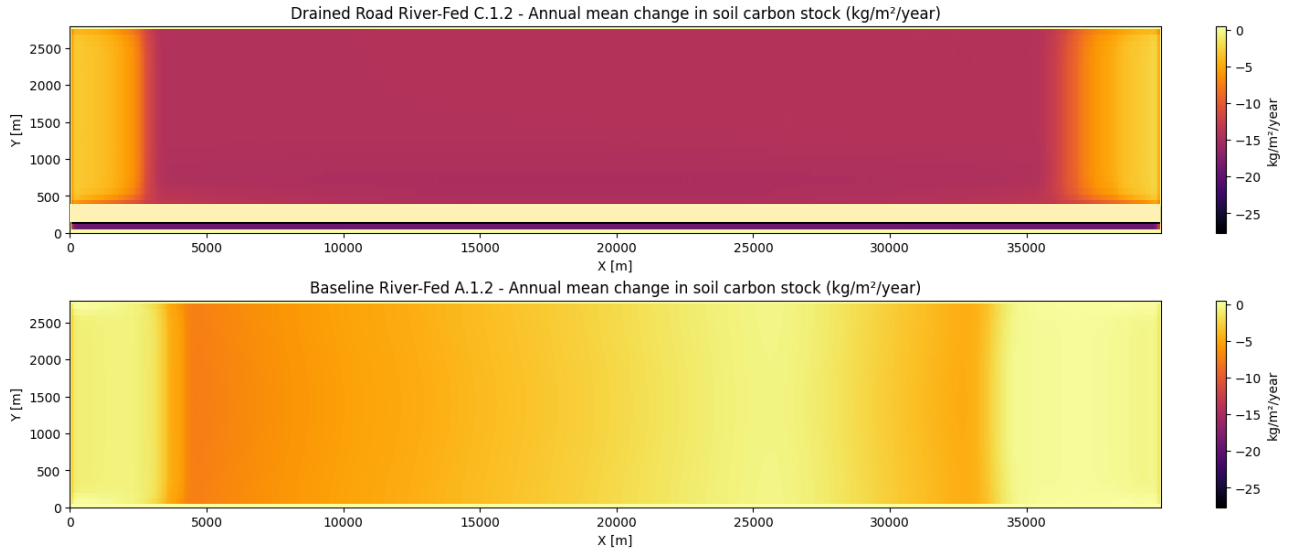

Figure 7.4 Annual mean change in soil carbon stock – Drained Road River-fed (C.1.2) vs Baseline River-fed (A.1.2)

7.3.4 Key Effects

(a) Groundwater levels stabilize at 2 meters depth under the road. (b) Drainage influence extends beyond the intervention area, reducing groundwater levels in adjacent zones. (c) Because of drainage, the area flooded by the boundary rivers decreases from 25% to 17% of the dome. (d) Peat decay increases everywhere because of the low water levels.

7.3.5 Recommendations

The effects of drainage during construction are substantial. The aim therefore is to limit their impact as far as possible. In river-fed peatlands, drainage can significantly reduce seasonal inundation, which is critical for maintaining peat saturation and preventing decomposition. During construction the following needs to be considered:

(1) temporary drainage systems – design drainage that minimizes water table drawdown and is easy to remove or block after construction; (2) install silt fences and sediment traps; (3) limit drainage duration; (4) rewet immediately after construction – block temporary ditches and allow natural water levels and flood pulses to return quickly; (5) use low-impact construction techniques – employ raised roads, geotextiles, or matting to reduce soil compaction and water flow disruption; (6) restore vegetation promptly – plant native wetland species to stabilize soil, retain moisture, and support floodplain hydrology.

7.4 Scenario D.1.2

7.4.1 Definition

What would happen in the peatlands under the following circumstances?

Development Intervention	(a) A settlement is developed in the peatland forest. (b) The topography is raised by 50 cm to prevent flooding. (c) Vegetation is cleared, and the soil surface is partially paved. (d) The peat is compressed under the load of buildings.
Climate	Rainfall, temperature and evapotranspiration between 2010 and 2020 are chosen to represent the current climate conditions.
Hydrological Region	The hydrological processes in the peatlands are driven by rainfall and evapotranspiration, as well as fluctuating water levels in bordering water bodies (e.g., river reaches). This is the mostly case in the riparian peatlands, mostly located in the Democratic Republic of Congo.

7.4.2 Hydrological results

Water levels in and around the intervention area are shown in Figure 7.5 for the current scenario (D.1.2) and the river-fed baseline scenario (A.1.2). As in the river-fed baseline simulation, the centre of the dome is not affected by river flooding (right graphs). Differences between scenarios D.1.2 and A.1.2 are therefore the same as in the rainfall driven simulations (see results in section 6.4).

In dry seasons, water table levels along the western boundary are higher than in the baseline scenario in the elevated settlement (upper left). The water table rises in the soil column because peat has a strong capillary potential. Water table depths are higher as the ground is elevated. During river flood event, water levels are the same as in the baseline scenario. The area flooded by rivers remains the same as in scenario A.1.2. Outside the intervention area, the water table slightly rises thanks to the influence of the settlement (middle left).

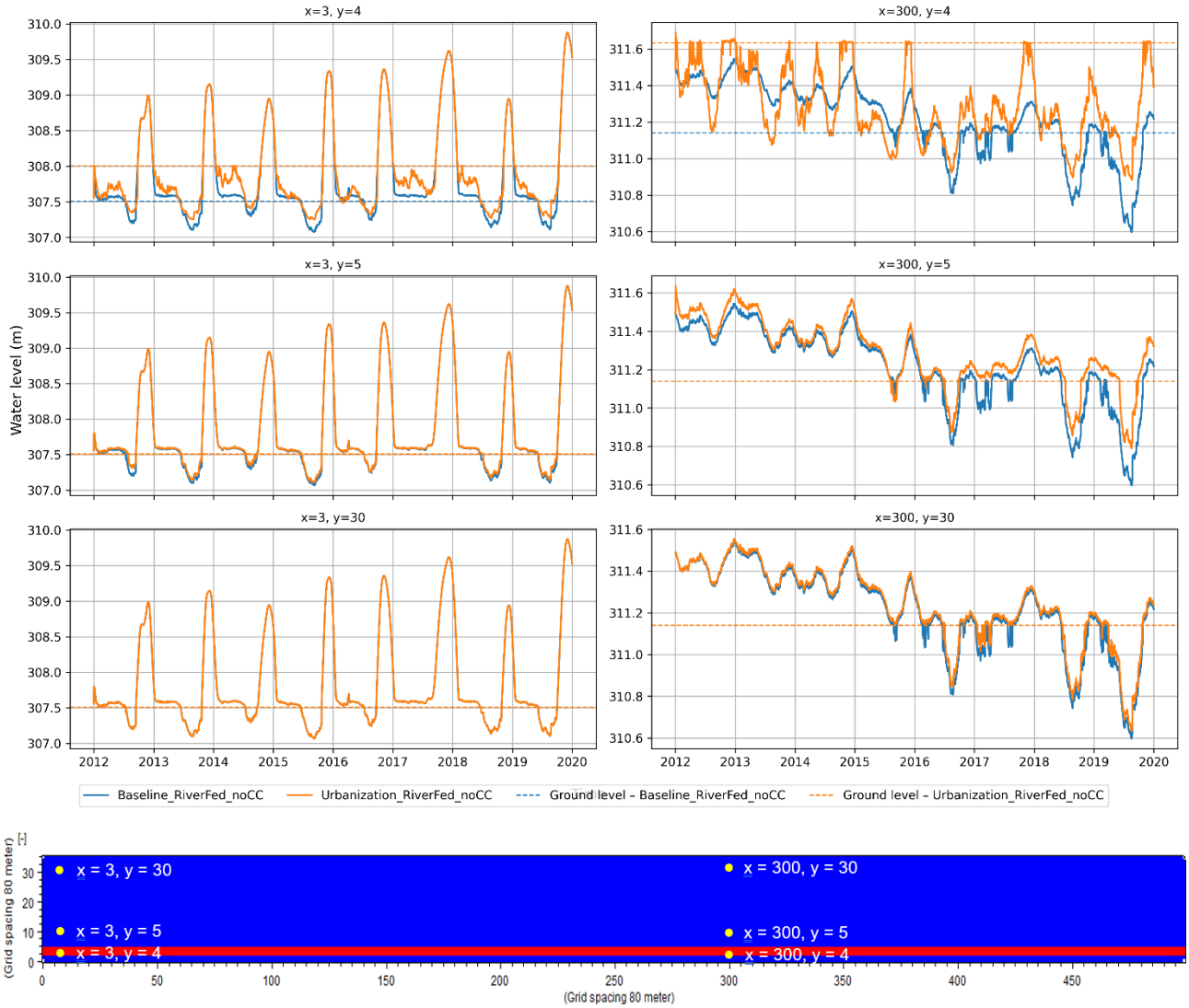

Figure 7.5 Water levels at six given locations within the model area; Scenario D.1.2 (Urbanization_RiverFed_noCC)

7.4.3 Indicators

Indicator values are displayed in the table below. As in the rainfall driven situation, oxic depth and groundwater table depth beneath the urbanized area are higher than the baseline scenario because the settlement was raised by 50 cm, which results in significant peat decay. Outside the settlement area, the mean groundwater table, located above ground, is higher than in the baseline scenario (see hydrological results). Oxic depth is reduced, leading to lower soil carbon losses than in scenario A.1.2.

Indicator Short Name	**Indicator Value D.1.2**	***Indicator Value A.1.2***	**Unit**
Oxic Depth Inside	0.34	*0.12*	m
Groundwater Depth Inside	0.35	*0.03*	m
Carbon Flux Inside	-8.10	*-2.82*	kg/m^2/year
Oxic Depth Outside	0.09	*0.12*	m
Groundwater Depth Outside	-0.01	*0.03*	m
Carbon Flux Outside	-2.08	*-2.82*	kg/m^2/year

A spatial representation of the mean change in soil carbon stock (see Figure 6.7) shows that building a settlement increases sharply carbon losses in the settlement footprint and reduces them in the surrounding cells. The area flooded by rivers, characterized by very limited peat decay, remains similar in both scenarios.

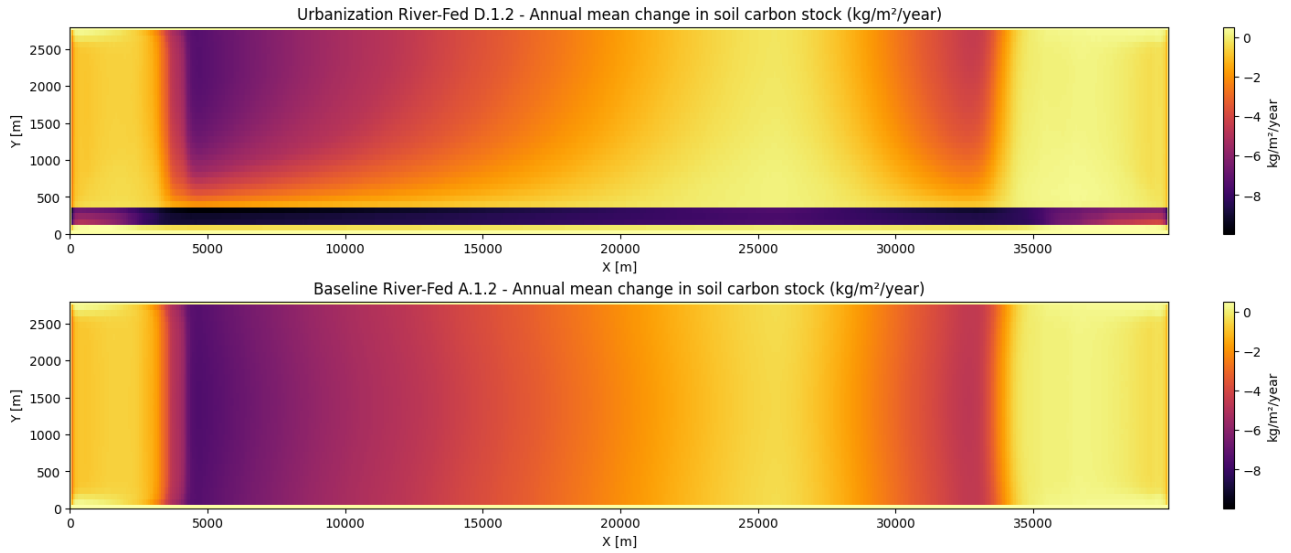

Figure 7.6 Annual mean change in soil carbon stock – Settlement (D.1.2) vs Baseline (A.1.2)

7.4.4 Key Effects

The key effects are like scenario D.1.1 and are valid inside and outside the floodplain: (a) Raising the settlement ground results in higher water levels but deeper groundwater tables. (b) Mean water levels rise outside the urban footprint, but the effect fades with distance. (c) Peat decay outside the intervention zone is reduced due to higher mean water levels.

7.4.5 Recommendations

Building a settlement in the peatlands would have serious environmental consequences, such as (1) reduced seasonal inundation, (2) increased carbon emissions due to lower water tables, (3) land subsidence, and (4) disruption of floodplain hydrology.

Mitigation measures to consider are: (a) zoning – use land-use planning to steer development away from flood-dependent peatlands; (b) minimal drainage design – use raised foundations or boardwalks to reduce the need for drainage and soil disturbance; (c) hydrological buffer zones – maintain surrounding wetland areas to preserve natural flood pulses and moisture retention; (d) flood-adapted infrastructure – design settlements to accommodate seasonal flooding without compromising peat integrity.

7.5 Scenario E.1.2

7.5.1 Definition

What would happen in the peatlands under the following circumstances?

Development Intervention (a) A forest fire completely clears the vegetation. (b) As a result, soil properties change: bulk density increases, and specific yield decreases.

Climate Rainfall, temperature and evapotranspiration between 2010 and 2020 are chosen to represent the current climate conditions.

Hydrological Region

The hydrological processes in the peatlands are driven by rainfall and evapotranspiration, as well as fluctuating water levels in bordering water bodies (e.g., river reaches). This is the mostly case in the riparian peatlands, mostly located in the Democratic Republic of Congo.

7.5.2 Hydrological results

Water levels in and around the intervention area are shown in Figure 7.7 for the current scenario (E.1.2) and the river-fed baseline scenario (A.1.2). As in the river-fed baseline simulation, the centre of the dome is not affected by river flooding. Differences between scenarios E.1.2 and A.1.2 are therefore the same as in the rainfall driven simulations (see results in section 6.5).

Near the western and eastern boundaries, water table levels in the burnt area are lower than in the A.1.2 baseline scenario outside of river flood events (see upper left graph). Indeed, given that the fire smoothed the terrain microtopography, the burnt area becomes the zone for preferential overland flow. With less storage in hollows, the water table drops quicker at the beginning of the dry season. Additionally, the water table falls deeper during dry seasons because the field capacity of burnt peat is reduced compared to untouched peat. For a given evaporated volume, a lower field capacity results indeed in a greater drop in water level. During river flood events, the water level remains like the river-fed baseline scenario. Outside the burnt area, differences between both scenarios are negligible (middle and lower left).

The graphs on the right show water tables variations in a cell located just outside the area influenced by river flooding. In this zone, water levels gradually rise above the baseline (upper right). As in the rainfall driven simulation, this decline results from reduced evaporation from the ground during dry seasons coupled with the absence of transpiration from the burnt area. The increase in water table level is also noticeable just outside the burnt area (middle right).

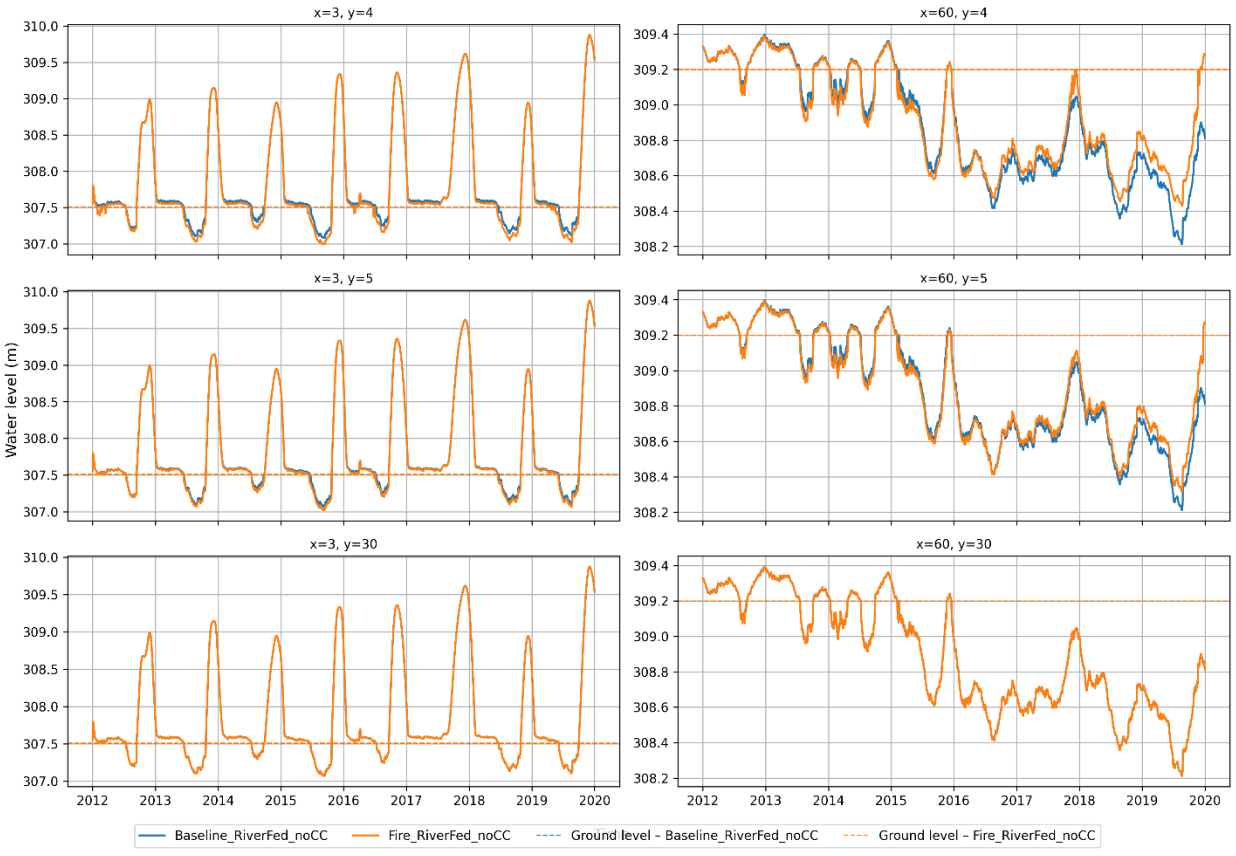

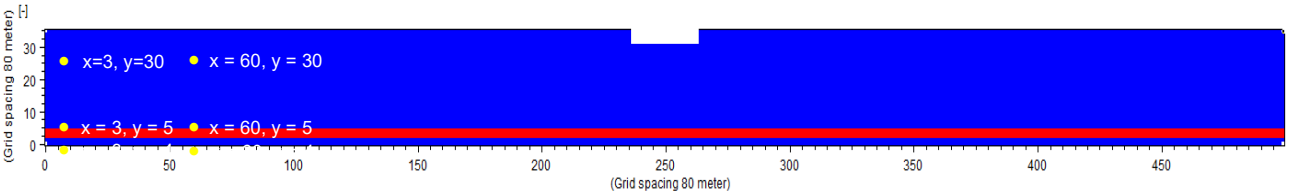

Figure 7.7 Water levels at six given locations near the western boundary; Scenario E.1.2 (Fire_RiverFed_noCC)

7.5.3 Indicators

Indicator values are displayed in the table below. Although average groundwater and oxic depths inside the footprint are nearly the same as in the baseline scenario, the net carbon outflow is higher as there is no carbon uptake by the burnt vegetation. Outside of the intervention footprint, carbon fluxes are similar to the baseline.

Indicator Short Name	Indicator Value E.1.2	*Indicator Value A.1.2*	Unit
Oxic Depth Inside	0.12	*0.12*	m
Groundwater Depth Inside	0.03	*0.03*	m
Carbon Flux Inside	-3.17	*-2.82*	kg/m^2/year
Oxic Depth Outside	0.12	*0.12*	m
Groundwater Depth Outside	0.03	*0.03*	m
Carbon Flux Outside	-2.85	*-2.82*	kg/m^2/year

Carbon losses in the burnt area are lower than in the baseline scenario over the whole length of the model (Figure 7.8).

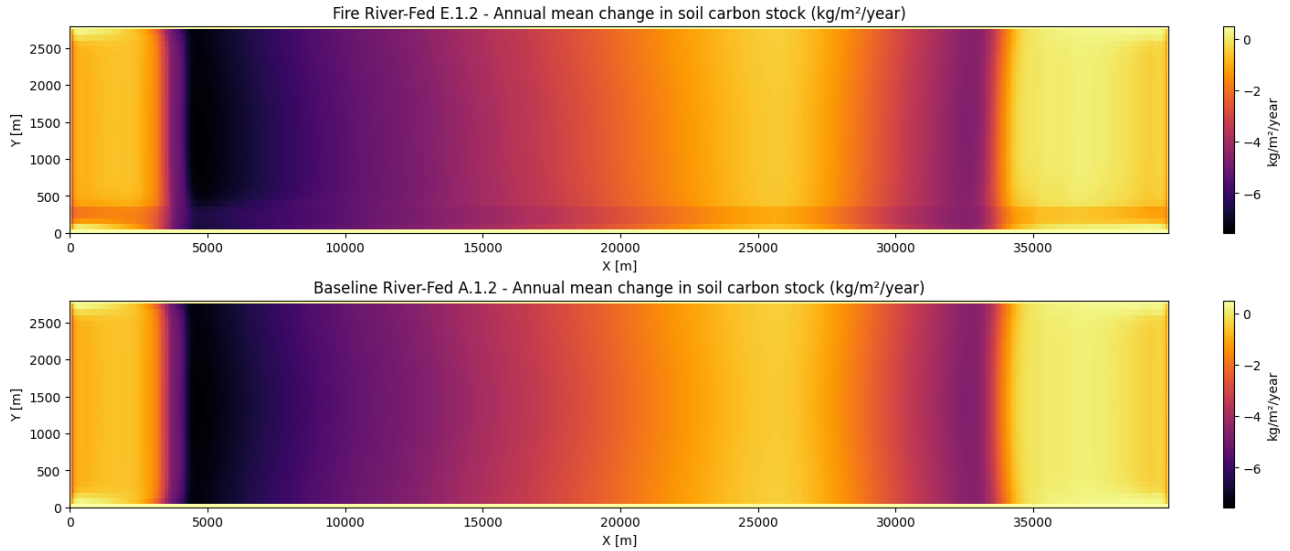

Figure 7.8 Annual mean change in soil carbon stock – Fire (E.1.2) vs Baseline (A.1.2)

7.5.4 Key Effects

(a) In the floodplain and at the centre of the dome, groundwater levels in the fire footprint are lower than under baseline conditions, while outside these zones they are higher due to reduced

evapotranspiration. (b) Outside the fire footprint, groundwater levels remain like those in the baseline scenario. (c) Despite similar oxic depths, net carbon outflow within the intervention footprint is higher as there is no carbon uptake by the burnt vegetation. Outside of the intervention footprint, carbon losses are similar to the baseline.

7.5.5 Recommendations

Forest fires in river-fed peatlands can disrupt seasonal flood dynamics and reduce peat saturation, especially in floodplain zones.

To mitigate these effects: (1) vegetation loss prevention – implement firebreaks and controlled burns to protect floodplain vegetation; (2) water tables maintaining or restoring – rewet burnt areas by blocking drainage channels and retaining floodwater; build small bunds or retention structures to preserve moisture during dry seasons; (3) post-fire restoration – replant native flood-adapted species to stabilize soil and restore evapotranspiration; apply soil amendments (e.g., organic mulches or biochar) to improve structure and water retention in floodplain soils.

7.6 Scenario F.1.2

7.6.1 Definition

What would happen in the peatlands under the following circumstances?

Development Intervention	Deforestation and Conversion to Oil Palm Plantations: (a) Natural vegetation is cleared to establish additional oil palm plantations. (b) Oil palms thrive with a mean water level 40 cm to 60 cm below ground. There is drainage at 50 cm depth. (c) Vegetation properties are altered according to 15-year-old mature oil palm plantation. (d) The microtopography is smoothed due to clearing. (e) Soil properties change by drainage: increased bulk density, reduced specific yield, and reduced hydraulic conductivity at saturation. (f) The topography is lowered by 50 cm due to soil subsidence induced by drainage.
Climate	Rainfall, temperature and evapotranspiration between 2010 and 2020 are chosen to represent the current climate conditions.
Hydrological Region	The hydrological processes in the peatlands are driven by rainfall and evapotranspiration, as well as fluctuating water levels in bordering water bodies (e.g., river reaches). This is the mostly case in the riparian peatlands, mostly located in the Democratic Republic of Congo.

7.6.2 Hydrological results

Water levels in and around the intervention area are shown in Figure 7.9 for the current scenario (F.1.2) and the river-fed baseline scenario (A.1.2). As in the river-fed baseline simulation, the centre of the dome is not affected by river flooding (right graphs). Differences between scenarios F.1.2 and A.1.2 are therefore the same as in the rainfall driven simulations (see results in section 6.6).

Water levels near the western model boundary drop rapidly compared to the baseline due to soil subsidence. When the water table falls to the drain level during dry seasons, it rises again quickly because of river flooding. Water depth in this zone is therefore only marginally higher than in the river-fed baseline. Outside the plantation, the water table is deeper: in the first few cells near the boundary this is due to subsidence alone, while further from the river it results from the combined effects of soil subsidence and drainage.

Water level peaks induced by river flooding are slightly attenuated (left graphs). Flood waves propagate indeed more slowly than in the baseline, as peat is drier due to drainage and soil subsidence. At most, 19% of the dome area is flooded by rivers, compared to 25% in the baseline scenario.

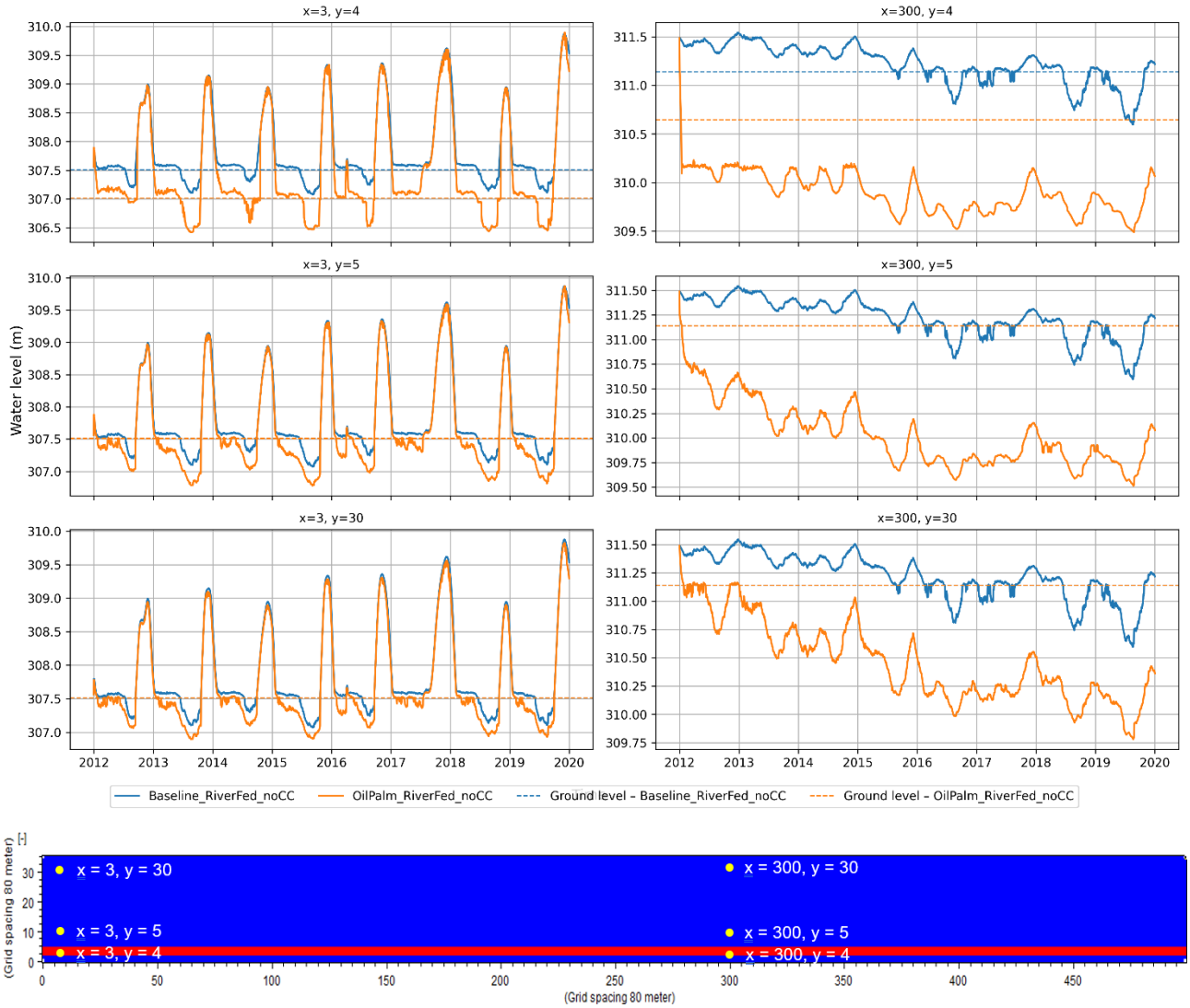

Figure 7.9 Water levels at six given locations within the model area; Scenario F.1.2 (OilPalm_RiverFed_noCC)

7.6.3 Indicators

Indicators are displayed in the table below. The groundwater table in and around the plantation is much lower than in the baseline scenario due to soil subsidence and drainage, which results in a carbon outflow 5 higher.

Indicator Short Name	Indicator Value F.1.2	*Indicator Value A.1.2*	Unit
Oxic Depth Inside	0.71	*0.12*	m
Groundwater Depth Inside	0.69	*0.03*	m
Carbon Flux Inside	-14.55	*-2.82*	kg/m^2/year
Oxic Depth Outside	0.65	*0.12*	m
Groundwater Depth Outside	0.64	*0.03*	m

Indicator Short Name	Indicator Value F.1.2	*Indicator Value A.1.2*	Unit
Carbon Flux Outside	-13.53	*-2.82*	kg/m^2/year

A spatial representation of the annual mean change in soil carbon stock (Figure 7.10) reveals that the area affected by river flooding is smaller than in the baseline scenario, and that carbon losses within this area are higher. The river floodplain is wider in the plantation footprint given the lower elevation. As in the rainfall driven scenario, there is more peat decay in the cells near the plantation footprint than in the footprint itself. Indeed, although water levels in and around the plantation footprint are close, the ground surface has subsided under the plantation, resulting in a shallower oxic zone.

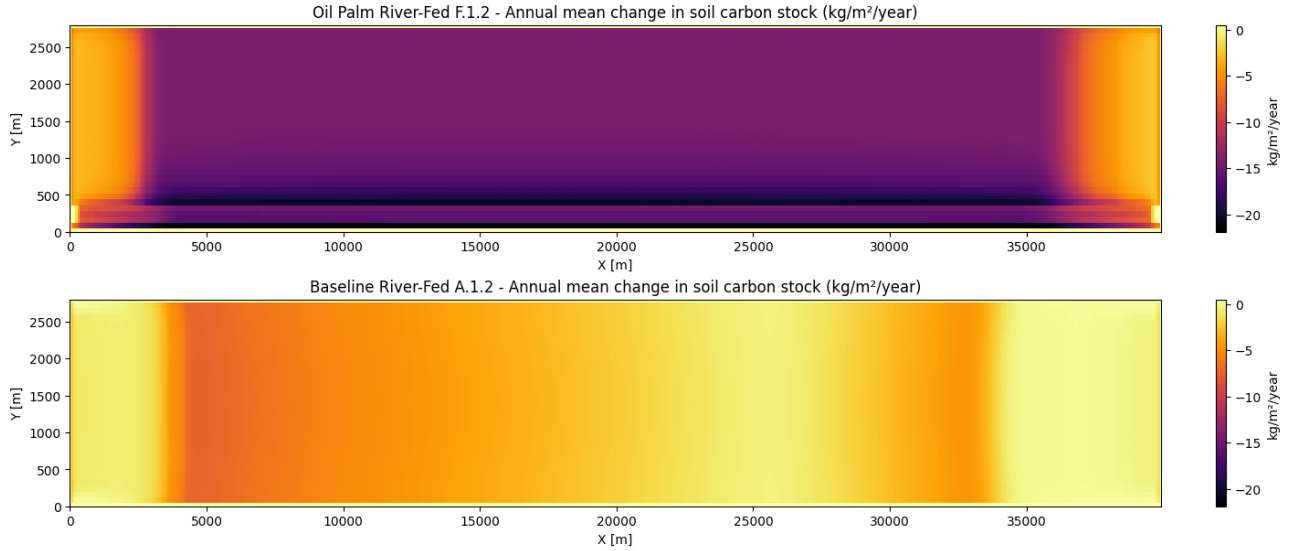

Figure 7.10 Annual mean net change in soil carbon – Oil Palm Plantation (F.1.2) vs Baseline (A.1.2)

7.6.4 Key Effects

(a) Groundwater levels under the plantation are lower than in the baseline situation, driven by drainage and soil subsidence. (b) A reduction in groundwater levels is observed throughout the area. (c) Peat decays is increased due to lower water levels. (d) Because of drainage and soil subsidence, the area flooded by the boundary rivers decreases from 25% to 19% of the dome.

7.6.5 Recommendations

Recommendations for mitigation: (1) hydrological management: (a) shallow drainage design by raising drainage depth closer to the surface (e.g., 30–40 cm) to reduce peat oxidation while still supporting oil palm growth, (b) controlled drainage systems using adjustable weirs or gates to manage seasonal water levels and maintain floodplain connectivity; (2) soil subsidence reduction: (a) minimize drainage intensity by reducing the duration and depth of drainage to slow peat decomposition and subsidence, (b) use ground covers by planting understory vegetation to reduce evaporation and protect soil structure; (3) vegetation and biodiversity buffers: retain natural vegetation strips along rivers and flood zones to preserve biodiversity and hydrological function; (4) carbon emission mitigation: rewet degraded areas by restoring abandoned or marginal plantation zones and reforesting; (5) topography and microtopography restoration: (a) avoid smoothing natural microtopography to maintain water retention and habitat diversity, (b) rebuild surface layers in degraded areas using organic mulches or compost to improve water retention and support seasonal inundation.

7.7 Scenario G.1.2

7.7.1 Definition

What would happen in the peatlands under the following circumstances?

Development Intervention	Deforestation and Conversion to Rice Cultivation: (a) Natural vegetation is removed and replaced with rice paddies. Rice is the most common seasonally flooded crop in the Cuvette Centrale. (b) There are two harvests per year. Paddies are flooded during the wet season. (c) Vegetation and surface properties/roughness vary with crop stage.
Climate	Rainfall, temperature and evapotranspiration between 2010 and 2020 are chosen to represent the current climate conditions.
Hydrological Region	The hydrological processes in the peatlands are driven by rainfall and evapotranspiration, as well as fluctuating water levels in bordering water bodies (e.g., river reaches). This is the mostly case in the riparian peatlands, mostly located in the Democratic Republic of Congo.

7.7.2 Hydrological results

Water levels in and around the intervention area are shown in Figure 7.11 for the current scenario (G.1.2) and the river-fed baseline scenario (A.1.2). As in the river-fed baseline simulation, the centre of the dome is not affected by river flooding (right graphs). Differences between scenarios G.1.2 and A.1.2 are therefore the same as in the rainfall driven simulations (see results in section 6.7).

Near the western and eastern boundaries, water table levels in the rice paddies are lower than in the A.1.2 baseline scenario outside of river flood events (see upper left graph). Indeed, given that the conversion to rice paddies smoothed the terrain microtopography, the plantation becomes the zone for preferential overland flow. Without storage in hollows, the water table drops quicker at the beginning of the dry season. During river flood events, the water level remains like the river-fed baseline scenario. Outside the rice paddies, differences between both scenarios are negligible (middle and lower left).

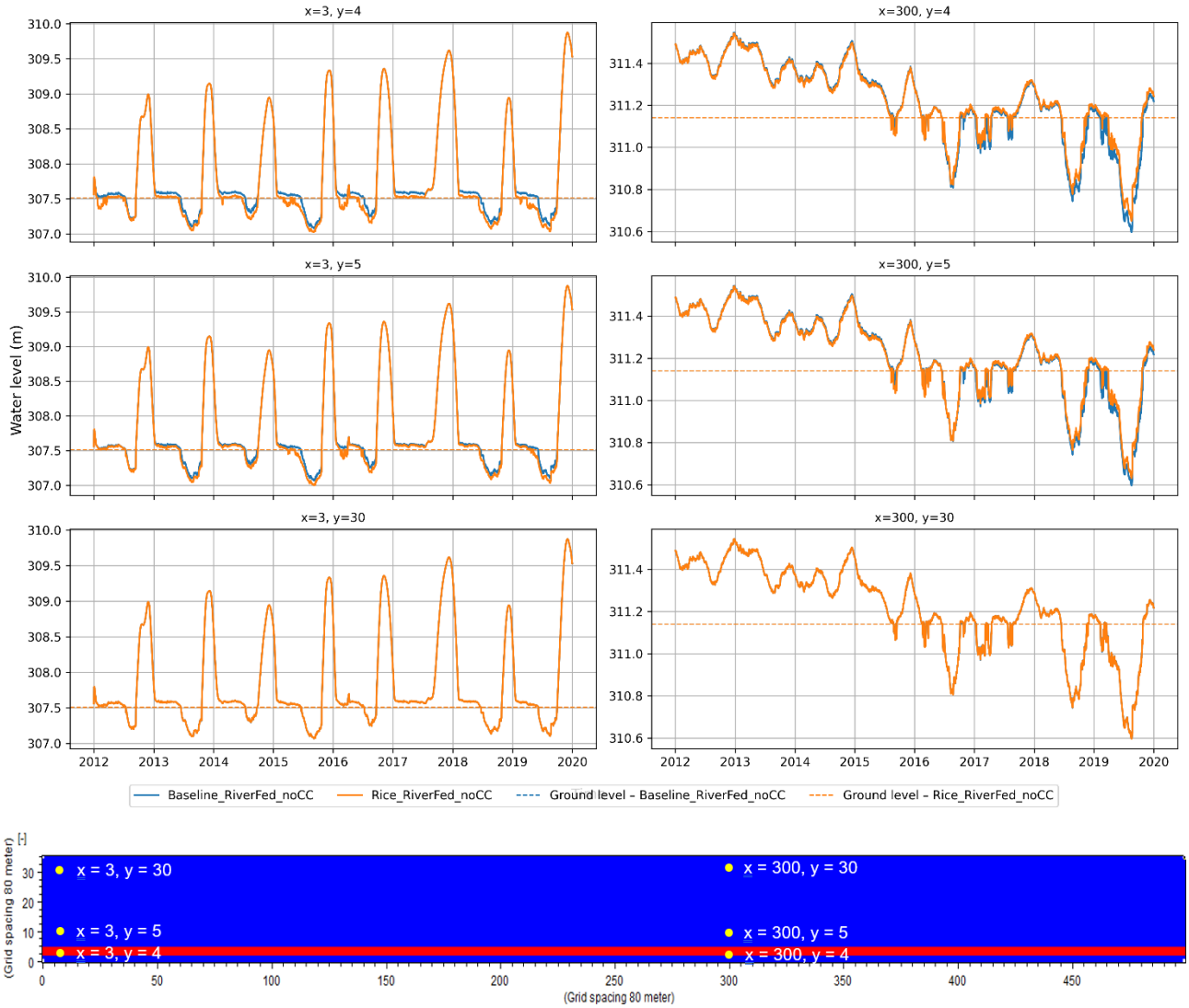

Figure 7.11 Water levels at six given locations within the model area; Scenario G.1.2 (Rice_RiverFed_noCC)

7.7.3 Indicators

Indicator values are displayed in the table below. Reduced evapotranspiration in the rice paddies outside the river floodplain results in higher soil moisture contents and therefore lower mean oxic depths and peat decay. Outside the intervention area, differences between scenarios G.1.2 and A.1.2 are small.

Indicator Short Name	Indicator Value G.1.2	*Indicator Value A.1.2*	Unit
Oxic Depth Inside	0.09	*0.12*	m
Groundwater Depth Inside	0.00	*0.03*	m
Carbon Flux Inside	-2.46	*-2.82*	kg/m^2/year
Oxic Depth Outside	0.12	*0.12*	m
Groundwater Depth Outside	0.03	*0.03*	m
Carbon Flux Outside	-2.79	*-2.82*	kg/m^2/year

Carbon losses from the rice plantation are higher than in the scenario A.1.2 in the river floodplain and at the centre of the dome but lower in between due to reduced evapotranspiration. Although water levels

at the centre of the dome are higher than in the baseline, the net carbon outflow is also higher as carbon uptake is reduced in the rice paddies. The area affected by river flooding is slightly wider in the rice paddies as the smooth surface acts as a preferential flow path.

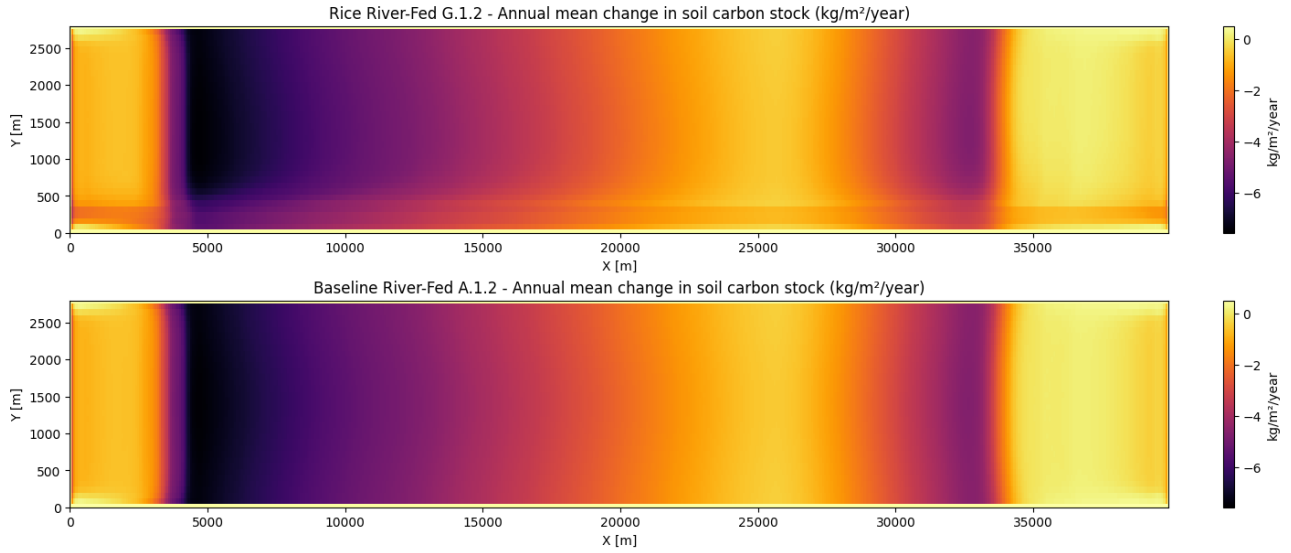

Figure 7.12 Annual mean net change in soil carbon stock – Rice (G.1.2) vs Baseline (A.1.2)

7.7.4 Key Effects

(a) In the river floodplain, groundwater levels in the rice paddies are lower than in the baseline scenario as overland ponding is reduced on the smooth surface, while outside the floodplain, they are higher by up to 25 cm due to reduced evapotranspiration. (b) Peat decay is reduced within the intervention zone - no major change outside the intervention area. Carbon losses are higher in the river floodplain and at the centre of the dome as the microtopography is smoother and carbon uptake by the vegetation is reduced.

7.7.5 Recommendations

(1) Water table stabilization: Use bunds and retention structures to reduce rapid drainage during dry seasons and maintain groundwater levels. (2) Preferential flow control: Restore microtopography or introduce shallow depressions to reduce overland flow and enhance water storage. (3) Evapotranspiration management: Apply alternate wetting and drying to balance water use and reduce CO_2 and methane emissions. (4) Soil enhancement: Use organic amendments (e.g. biochar, mulch) to improve water retention and reduce peat degradation. (5) Floodplain buffering: Maintain vegetation buffers near river margins to slow floodwater spread.

7.8 Summary of Results

Water levels and carbon fluxes across the model area were analysed for various interventions. The model area is hydrologically heterogeneous, with a flat peat dome centre that is nearly permanently waterlogged and steep boundary zones which are subject to yearly river flooding. Rivers flood the cells near the boundaries and replenish the aquifer. Peat decay in the floodplain area occurs between the river flooding events when water levels are below ground.

The river inflow produces a sustained rise in the water table compared to the baseline rainfall driven scenario, which results in low carbon losses in the boundary zones. As in the baseline rainfall driven scenario, the carbon outflow from the dome centre is low because the water table is mainly above ground and the oxic depth is therefore very low. The highest carbon losses are located at the periphery of the river-flooded area.

The modelled interventions modify topography, peat hydraulic properties, vegetation, and land use. These changes are represented in a 240-m-wide horizontal stripe extending along the entire length of the model area. The hydrological and carbon flux impacts of the interventions are assessed within and around the intervention footprint. Indicator values are summarised in the table below. Values highlighted in red and green indicate, respectively, high and low peat carbon losses.

Indicator Short Name	Unit	Indicator Values for Scenarios						
		A.1.2	B.1.2	C.1.2	D.1.2	E.1.2	F.1.2	G.1.2
Oxic Depth Inside	m	0.12	0.89	2.12	0.34	0.12	0.71	0.09
Groundwater Depth Inside	m	0.03	1.03	2.01	0.35	0.03	0.69	0.00
Carbon Flux Inside	kg/m^2/year	**-2.82**	0.00	0.00	-8.10	-3.17	-14.55	-2.46
Oxic Depth Outside	m	0.12	0.07	0.61	0.09	0.12	0.65	0.12
Groundwater Depth Outside	m	0.03	-0.05	0.59	-0.01	0.03	0.64	0.03
Carbon Flux Outside	kg/m^2/year	**-2.82**	-1.40	-12.88	-2.08	-2.85	--13.53	-2.79

Carbon fluxes inside and outside the footprint follow the same trend relative to the baseline as in the rainfall driven scenarios: if carbon losses for a given intervention are lower than the baseline in the rainfall driven case, they are also lower in the river-fed case.

As in the rainfall driven case, drainage and topographic changes have a significant impact on water levels both within and outside the footprint, while changes in soil properties and vegetation have a lesser impact. Since the results outside the river floodplains are like those in the rainfall driven scenarios, only the situation in the areas flooded by rivers is described here.

As drainage reduces soil moisture in the unsaturated zone compared to the river-fed baseline scenario, more infiltration occurs into the peat during river flooding events. Floods therefore propagate more slowly, which explains why the floodplain is smaller in the drained road scenario (C.1.2) and in the oil palm scenario (F.1.2) than in the River-fed baseline. Soil carbon losses within the floodplains are higher in both scenarios, as water levels are deeper during dry seasons. Drainage thus results in higher carbon losses in both rainfall driven and river-fed zones.

Topographic changes affect water tables in the floodplain and thus carbon fluxes, mainly in the same way as in rainfall driven areas. Nevertheless, a few specific features of river-fed areas can be highlighted. In the road scenario (B.1.2), flood peaks beneath the road are smaller and broader because the water table lies below ground and groundwater dynamics are much slower than overland flow. Flood peaks are also broader under the elevated settlement (D.1.2). In the oil palm scenario (F.1.2), the floodplain expands further under the plantation because of ground subsidence.

Although less significant than in rainfall driven areas, changes in soil properties and vegetation also influence water tables and thus carbon fluxes in the floodplain. Microtopography is smoothed in the fire (E.1.2) and rice (G.1.2) scenarios, reducing ponding compared to the river-fed baseline and increasing overland flow towards lower-lying cells. This outflow causes the water table in the floodplain to drop more quickly in the footprint at the beginning of the dry season. In the fire scenario (E.1.2), the decrease in water level during dry periods may also be partly explained by the higher specific yield of the soil resulting from peat smouldering.

The specific features of river-fed peatlands highlighted here should not disguise the fact that the simulated interventions have broadly similar impacts in both rainfall driven and the river-fed cases. Within the footprint, soil carbon losses increase in the settlement (D.1) and oil palm plantation (C.1), but decrease in the rice paddies (G.1). Outside the footprint, carbon losses rise for the drained road (C.1) and oil palm scenarios (F.1), while they decrease for the road (B.1) and settlement (D.1) scenarios. These simulations were carried out under current climate conditions. The next section examines climate change scenarios to assess whether the impacts of the interventions would remain similar in the future.

8 Effects of climate change

This section aims at comparing the hydrological and carbon dioxide emissions results for various climate change scenarios. Two Shared Socio-Economic Pathways (SSP) are compared here: SSP1-2.6 and SSP3-7.0 (see section 5.2).

8.1 Intervention A – Baseline

8.1.1 Rainfall driven case

Water levels at the peat centre and near the western boundary are shown in Figure 8.1 for both SSP1-2.6 and SSP3-7.0. Under SSP1-2.6, water levels drop more than under current climate conditions. As in the current climate, the water table at the centre of the dome declines during the dry years 2015 and 2016 and does not recover afterwards. After 2015, water levels remain mostly below the ground surface, reaching up to 20 cm lower than under current conditions. Water levels under SSP3-7.0 are much lower than under current climate conditions. The water table declines across the entire peat dome, reaching up to 1 m lower than under present conditions at the centre of the dome. Near the western and eastern boundaries, the water table drops so severely during the simulation that it reaches the bottom of the peat layer by the end of the period.

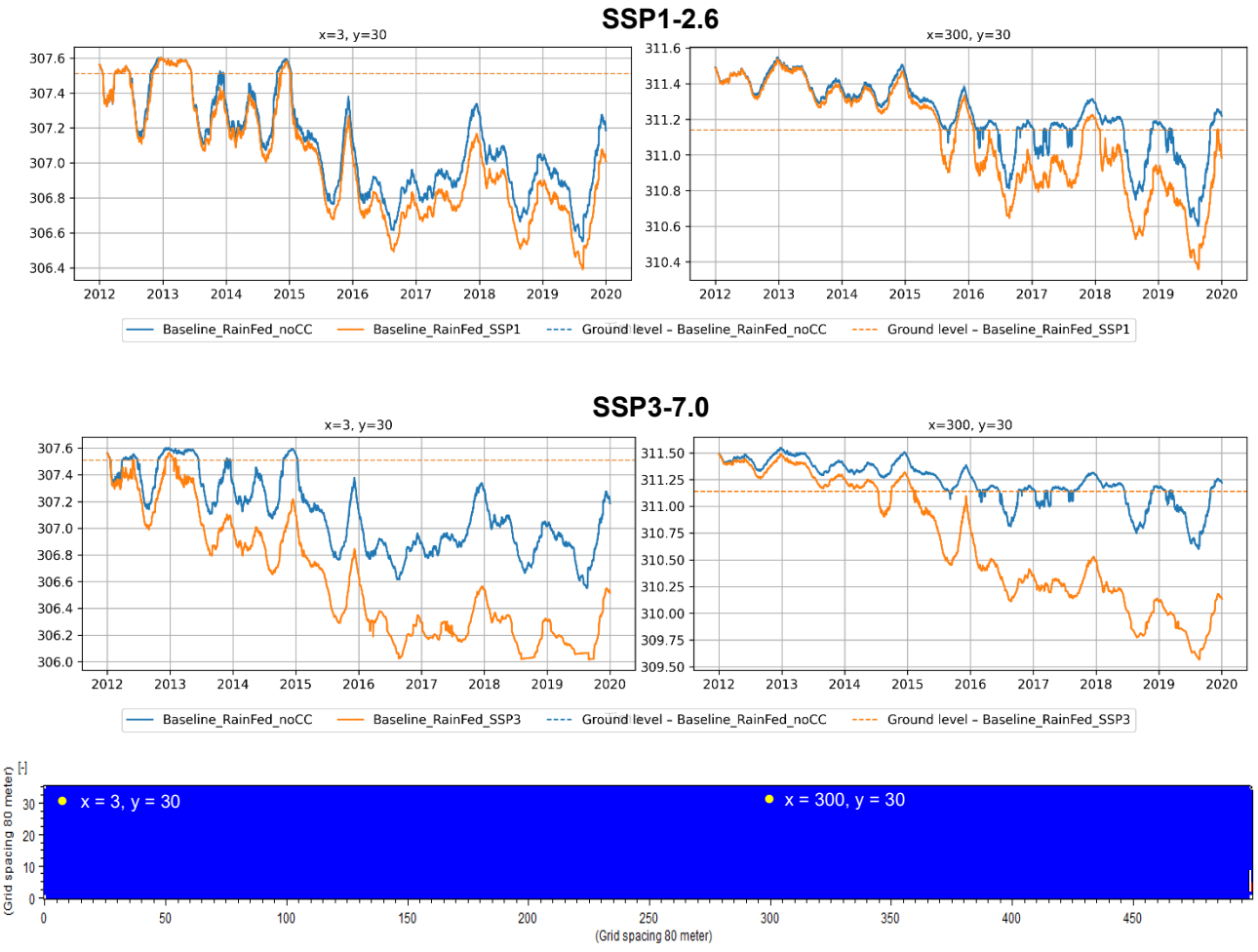

Figure 8.1 Water levels at the peat centre and near the western boundary
Scenario A.2.1 (top, Baseline_RainFed_SSP1) & A.3.1 (bottom, Baseline_RainFed_SSP3)

Lower water tables in both SSPs can be explained by a greater increase in evapotranspiration compared to rainfall. Indeed, actual evapotranspiration increase by 2.4% annually under SSP1-2.6 and by 3.7% under SSP3-7.0, while annual rainfall rises by 1.5% under SSP1-2.6 and decreases by 0.1% under SSP3-7.0. The water table is much lower under SSP3-7.0 than under SSP1-2.6.

Indicator values are displayed in the table below. For both climate change scenarios, peat decay is higher than under current climate conditions (A.1.1) because of lowered water levels and increased exposure of peat to aerobic conditions.

Indicator Short Name	***Indicator Value A.1.1 Rainfall driven Current Climate***	**Indicator Value A.2.1 Rainfall driven SSP1-2.6**	**Indicator Value A.3.1 Rainfall driven SSP3-7.0**	**Unit**
Oxic Depth Inside/Outside	*0.20*	0.31	0.74	m
Groundwater Depth Inside/Outside	*0.15*	0.27	0.71	m
Carbon Flux Inside/Outside	*-4.72*	-7.66	-16.11	kg/m^2/year

A spatial representation of the annual mean change in peat carbon stock under SSP1-2.6 and SSP3-7.0 (see Figure 8.2) shows that carbon losses are higher than under current climate conditions throughout the whole model area.

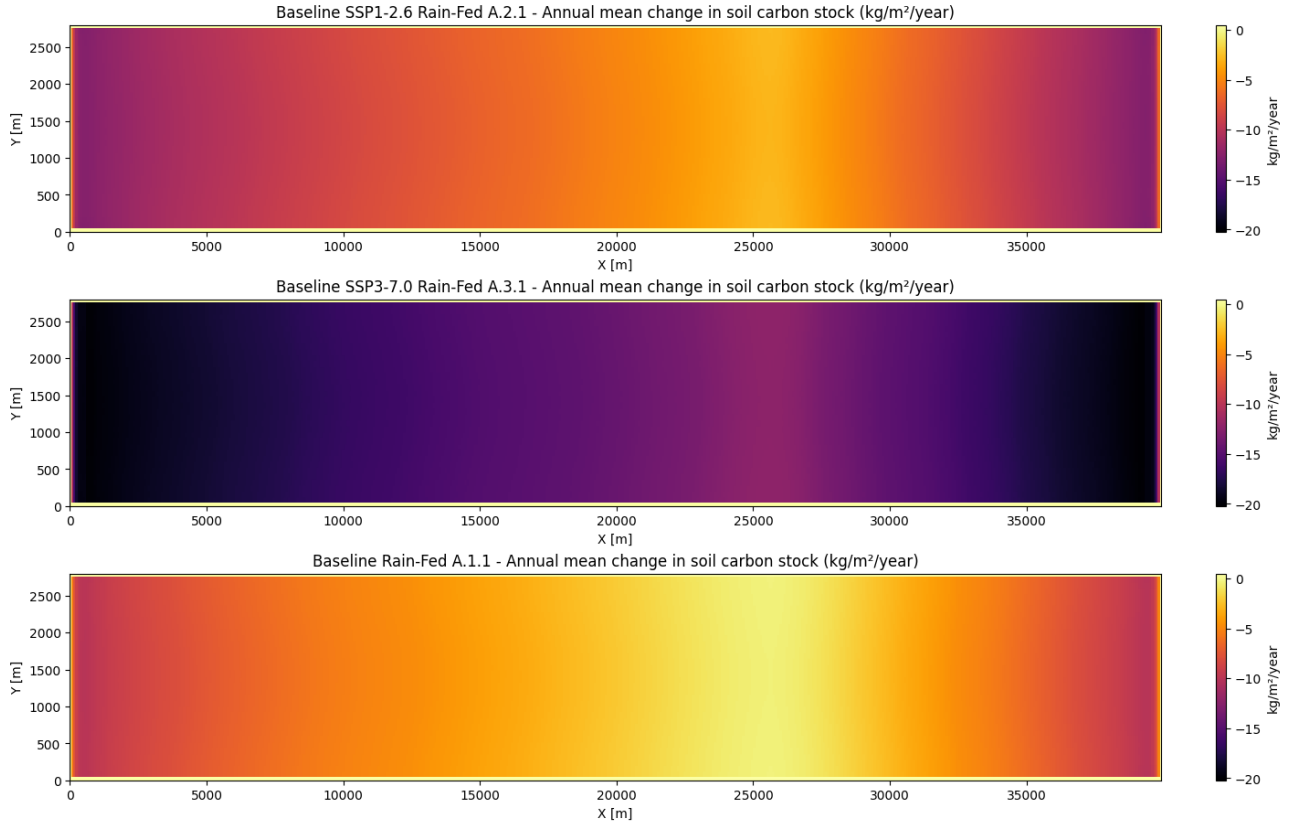

Figure 8.2 Annual mean net change in soil carbon stock– Baseline SSP1-2.6 Rainfall driven (A.2.1) vs Baseline SSP3-7.0 Rainfall driven (A.3.1) vs Baseline Rainfall driven (A.1.1)

8.1.2 River-fed case

Water levels at the peat centre and near the western boundary are shown in Figure 8.3 for both SSP1-2.6 (A.2.2) and SSP3-7.0 (A.3.2). As in the rainfall driven case, the centre of the dome is not affected by river flooding (right graphs). Differences between scenarios A.2.2/A.3.2 and A.1.2 are therefore the same as in the rainfall driven simulations (see results in section 8.1.1).

Results near the western and eastern boundaries are similar between the two SSPs but differ from the baseline. During dry seasons, the water table is deeper for both SSPs than under current climate conditions. Water levels are like those in scenario A.1.2 during wet seasons as the impacts of temperature and precipitation changes on river levels weren't included in this study (see justification in section 7.1).

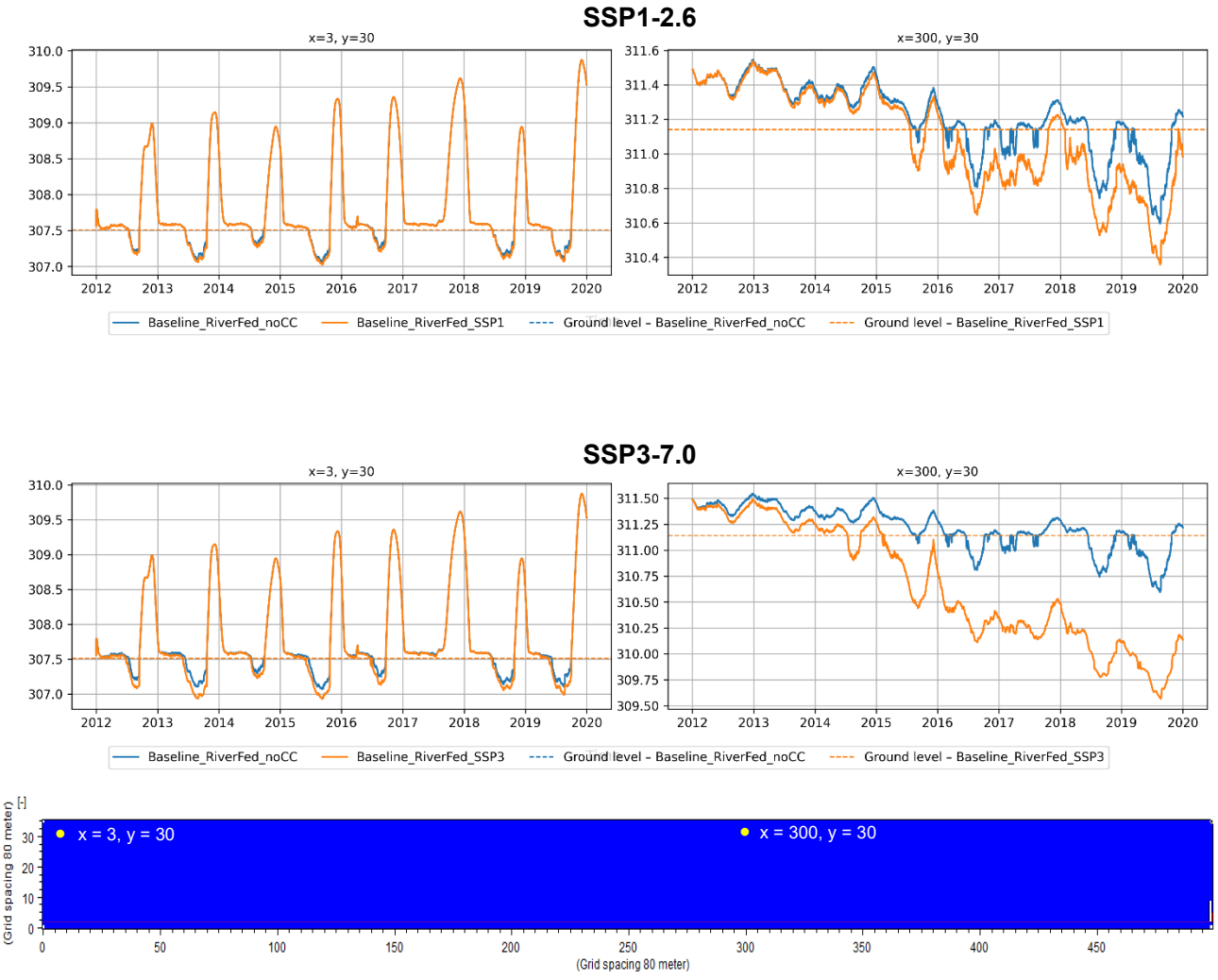

Figure 8.3 Water levels at the peat centre and near the western boundary
Scenario A.2.2 (top, Baseline_RiverFed_SSP1) & A.3.2 (bottom, Baseline_RiverFed_SSP3)

Indicator values are displayed in the table below. Under SSP1-2.6, the oxic zone is in average 10 cm deeper than in the baseline A.1.2 scenario, and carbon losses are nearly twice as high. Under SSP3-7.0, the oxic depth and carbon losses are 4/5 times higher than in the baseline A.1.2 scenario.

Indicator Short Name	*Indicator Value A.1.2 River-fed Current Climate*	Indicator Value A.2.2 River-fed SSP1-2.6	Indicator Value A.3.2 River-fed SSP3-7.0	Unit
Oxic Depth Inside/Outside	*0.12*	0.21	0.55	m
Groundwater Depth Inside/Outside	*0.03*	0.12	0.48	m
Carbon Flux Inside/Outside	*-2.82*	-5.16	-12.28	kg/m^2/year

A spatial representation of the annual mean change in soil carbon stock for the three climate scenarios (see Figure 8.4) shows that soil carbon losses outside of the floodplain are higher under SSP3-7.0 than under SSP1-2.6, which are themselves higher than those of the A.1.2 baseline scenario. The area affected by river flooding under SSP1-2.6 and SSP3-7.0 is narrower than in the baseline scenario.

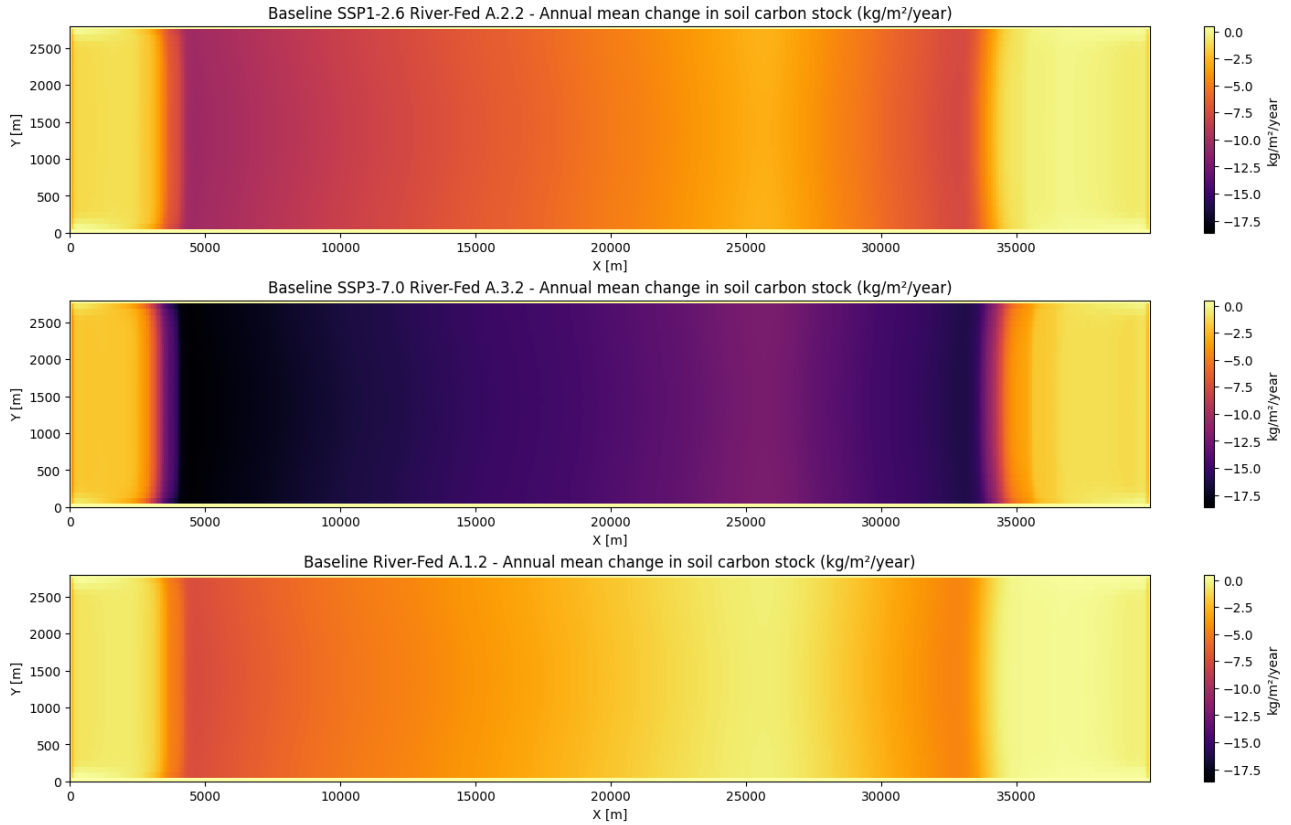

Figure 8.4 Annual mean net CO_2 emissions – Baseline SSP1-2.6 River-fed (A.2.2) vs Baseline SSP3-7.0 River-fed (A.3.2) vs Baseline River-fed (A.1.2)

8.2 Intervention B – Road Built and Operational

As water levels drop with climate change, peat decay increases near the road footprint while remaining lower than in the baseline scenario. Inside the road footprint, the carbon flux remains zero because the water table stays above the base of the road embankment.

8.2.1 Rainfall driven case

Indicator Short Name	*Indicator Value B.1.1 Rainfall driven Current Climate*	Indicator Value B.2.1 Rainfall driven SSP1-2.6	Indicator Value B.3.1 Rainfall driven SSP3-7.0	Unit
Oxic Depth Inside	*0.92*	0.95	1.13	m
Groundwater Depth Inside	*1.06*	1.10	1.26	m
Carbon Flux Inside	*0.00*	0.00	0.00	kg/m^2/year
Oxic Depth Outside	*0.13*	0.21	0.61	m
Groundwater Depth Outside	*0.05*	0.16	0.58	m
Carbon Flux Outside	*-2.90*	-5.27	-13.75	kg/m^2/year

8.2.2 River-fed case

Indicator Short Name	*Indicator Value B.1.2 River-fed Current Climate*	Indicator Value B.2.2 River-fed SSP1-2.6	Indicator Value B.3.2 River-fed SSP3-7.0	Unit
Oxic Depth Inside	*0.89*	0.92	1.07	m
Groundwater Depth Inside	*1.03*	1.06	1.20	m
Carbon Flux Inside	*0.00*	0.00	0.00	kg/m^2/year
Oxic Depth Outside	*0.07*	0.13	0.44	m
Groundwater Depth Outside	*-0.05*	0.03	0.37	m
Carbon Flux Outside	*-1.40*	-3.23	-10.29	kg/m^2/year

8.3 Intervention C – Road during Construction

As water levels drop with climate change, peat decay increases near the drained road footprint while remaining much higher than in the baseline scenario. However, the decrease in water level due to drainage is so important that the impact of climate change on water levels is reduced compared to the baseline intervention. Inside the road footprint, the carbon flux remains zero because the water table stays above the base of the road embankment.

8.3.1 Rainfall driven case

Indicator Short Name	*Indicator Value C.1.1 Rainfall driven Current Climate*	Indicator Value C.2.1 Rainfall driven SSP1-2.6	Indicator Value C.3.1 Rainfall driven SSP3-7.0	Unit
Oxic Depth Inside	*2.12*	2.12	2.12	m
Groundwater Depth Inside	*2.01*	2.02	2.06	m
Carbon Flux Inside	*0.00*	0.00	0.00	kg/m^2/year
Oxic Depth Outside	*0.68*	0.77	1.08	m

Indicator Short Name	*Indicator Value C.1.1 Rainfall driven Current Climate*	Indicator Value C.2.1 Rainfall driven SSP1-2.6	Indicator Value C.3.1 Rainfall driven SSP3-7.0	Unit
Groundwater Depth Outside	*0.68*	0.78	1.06	m
Carbon Flux Outside	*-14.26*	-16.42	-20.64	kg/m^2/year

8.3.2 River-fed case

Indicator Short Name	*Indicator Value C.1.2 River-fed Current Climate*	Indicator Value C.2.2 River-fed SSP1-2.6	Indicator Value C.3.2 River-fed SSP3-7.0	Unit
Oxic Depth Inside	*2.12*	2.12	2.12	m
Groundwater Depth Inside	*2.01*	2.02	2.06	m
Carbon Flux Inside	*0.00*	0.00	0.00	kg/m^2/year
Oxic Depth Outside	*0.61*	0.69	0.96	m
Groundwater Depth Outside	*0.60*	0.67	0.92	m
Carbon Flux Outside	*-12.88*	-14.81	-18.63	kg/m^2/year

8.4 Intervention D – Settlements developed

As water levels drop with climate change, peat decay increases inside and outside the settlement footprint, while remaining lower than under current climate conditions outside the footprint. In the rainfall driven case, as actual evapotranspiration outside the footprint is very high under SSP3-7.0, water levels under the footprint are shallower than outside -and thus carbon losses lower-, unlike under current climate conditions and SSP1-2.6. In the river-fed case under SSP3-7.0, although carbon losses outside the footprint remain lower than inside, they are also lower than in the baseline scenario because of the very high actual evapotranspiration outside the footprint. Outside of the intervention footprint, carbon losses are similar to the baseline scenario.

8.4.1 Rainfall driven case

Indicator Short Name	*Indicator Value D.1.1 Rainfall driven Current Climate*	Indicator Value D.2.1 Rainfall driven SSP1-2.6	Indicator Value D.3.1 Rainfall driven SSP3-7.0	Unit
Oxic Depth Inside	*0.37*	0.40	0.52	m
Groundwater Depth Inside	*0.40*	0.43	0.55	m
Carbon Flux Inside	*-8.77*	-9.93	-12.56	kg/m^2/year
Oxic Depth Outside	*0.16*	0.26	0.67	m
Groundwater Depth Outside	*0.10*	0.21	0.64	m
Carbon Flux Outside	*-3.80*	-6.46	-14.80	kg/m^2/year

8.4.2 River-fed case

Indicator Short Name	*Indicator Value D.1.2 River-fed Current Climate*	Indicator Value D.2.2 River-fed SSP1-2.6	Indicator Value D.3.2 River-fed SSP3-7.0	Unit
Oxic Depth Inside	*0.34*	0.37	0.48	m
Groundwater Depth Inside	*0.35*	0.38	0.49	m
Carbon Flux Inside	*-8.10*	-9.18	-11.56	kg/m^2/year
Oxic Depth Outside	*0.09*	0.17	0.49	m
Groundwater Depth Outside	*-0.01*	0.08	0.42	m
Carbon Flux Outside	*-2.08*	-4.18	-11.77	kg/m^2/year

8.5 Intervention E – Forest Fire / Deforestation

As water levels drop with climate change, peat decay increases both inside and outside the fire footprint. In the intervention footprint, carbon losses under SSP1-2.6 and SSP3-7.0 are lower than the baseline. Evapotranspiration from the burnt area is indeed reduced when the water table drops deep below ground, which results in an increase in the water table. Carbon fluxes outside the fire footprint are similar to the baseline.

8.5.1 Rainfall driven case

Indicator Short Name	*Indicator Value E.1.1 Rainfall driven Current Climate*	Indicator Value E.2.1 Rainfall driven SSP1-2.6	Indicator Value E.3.1 Rainfall driven SSP3-7.0	Unit
Oxic Depth Inside	*0.18*	0.25	0.43	m
Groundwater Depth Inside	*0.14*	0.22	0.43	m
Carbon Flux Inside	*-4.67*	-6.64	-10.83	kg/m^2/year
Oxic Depth Outside	*0.20*	0.31	0.73	m
Groundwater Depth Outside	*0.16*	0.27	0.70	m
Carbon Flux Outside	*-4.78*	-7.65	-15.88	kg/m^2/year

8.5.2 River-fed case

Indicator Short Name	*Indicator Value E.1.2 River-fed Current Climate*	Indicator Value E.2.2 River-fed SSP1-2.6	Indicator Value E.3.2 River-fed SSP3-7.0	Unit
Oxic Depth Inside	*0.12*	0.18	0.34	m
Groundwater Depth Inside	*0.03*	0.11	0.29	m
Carbon Flux Inside	*-3.17*	-4.91	-8.72	kg/m^2/year
Oxic Depth Outside	*0.12*	0.21	0.54	m
Groundwater Depth Outside	*0.03*	0.12	0.47	m

Indicator Short Name	*Indicator Value E.1.2 River-fed Current Climate*	Indicator Value E.2.2 River-fed SSP1-2.6	Indicator Value E.3.2 River-fed SSP3-7.0	Unit
Carbon Flux Outside	*-2.85*	-5.16	-12.09	kg/m^2/year

8.6 Intervention F – Forest replaced by Oil Palm Plantations

Climate change under SSP1-2.6 increases evapotranspiration, further lowering water tables across the peat dome. However, the decrease in water level due to soil subsidence and drainage is so important that the impact of climate change on water levels is reduced compared to the baseline intervention. Peat decay increases compared to current climate conditions due to lower water tables. Carbon losses remain much higher than in the baseline scenario (A.2.1) both inside and outside the plantation footprint.

8.6.1 Rainfall driven case

Indicator Short Name	*Indicator Value F.1.1 Rainfall driven Current Climate*	Indicator Value F.2.1 Rainfall driven SSP1-2.6	Indicator Value F.3.1 Rainfall driven SSP3-7.0	Unit
Oxic Depth Inside	*0.77*	0.82	1.05	m
Groundwater Depth Inside	*0.79*	0.84	1.04	m
Carbon Flux Inside	*-15.64*	-17.13	-20.37	kg/m^2/year
Oxic Depth Outside	*0.73*	0.83	1.13	m
Groundwater Depth Outside	*0.73*	0.83	1.12	m
Carbon Flux Outside	*-15.01*	-17.17	-21.25	kg/m^2/year

8.6.2 River-fed case

Indicator Short Name	*Indicator Value F.1.2 River-fed Current Climate*	Indicator Value F.2.2 River-fed SSP1-2.6	Indicator Value F.3.2 River-fed SSP3-7.0	Unit
Oxic Depth Inside	*0.71*	0.75	0.94	m
Groundwater Depth Inside	*0.69*	0.74	0.91	m
Carbon Flux Inside	*-14.55*	-15.87	-18.70	kg/m^2/year
Oxic Depth Outside	*0.65*	0.74	1.00	m
Groundwater Depth Outside	*0.64*	0.72	0.97	m
Carbon Flux Outside	*-13.53*	-15.45	-19.17	kg/m^2/year

8.7 Intervention G – Forest replaced by Rice Plantations

As water levels drop with climate change, peat decay increases both inside and outside the rice plantation. In the intervention footprint, like under the current climate, carbon losses under SSP1-2.6 and SSP3-7.0 are lower than the baseline. Evapotranspiration from the rice paddies is indeed reduced

when the water table drops deep below ground, which mitigates the drop in water level. Carbon fluxes outside the rice footprint are similar to the baseline.

8.7.1 Rainfall driven case

Indicator Short Name	*Indicator Value G.1.1 Rainfall driven Current Climate*	Indicator Value G.2.1 Rainfall driven SSP1-2.6	Indicator Value G.3.1 Rainfall driven SSP3-7.0	Unit
Oxic Depth Inside	*0.14*	0.22	0.50	m
Groundwater Depth Inside	*0.10*	0.19	0.49	m
Carbon Flux Inside	*-3.77*	-5.97	-12.34	kg/m^2/year
Oxic Depth Outside	*0.20*	0.31	0.73	m
Groundwater Depth Outside	*0.15*	0.27	0.70	m
Carbon Flux Outside	*-4.70*	-7.57	-15.91	kg/m^2/year

8.7.2 River-fed case

Indicator Short Name	*Indicator Value G.1.2 River-fed Current Climate*	Indicator Value G.2.2 River-fed SSP1-2.6	Indicator Value G.3.2 River-fed SSP3-7.0	Unit
Oxic Depth Inside	*0.09*	0.15	0.39	m
Groundwater Depth Inside	*0.00*	0.08	0.34	m
Carbon Flux Inside	*-2.46*	-4.27	-9.91	kg/m^2/year
Oxic Depth Outside	*0.12*	0.20	0.54	m
Groundwater Depth Outside	*0.03*	0.12	0.47	m
Carbon Flux Outside	*-2.79*	-5.10	-12.14	kg/m^2/year

8.8 Summary of Results

Water levels in the peatland are expected to drop under both SSP1-2.6 and SSP3-7.0. Although rainfall should increase by 1.5% annually under SSP1-2.6, the rise in actual evapotranspiration is sharper. Under SSP3-7.0, a substantial increase in actual evapotranspiration coupled with a slight decrease in rainfall leads to lower water levels.

As water levels drop under climate change, peat decay increases. In rainfall driven peatlands, soil carbon losses should rise consistently throughout the model area, the cells located near the western and eastern boundaries remaining important carbon sources. In river-fed peatlands, carbon losses also rise throughout the whole model area, while the floodplain is narrower than under current climate conditions.

Across all interventions except the settlement and fire interventions, carbon fluxes inside and outside the footprint follow the same trend relative to the baseline under all climate conditions: if carbon losses for a given intervention are lower than the baseline under current climate conditions, they are also lower under SSP1-2.6 and SSP3-7.0. In the road scenarios (B and C), carbon fluxes from the gravel embankment are zero. This means they are lower than the baseline under all climate scenarios.

For the settlement intervention, carbon losses inside the footprint are higher than the baseline under current climate conditions and under SSP1-2.6 but lower under SSP3-7.0. Under the current climate, the water table under the footprint is deeper than in the surrounding cells as the ground is raised. Actual evapotranspiration is slightly reduced compared to the area outside of the footprint. Under SSP3-7.0, as actual evapotranspiration in the baseline is so high compared to the settlement, the average water table is shallower in the settlement footprint than in the baseline, which results in reduced peat decay.

For the fire intervention, soil carbon losses inside the footprint are lower than the baseline under SSP1-2.6 and SSP3-7.0, unlike under current climate conditions. In river-fed peatlands, carbon losses in the burnt area are higher than the baseline under the current climate, because of ground smoothening, peat compaction through burning and reduced carbon uptake by the burnt vegetation. In rainfall driven peatlands, carbon fluxes in the burnt area are similar to the baseline as the aforementioned effects are offset by the lower actual evapotranspiration. As water levels drop under SSP1-2.6 and SSP3-7.0, actual evapotranspiration increases sharply in the baseline intervention but only slightly in the burnt area because the top soil layer dries out, resulting in comparatively lower carbon losses for the fire intervention.

9 Applicability and Limitations of the Methodology

The method presented here acknowledges that understanding the hydrology of the peatlands is essential for estimating changes in soil carbon stocks and relies thus on a joint hydrological model and carbon flux approach. Although the developed tool provides an assessment of the impacts of interventions on water levels and carbon fluxes, there are limitations of the methodology.

9.1 Hydrological setup and model validation

Due to limited availability of comprehensive data, a georeferenced model could not be developed. Instead, a conceptual model was adopted, focusing on the dominant hydrological processes that shape peatland dynamics. This “experimental” approach is tailored to the region’s data constraints and supports robust scenario analysis despite inherent uncertainties. To reflect the hydrological diversity of the Cuvette Centrale, the model incorporates two distinct representations: one for rainfall-driven peatlands and another for those influenced by river flooding. This ensures that both hydrological regimes are adequately captured. The model structure and parameterization are designed to align with the region’s hydrological, climatic, and geomorphological characteristics, while also accounting for existing data gaps. Its spatial extent was defined through iterative testing of local interventions, ensuring relevance to the scenarios being assessed.

Simulated water levels were compared to measurements along several transects in the Cuvette Centrale in 2013-2014 and 2018-2019 (Dargie et al., 2017; Crezee et al., 2022). The model being conceptual, standard calibration procedures using established performance evaluation metrics to validate its accuracy couldn’t be carried out. Therefore, the emphasis was rather on qualitative plausibility checks of water level ranges and fluctuation patterns.

The **comparison of simulated water levels with observations** shows that they fall within the same range and exhibit similar seasonal fluctuations (see section 3.3). Measurements indicate rapid groundwater rises following rainfall events, followed by gradual declines; however, this pattern is not well reproduced in the MIKE SHE model. The model also clearly separates rapid overland flow from slower groundwater dynamics – it should rather be less pronounced.

Peat depth and elevation measurements from the region (see Dargie et al., 2017; Crezee et al., 2022) were used to design the gently sloped peat dome model. Model results show deeper water tables in the steep areas near the western and eastern boundaries than at the flat centre of the dome. However, the available measurements provide no evidence that the water table is in fact deeper at the steep fringes of the peat dome (see section 3.3). Additional fieldwork in the Cuvette Centrale would therefore needed to better understand the **spatial variability of water levels across peat domes**. Accurate mapping of areas with deep water tables is essential, as these areas are responsible for most carbon emissions. If simulated water levels along the dome edges are too low, the resulting drop in carbon losses simulated for river-fed peatlands relative to rain-fed peatlands would be overestimated.

9.2 Hydrological processes

Estimating **evapotranspiration** accurately is essential to describe the water balance of the Cuvette Centrale. Transpiration is modelled in MIKE SHE based on reference evapotranspiration and plant-specific parameters which vary depending on the simulated intervention. It is simulated using a logarithmic root-density distribution in the soil column, with higher extraction in the topsoil. This distribution depends on the maximum root depth, which is an input parameter of the model. Sciumbata et al. (2023) measured fine root production to a depth of 1 m in the peatlands of the Cuvette Centrale and found evidence of fine roots throughout the entire soil column. The maximum root depth is therefore set to 1 m in this study.

Sciumbata et al. also observed that fine root production decreases sharply with depth in the Cuvette Centrale peatlands. By contrast, the default MIKE SHE roots distribution decreases more gradually with depth, allowing for relatively deeper roots. As a result, transpiration and thus water table depth may be overestimated in the model during dry periods.

Peat hydraulic properties such as hydraulic conductivity and specific yield determine how water infiltrates and flows through peat. Because no measurements of soil hydraulic parameters are available for the Cuvette Centrale, parameter values are derived from literature on Southeast Asian tropical peatlands. It is also unknown how these properties vary with depth in the study region. To better represent subsurface water dynamics in the peatlands of the Cuvette Centrale, measurements of hydraulic properties should be conducted.

The water balance in scenario A.1.1 shows very little flow towards the western and eastern boundaries (see section 3.3.3), although some studies demonstrate that outflow towards rivers is high in the Congolese peatlands. The river-fed simulations show that low river levels appear not to affect the water table beyond two cells away from the boundary. Groundwater flow from and to rivers and more generally **lateral groundwater flow** could be underestimated in the current model configuration. Field measurements should be made to quantify lateral groundwater flow in the peatlands of the Cuvette Centrale.

9.3 Scenarios

River-fed simulations indicate that the area flooded by rivers gradually expands from year to year as river inflows replenish the unsaturated zone. This suggests that hydrological equilibrium is not reached during the simulation. Therefore, it would be better to run the river-fed model over a longer period to fully capture the impacts of river flooding on the entire model area.

The **interventions** modelled could be improved with local knowledge and data. Geotechnical data would help refine the model configuration for the road and settlement interventions. For the oil palm and rice plantations, more info on drainage patterns in the Cuvette Centrale would be valuable for improving the model setups. Local soil measurements should also be carried out in degraded patches of the peatland. To better understand the hydrological impacts of the various interventions, the hydraulic properties of peat that is subjected to compression, burning, or drainage should be monitored.

The **climate models** included in the CMIP6 multi-model ensemble show conflicting results regarding rainfall trends in the study area (see section 5.2.2). The significant uncertainties associated with the precipitation predictions in the region mean that the results of the climate change scenarios are to be interpreted with caution. While the ensemble median suggests a slight increase in rainfall under SSP1-2.6 and a decrease under SSP3-7.0, some models predict much larger increases or decreases. If one of the wetter rainfall scenarios were to materialize, the impact of climate change on water levels would likely be less severe. For greater accuracy, however, the p10 and p90 rainfall projections should also be considered to provide insight into the full range of possible climate futures. Furthermore, additional scientific studies are needed to assess the effects of climate change on river discharge across the region, which plays a crucial role in the hydrology of river-fed peatlands.

9.4 Carbon accumulation and loss model

In the current model, carbon storage is assumed to remain constant throughout the simulation period. In reality, the total amount of carbon stored through plant photosynthesis, referred to as **Gross Primary Productivity (GPP), depends on both weather and hydrological conditions.** Photosynthesis, for example, slows on cloudy days. Hirano et al. (2012) observed that GPP decreased in burnt peatland forests in Indonesia due to the dense smoke generated by peat fires. Incorporating this effect into the fire scenario would improve the accuracy of the carbon flux estimates. Carbon storage is also influenced by hydrology, as plants become stressed when the water table is either too low or too high.

To better capture this effect, a reduction factor for carbon storage could be introduced when the water table lies outside an optimal range.

Prolonged periods of **peat decay lead to soil subsidence**. In the oil palm hydrological model, this effect is represented by lowering the ground surface by 50 cm. A more accurate approach would be to explicitly couple the carbon flux and hydrological models, adjusting ground elevation dynamically according to carbon dynamics. However, this would considerably increase the complexity of the modelling process.

Several studies have shown that **peat hydraulic properties influence decay rates**. For example, Hirano et al. (2012) demonstrated that a similar drop in the average yearly water table results in greater CO_2 emissions in untouched peatlands than in drained peatlands. Decay rates could therefore be estimated more accurately if soil properties were incorporated into the carbon flux model. However, literature data on the effects of peat properties on decay rates remain limited, which is why the method presented here does not account for soil hydraulic properties.

The present study **focuses on carbon balance rather than greenhouse gas emissions**, which prevents drawing firm conclusions about the effects of the different peatland interventions on global warming. Under oxic conditions, most peat carbon is converted to CO_2, whereas under anoxic conditions, substantial amounts of methane and dissolved organic carbon can be produced. The relative contribution of each carbon outflow pathway depends on the physical and chemical properties of the peat. Because, across all model scenarios, most peat decomposition occurs under oxic conditions, CO_2 emissions can be approximated from peat carbon loss. However, a more comprehensive assessment of carbon outflows under both oxic and anoxic conditions would require additional field measurements.

9.5 Conclusion

The combined modelling approach described here enables decision-makers to assess the effects of specific interventions on water levels and carbon dioxide emissions under various hydrological and climate conditions. The accuracy of the model is constrained by the limited understanding of peatland hydrology in the Cuvette Centrale, particularly the exchanges between rivers and peatlands. Field measurements would help refine the model, especially soil hydraulic parameters and water level time series for validation. To estimate more precisely the impacts of a given intervention in a specific area, the current conceptual rectangular-shaped model could be converted into a georeferenced model that covers the actual intervention zone with appropriate site-specific parameters.

10 Summary and Conclusion

This report has presented the development and application of a Hydrological Decision Support System (HDSS) tailored to the unique characteristics of the Congo Basin peatlands. Through the integration of a conceptual hydrological model (MIKE SHE) and a heuristic biodegradation model, the HDSS provides a framework for understanding the interplay between water dynamics and carbon emissions in the Cuvette Centrale.

The hydrological model simulates key processes such as precipitation, evapotranspiration, infiltration, groundwater flow, and overland flow. Two distinct hydrological zones are modelled: (1) rainfall driven only, and (2) rainfall driven and river-fed. Despite the conceptual nature of the model and the limited availability of in-situ data, the calibration results align well with observed seasonal and spatial patterns of groundwater levels from literature. The model captures the sensitivity of the peatland system to climatic variability, particularly the drying trend observed over recent decades.

Coupled with the biodegradation model, the carbon fluxes are estimated based on oxic and anoxic soil conditions. The heuristics distinguish between labile and recalcitrant organic matter and account for their respective degradation rates under varying saturation levels. This approach provides an understanding of how hydrological changes - whether from climate variability or human interventions - translate into carbon fluxes.

Scenario analyses demonstrate the significant impact of development interventions such as road construction, settlement expansion, and land-use conversion on peatland hydrology and carbon losses. For example, drainage associated with infrastructure development can drastically lower groundwater tables, increasing oxic depth and accelerating peat decomposition. Conversely, scenarios that maintain or restore high water tables show reduced emissions and better preservation of peat carbon stocks.

The scenario analyses conducted in this study highlight several critical vulnerabilities of the peatlands, arising from their hydrological sensitivity, the nature of development interventions, and the impacts of climate change.

- **Hydrological Vulnerabilities**: The peatlands are highly sensitive to changes in water table levels. Lowering of the groundwater table - whether through drainage, infrastructure development, or prolonged dry periods - exposes peat to oxic conditions, thereby accelerating decomposition and increasing carbon losses. The loss of microtopography and increased overland flow further exacerbate water loss, particularly in areas where natural surface features are altered.
- **Vulnerabilities from Development Interventions**: Infrastructure development, such as road construction, settlement expansion, and conversion to agriculture (e.g., oil palm or rice cultivation), typically involves drainage and compression of peat soils. These interventions result in a significant lowering of the water table, increased oxic depth, and enhanced peat decomposition. Removal of natural vegetation and smoothing of the land surface reduce the peatland's capacity to retain water and buffer against hydrological extremes.
- **Climate Change Vulnerabilities**: With climate change, the peatlands of the Cuvette Centrale are expected to become drier. Evapotranspiration rates are projected to increase substantially, driven by rising temperatures in the region. This projection is particularly concerning for the Cuvette Centrale, where peatlands are more vulnerable to drought than their Southeast Asian counterparts due to lower annual precipitation. The region could experience longer and more intense dry seasons, leading to lower water tables, an increased risk of fire, and accelerated carbon loss.
  The interaction between these uncertain climate trajectories and ongoing human interventions poses a significant challenge to the long-term resilience and stability of the peatland ecosystem. However, these findings should be interpreted with caution given the high uncertainty of CMIP6 rainfall projections. While the ensemble median shows only modest rainfall changes, individual models project a much wider range—from strong increases to strong decreases—highlighting the importance of also considering p10 and p90 scenarios. Additional research on regional river discharge is needed, as it is a key driver of water levels in river-fed peatlands.

To address these vulnerabilities, the following management actions are recommended:

- **Maintain High Water Tables**: Prioritize hydrological management practices that keep the groundwater table close to the surface. Where drainage is unavoidable, limit the depth and duration of drainage to minimize peat oxidation and subsidence.
- **Protect and Restore Vegetation**: Retain natural vegetation buffers, especially along waterways and peat dome margins, to support water retention and ecosystem resilience. Restoration of degraded areas through rewetting and reforestation should be promoted to reduce emissions and enhance peatland function.
- **Minimize Surface Disturbance**: Avoid large-scale smoothing of natural microtopography and limit soil compaction from heavy infrastructure. Where possible, design interventions to preserve or mimic natural surface features.
- **Implement Adaptive Drainage**: Where drainage is necessary for development, employ controlled drainage systems (e.g., adjustable weirs) to allow dynamic management of water levels in response to seasonal and climatic variability.
- **Monitor and Adapt**: Establish long-term monitoring of hydrological and ecological indicators to inform adaptive management and ensure that interventions do not compromise peatland integrity.

In summary, the Congo Basin peatlands are highly vulnerable to hydrological disturbance, unsustainable land use, and climate change. Maintaining high water tables, protecting natural vegetation, and restoring degraded areas are essential to safeguard their carbon stocks, biodiversity, and hydrological functions.

The HDSS developed in this project lays the groundwork for evidence-based governance and sustainable planning in the Congo Basin peatlands. Looking ahead, the following key direction can be envisioned: Stakeholder Engagement and Policy Integration: The HDSS outputs can inform land-use planning, conservation strategies, and infrastructure development guidelines. Continued collaboration with local stakeholders and policymakers will be essential to ensure the system's relevance and impact.

Future efforts should focus on improving in-situ data collection, refining soil hydraulic parameters, and expanding the spatial resolution of the model. In conclusion, the HDSS represents a significant step towards the application of integrating hydrology, carbon dynamics, and climate projections into a unified decision support framework for sustainable management and conservation of peatlands in the Congo Basin.

11 List of Figures and Tables

Figures

Tables

12Abbreviations

AWD:	Alternate Wetting and Drying
BRF:	Business Rule Framework
CORDEX:	Coordinated Regional Downscaling Experiment
DAHITI:	Database for Hydrological Time Series of Inland Waters
DRC:	Democratic Republic of Congo
ECMWF:	European Centre for Medium-Range Weather Forecasts
ET:	Evapotranspiration
GCM:	Global Climate Model
GIS:	Geographic Information System
GPP:	Gross Primary Productivity
GWT:	Groundwater
HDSS:	Hydrological Decision Support System
IKI:	Internationale Klimaschutzinitiative (International Climate Initiative)
IPCC:	Intergovernmental Panel on Climate Change
LAI:	Leaf Area Index
MAE:	Mean Absolute Error
MODIS:	Moderate Resolution Imaging Spectroradiometer
OCIV:	Observatoire Congolais des Inondations et de la Vulnérabilité
OL:	Overland Flow
PDF:	Probability Density Function
PSEAU:	Programme Solidarité Eau
RCP:	Representative Concentration Pathway
SSP:	Shared Socioeconomic Pathway
UNEP:	United Nations Environment Programme

13 References

/1/ Aloysius, N., & Saiers, J. (2017). Simulated hydrologic response to projected changes in precipitation and temperature in the Congo River basin. *Hydrology and Earth System Sciences*, *21*(8), 4115-4130.

/2/ Apers, M. E., Crezee, B., Dargie, G. C., Sjögersten, S., Bocko, Y. E., Ewango, C. E. N., ... & Lawson, I. T. (2022). Hydrology of the central Congo peatlands: Seasonal dynamics and their influence on the carbon cycle. *Environmental Research Letters, 17*(6), 064028. https://doi.org/10.1088/1748-9326/ac6e57

/3/ Awal, M. A., & Wan Ishak, W. I. (2008). *Measurement of oil palm LAI by manual and LAI-2000 method*. Asian Journal of Scientific Research, 1(1), 49–56. https://doi.org/10.3923/ajsr.2008.49.56 scialert.net

/4/ Cook, K. H., Liu, Y., & Vizy, E. K. (2020). Congo Basin drying associated with poleward shifts of the African thermal lows. *Climate Dynamics, 54*(1–2), 863–883. https://doi.org/10.1007/s00382-019-05033-3

/5/ Crezee, B., Dargie, G. C., Ewango, C. E. N., Mitchard, E. T. A., Emba B., O., Kanyama T., J., Bola, P., Ndjango, J.-B. N., Girkin, N. T., Bocko, Y. E., Ifo, S. A., Hubau, W., Seidensticker, D., Batumike, R., Imani, G., Cuní-Sanchez, A., Kiahtipes, C. A., Lebamba, J., Wotzka, H.-P., Bean, H., Baker, T. R., Baird, A. J., Boom, A., Morris, P. J., Page, S. E., Lawson, I. T., Lewis, S. L., 2022. *Mapping peat thickness and carbon stocks of the central Congo Basin using field data.* Nature Geoscience 15, 639-644. https://doi.org/10.1038/s41561-022-00966-7.

/6/ Dargie, G. C. (2015). *Quantifying and understanding the tropical peatlands of the central Congo Basin* (Doctoral dissertation, University of Leeds).

/7/ Dargie, G. C., Lewis, S. L., Lawson, I. T., Mitchard, E. T., Page, S. E., Bocko, Y. E., & Ifo, S. A. (2017). Age, extent and carbon storage of the central Congo Basin peatland complex. *Nature*, *542*(7639), 86-90.

/8/ Evans, C. D., Williamson, J. M., Kacaribu, F., Irawan, D., Suardiwerianto, Y., Hidayat, M. F., ... & Page, S. E. (2019). Rates and spatial variability of peat subsidence in Acacia plantation and forest landscapes in Sumatra, Indonesia. *Geoderma*, *338*, 410-421.

/9/ Food Security Cluster. (2024, May 2). *Annexes – Lignes Directrices Cluster Sécurité Alimentaire* [PDF file]. Food Security Cluster, Democratic Republic of the Congo. FSCluster.org. Retrieved from FSCluster.org

/10/ Ginting, E. N., Darlan, N. H., & Winarna. (2016). Effective water management for oil palm in peatland: for peat conservation and yield optimization. In *15th International peat congress* (Vol. 2016, pp. 497-501).

/11/ Gorham, E. (1991). Northern peatlands: Role in the carbon cycle and probable responses to climatic warming. *Ecological Applications, 1*(2), 182–195. https://doi.org/10.2307/1941811

/12/ Hirano, T., Sundari, S., & Yamada, H. (2012). CO_2 Balance of Tropical Peat Ecosystems. In *Tropical Peatland Ecosystems* (pp. 329-337). Springer. https://doi.org/10.1007/978-4-431-55681-7_21 link.springer.com

/13/ Hooijer, A., Silvius, M., Wösten, H., & Page, S. (2006). PEAT-CO2. Assessment of CO2 emissions from drained peatlands in SE Asia.

/14/ Hooijer, A., Page, S., Canadell, J. G., Silvius, M., Kwadijk, J., Wösten, H., & Jauhiainen, J. (2010). Current and future CO_2 emissions from drained peatlands in Southeast Asia. *Biogeosciences, 7*(5), 1505–1514. https://doi.org/10.5194/bg-7-1505-2010

/15/Hooijer, A., Page, S., Jauhiainen, J., Lee, W. A., Lu, X. X., Idris, A., & Anshari, G. (2012). Subsidence and carbon loss in drained tropical peatlands. *Biogeosciences*, *9*(3), 1053-1071.

/16/Jelisic, N. (2005). Geotechnical properties of stabilized peat. In *Proceedings of the 16th International Conference on Soil Mechanics and Geotechnical Engineering* (pp. 1203-1206). IOS Press.

/17/Karam, S., Zango, B. S., Seidou, O., Perera, D., Nagabhatla, N., & Tshimanga, R. M. (2023). Impacts of climate change on hydrological regimes in the Congo River Basin. *Sustainability*, *15*(7), 6066.

/18/Kurnianto, S., Warren, M., Talbot, J., Kauffman, B., Murdiyarso, D., & Frolking, S. (2015). Carbon accumulation of tropical peatlands over millennia: a modeling approach. *Global change biology*, *21*(1), 431-444.

/19/Lampela, M., Jauhiainen, J., Kämäri, I., Koskinen, M., Tanhuanpää, T., Valkeapää, A., & Vasander, H. (2016). Ground surface microtopography and vegetation patterns in a tropical peat swamp forest. *Catena*, 139, 127–136. https://doi.org/10.1016/j.catena.2015.12.016

/20/Lampela, M., Jauhiainen, J., Sarkkola, S., & Vasander, H. (2017). Promising native tree species for reforestation of degraded tropical peatlands. *Forest Ecology and Management*, *394*, 52-63.

/21/Li, W., O'Kelly, B. C., Yang, M., & Fang, K. (2020). Compressibility behaviour and properties of peaty soils from Dian-Chi Lake area, China. *Engineering Geology*, *277*, 105778.

/22/Liu, H., Price, J., Rezanezhad, F., & Lennartz, B. (2020). Centennial-scale shifts in hydrophysical properties of peat induced by drainage. Water Resources Research, 56(10), e2020WR027538.

/23/Mahajan, G., Timsina, J., Jhanji, S., Sekhon, N. K., & Kuldeep-Singh. (2012). Cultivar response, dry-matter partitioning, and nitrogen-use efficiency in dry direct-seeded rice in northwest India. *Journal of Crop Improvement*, *26*(6), 767-790.

/24/Mander, Ü., Pärn, J., Espenberg, M., Soosaar, K., Ndolo Ebika, S., Bouka Dipelet, G., Kuusemets, L., Mander, S., Khanongnuch, R., Kanger, K., Brugière, D., & Loumeto, J. (2025, April 27-May 2). *Greenhouse gas fluxes and microbiome in a peatland forest and peaty savanna in Epena, Republic of the Congo* [Abstract EGU25-7308, EGU General Assembly]. Copernicus Meetings. https://doi.org/10.5194/egusphere-egu25-7308

/25/Mayengo, A., Macaire, J., & van Assche, A. (2005). *Guide pratique pour une exploitation agricole située à Kinshasa et sa périphérie*. OCIV–Entreprendre Cedita. Retrieved from PSEAU website

/26/McCalmont, J., Kho, L. K., Teh, Y. A., Lewis, K., Chocholek, M., Rumpang, E., & Hill, T. (2021). Short-and long-term carbon emissions from oil palm plantations converted from logged tropical peat swamp forest. *Global Change Biology*, *27*(11), 2361-2376.

/27/Moore, S., Adu-Bredu, S., Duah-Gyamfi, A., Addo-Danso, S. D., Ibrahim, F., Mbou, A. T., ... & Malhi, Y. (2018). Forest biomass, productivity and carbon cycling along a rainfall gradient in West Africa. *Global change biology*, *24*(2), e496-e510.

/28/Page, S. E., Rieley, J. O., & Banks, C. J. (2011). Global and regional importance of the tropical peatland carbon pool. *Global Change Biology, 17*(2), 798–818. https://doi.org/10.1111/j.1365-2486.2010.02279.x

/29/Prabhakar, M., Gopinath, K. A., Ravi Kumar, N., Thirupathi, M., Sai Sravan, U., Srasvan Kumar, G., ... & Singh, V. K. (2024). Mapping leaf area index at various rice growth stages in Southern India using airborne hyperspectral remote sensing. *Remote Sensing*, *16*(6), 954.

/30/Ribeiro, K., Pacheco, F. S., Ferreira, J. W., de Sousa-Neto, E. R., Hastie, A., Krieger Filho, G. C., ... & Ometto, J. P. (2021). Tropical peatlands and their contribution to the global carbon cycle and climate change. *Global change biology*, *27*(3), 489-505.

/31/Rieley, J. O., Wüst, R. A. J., Jauhiainen, J., Page, S. E., Wösten, H., Hooijer, A., ... & Stahlhut, M. (2008). Tropical peatlands: carbon stores, carbon gas emissions and contribution to climate change processes. *Peatlands and climate change. Calgary: Peat Society*, 44-70.

/32/Rusli, N., & Majid, M. R. (2014, February). Monitoring and mapping leaf area index of rubber and oil palm in small watershed area. In *IOP Conference Series: Earth and Environmental Science* (Vol. 18, No. 1, p. 012036). IOP Publishing.

/33/Samejima, H., & Tsunematsu, H. (2016). Genotypic variation in rice varieties screened for deep rooting under field conditions in West Africa. *Plant Production Science*, *19*(1), 181-192.

/34/Safitri, L., Suryanti, S., Kautsar, V., Kurniawan, A., & Santiabudi, F. (2018, March). Study of oil palm root architecture with variation of crop stage and soil type vulnerable to drought. In *IOP Conference Series: Earth and Environmental Science* (Vol. 141, p. 012031). IOP Publishing.

/35/Schwatke, C., Dettmering, D., Bosch, W., & Seitz, F. (2015). DAHITI–an innovative approach for estimating water level time series over inland waters using multi-mission satellite altimetry. *Hydrology and Earth System Sciences*, *19*(10), 4345-4364.

/36/Sinclair, A. L., Graham, L. L., Putra, E. I., Saharjo, B. H., Applegate, G., Grover, S. P., & Cochrane, M. A. (2020). Effects of distance from canal and degradation history on peat bulk density in a degraded tropical peatland. Science of the Total Environment, 699, 134199.

/37/Sonwa, D. J., Oumarou Farikou, M., Martial, G., & Félix, F. L. (2020). Living under a fluctuating climate and a drying Congo Basin. *Sustainability, 12*(7), 2936. https://doi.org/-2.8290/su12072936

/38/Surahman, A., Soni, P., & Shivakoti, G. P. (2018). Are peatland farming systems sustainable? Case study on assessing existing farming systems in the peatland of Central Kalimantan, Indonesia. *Journal of Integrative Environmental Sciences*, *15*(1), 1-19.

/39/Tshimanga, R. M., & Hughes, D. A. (2012). Climate change and impacts on the hydrology of the Congo Basin: The case of the northern sub-basins of the Oubangui and Sangha Rivers. *Physics and Chemistry of the Earth, Parts A/B/C*, *50*, 72-83.